ENGINEERING MONOGRAPH No. 23

United States Department of the Interior
BUREAU OF RECLAMATION

PHOTOELASTIC AND EXPERIMENTAL ANALOG PROCEDURES

By W. T. Moody and H. B. Phillips

Denver, Colorado

(Revised March 1967)

$2.00

On November 6, 1979, the Bureau of Reclamation was renamed the Water and Power Resources Service in the U.S. Department of the Interior. The new name more closely identifies the agency with its principal functions—supplying water and power.

The text of this publication was prepared prior to adoption of the new name; all references to the Bureau of Reclamation or any derivative thereof are to be considered synonymous with the Water and Power Resources Service.

United States Department of the Interior

STEWART L. UDALL, Secretary

Bureau of Reclamation

FLOYD E. DOMINY, Commissioner

B. P. BELLPORT, Chief Engineer

Engineering Monograph

No. 23

PHOTOELASTIC AND EXPERIMENTAL ANALOG PROCEDURES

by
W. T. Moody and
H. B. Phillips
Experimental Design Analysis Section
Design Division

Technical and Foreign Services Branch
Denver Federal Center
Denver, Colorado

In its assigned function as the Nation's principal natural resource agency, the Department of the Interior bears a special obligation to assure that our expendable resources are conserved, that renewable resources are managed to produce optimum yields, and that all resources contribute their full measure to the progress, prosperity, and security of America, now and in the future.

ENGINEERING MONOGRAPHS are published in limited editions for the technical staff of the Bureau of Reclamation and interested technical circles in government and private agencies. Their purpose is to record developments, innovations, and progress in the engineering and scientific techniques and practices that are employed in the planning, design, construction, and operation of Reclamation structures and equipment. Copies may be obtained from the Bureau of Reclamation, Denver Federal Center, Denver, Colorado, and Washington, D. C.

First printing July 1955

Revised and reprinted, March 1967

CONTENTS

LIST OF FIGURES

INTRODUCTION

This monograph has been prepared to explain the use of the instruments available in the Bureau of Reclamation for stress analysis studies. It is intended primarily as an explanation of technique and procedure rather than an explanation of the theory underlying the methods used. For that reason the development and justification of the theories involved in the methods of analysis discussed herein have been almost entirely eliminated or greatly condensed. The primary purpose of these experimental studies is to provide an analysis of each problem considered that will assist the designer in making safe, economical designs. Thus, emphasis has been placed on the actual procedures involved and their application to the design problems encountered.

The phenomena of double refraction and photoelastic stress patterns have been known and discussed in technical publications since the time of the British physicist, Sir David Brewster. Brewster [1], in 1816, experimented with polarized light and clear glass plates subjected to stress. He observed the development of a fringe pattern in the glass plates and surmised it was due to double refraction of the glass while under stress. Very little was done experimentally from the time of Brewster until the beginning of the Twentieth Century to utilize this knowledge for design purposes. However, the theories underlying the photoelastic phenomena were thoroughly investigated by many of the scientists of the period. These included such men as Biot [2], Fresnel [3], Neumann [4], Wertheim [5], Maxwell [6], and others.

Experimental photoelastic stress analysis had its real beginning with the British scientists, Coker and Filon [7], who pioneered the field starting about the turn of the century. Since that time, photoelastic stress analysis has become an accepted design tool. Nearly all engineering colleges and large industrial firms are now equipped with photoelastic polariscopes and related instruments.

[1]Superior figures refer to items in the Bibliography.

Photoelastic studies were started by the Bureau of Reclamation at Denver, Colorado, in 1934 to assist primarily in the problems being encountered in the planning and design of Grand Coulee Dam. Original photoelastic equipment was an 8-inch reflector-type polariscope. Since that time additional equipment has been added, existing equipment modified or replaced, and operating technique developed and perfected. At the present time instruments and equipment are available for performing a great variety of stress analysis studies not only in photoelasticity but also in related fields. The major instruments for this work are described in detail in the succeeding sections. A brief discussion of the principal use of each instrument follows.

The Photoelastic Polariscope provides a direct method for the determination of the difference between the two principal stresses, or the maximum shear, in two-dimensional structures. At free boundaries of the structure, the stress condition is immediately known. It is particularly adapted to the analysis of massive structures.

The Photoelastic Interferometer is suitable for use in analyzing the same type of two-dimensional structures that are studied in the photoelastic polariscope. However, the information obtained gives a complete picture of the state of stress at any desired point in the structure since each individual principal stress and its direction are determined.

The Babinet Compensator provides the same type of information as the photoelastic polariscope. However, it is a very precise instrument and will measure variations of the order of one-hundredth of a fringe. Stresses are determined at points on the model rather than observing the entire model as is done in the photoelastic polariscope.

The Beggs Deformeter utilizes microscopic deformations of scale models to determine influence lines for statically indeterminate structures. From the influence lines, the reactions required to make a structure statically determinate can be found. Its principal use is in frame structure analysis.

The Electrical Analogy Tray is an experimental method of obtaining solutions to steady-state potential flow problems. It is most often used to study the steady-state flow of water through earth or other pervious material. It can be applied to two- or three-dimensional studies of the flow and pressure conditions in earth and concrete dams, and in drainage systems.

The Membrane Analogy is used by the Bureau of Reclamation to determine the torsional stresses in structural shapes. It also can be used in problems of potential flow, as is the electrical analogy tray, and to obtain the sum of the principal stresses in a structure.

THE PHOTOELASTIC POLARISCOPE

General

The ultimate objective of any stress analysis study is the determination of the state of stress in the structure being investigated with sufficient accuracy and at enough points to provide information for an adequate design. For the two-dimensional, or plane, stress case, the complete state of stress at any point in the plane is defined when the maximum principal stress, σ_1, the minimum principal stress, σ_2, and their orientation, θ, with respect to a reference axis, are known. Hence, the solution of problems in plane stress resolves into a determination of these three values: σ_1, σ_2, and θ.

The photoelastic polariscope provides a means for determining the difference between the two principal stresses, and their directions. On a free boundary where one stress is zero and the direction of the other stress is parallel to the boundary, it provides a very rapid method of experimentally determining the stress at that boundary. In a great many studies this provides sufficient information for design purposes.

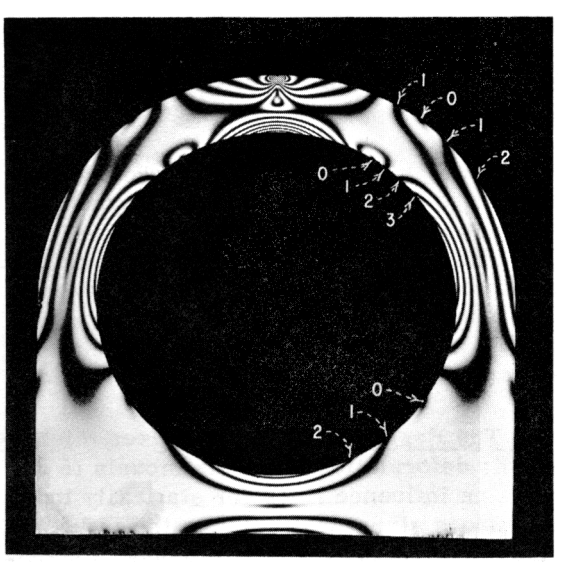

FIGURE 1 -- Typical photoelastic fringe pattern.

The photoelastic polariscope is particularly well suited to the analysis of massive two-dimensional structures, although methods do exist for its use in the analysis of three-dimensional problems.

Theory

General--In its simplest form, the photoelastic polariscope consists of a light source, a polarizing device called the polarizer, the photoelastic model, and a second polarizing device called the analyzer. Refinements of the basic system may be a ground glass or viewing screen, and other parts for convenience in viewing or photographing the stress pattern. When the model is stressed, the photoelastic stress pattern becomes visible on the ground glass or viewing screen of the photoelastic polariscope. Figure 1 is a typical photoelastic fringe pattern. It shows the fringes developed in an outlet conduit due to a concentrated load applied at the crown with the conduit uniformly supported along its base.

Nature of Light and Plane Polarization--For the purposes of this discussion, light may be considered to behave as a wave motion. These waves or vibrations are transverse to the rays of light. In general, they vibrate in all directions, perpendicular to the light ray, in a manner similar to the vibrations of a violin string.

A particular type of light, called plane-polarized light, is produced when the light vibrations are all oriented in one direction. This orientation can be accomplished in several ways, such as by reflection, refraction, Nicol prisms, or other crystals. The polarizing device in most common use is the commercial product, polaroid. The polaroid element is composed of long, needle-like crystals of an iodine salt with their axes all oriented in one direction. This mass of needle-like crystals behaves like a series of slits and permits only those light vibrations to pass which have the same orientation as the needles. All other light vibration components are absorbed or filtered by the polaroid. The emitted light is plane-polarized. In the simple polariscope, the light can be imagined as emerging from the first polaroid disk or polarizer and vibrating in a vertical direction, as shown at (A) in Figure 2. The second polaroid or analyzer is "crossed" with respect to the first. This means that it is oriented to pass light that is vibrating in a horizontal direction such as shown at (D) in Figure 2. When polaroid disks are "crossed" the first polaroid absorbs or filters all except the vertical components of the light ray, and the second polaroid absorbs or filters all except the horizontal components. All light is therefore absorbed, and the "crossed" polaroids, each of which is transparent, appear black when viewed together.

Double Refraction or Birefringency--When a ray of polarized light is passed through certain crystalline materials, the ray is divided into two components vibrating at right angles to each other. Materials such as mica, calcite, and tourmaline possess this property. Similarly, glass, celluloid, and certain plastics also possess this property of double refraction or birefringency while they are subjected to stress. Unstressed, no change occurs to a light ray in passing through these materials, but when subjected to stress the materials will cause the light ray to divide into two components at right angles to each other and lying in the principal stress planes.

Interference Fringes or Isochromatics--As discussed above, polarized light in passing through a stressed model will form wave components vibrating in the two principal stress planes at each point in the model. The two ray components will have different velocities in the two planes; therefore, while passing through the model, the wave front of one ray will pass the wave front of the other ray a small distance, δ. This distance, δ, is called the relative optical displacement of the two ray components. Now, if the two components are combined after leaving the stressed plate by passing them through a second polarizer so that they will vibrate again in the same plane, interference will take place due to the relative optical displacement, δ

Complete interference will occur when $\delta = 0, 1, 2, 3, \ldots, N$, wave lengths; thus furnishing a means of measuring the relative optical displacement. It has been shown theoretically [8] and verified experimentally [9] that the difference in magnitude of the two principal stresses, σ_1 and σ_2, at the line of passage of a ray is in direct proportion to the relative optical displacement, δ. When a field rather than a single ray of plane-polarized light is passed through a stressed model, bands will form connecting points in the model having the same relative optical displacement of the light rays or the same difference of principal stresses. These bands have been called isochromatic fringes.

The equation expressing the optical effect is

$$\sigma_1 - \sigma_2 = NC \quad . \quad . \quad . \quad . \quad . \quad . \quad . \quad . \quad . \quad (1)$$

where

σ_1, represents maximum principal stress,

σ_2, minimum principal stress,

N, order of interference or fringe order as counted on the isochromatic fringe pattern, and

C, a constant which is a function of the model material, its thickness, and the wave length of the light source.

When a stress-free model is viewed in the photoelastic polariscope, it will appear uniformly dark. As the model is stressed,

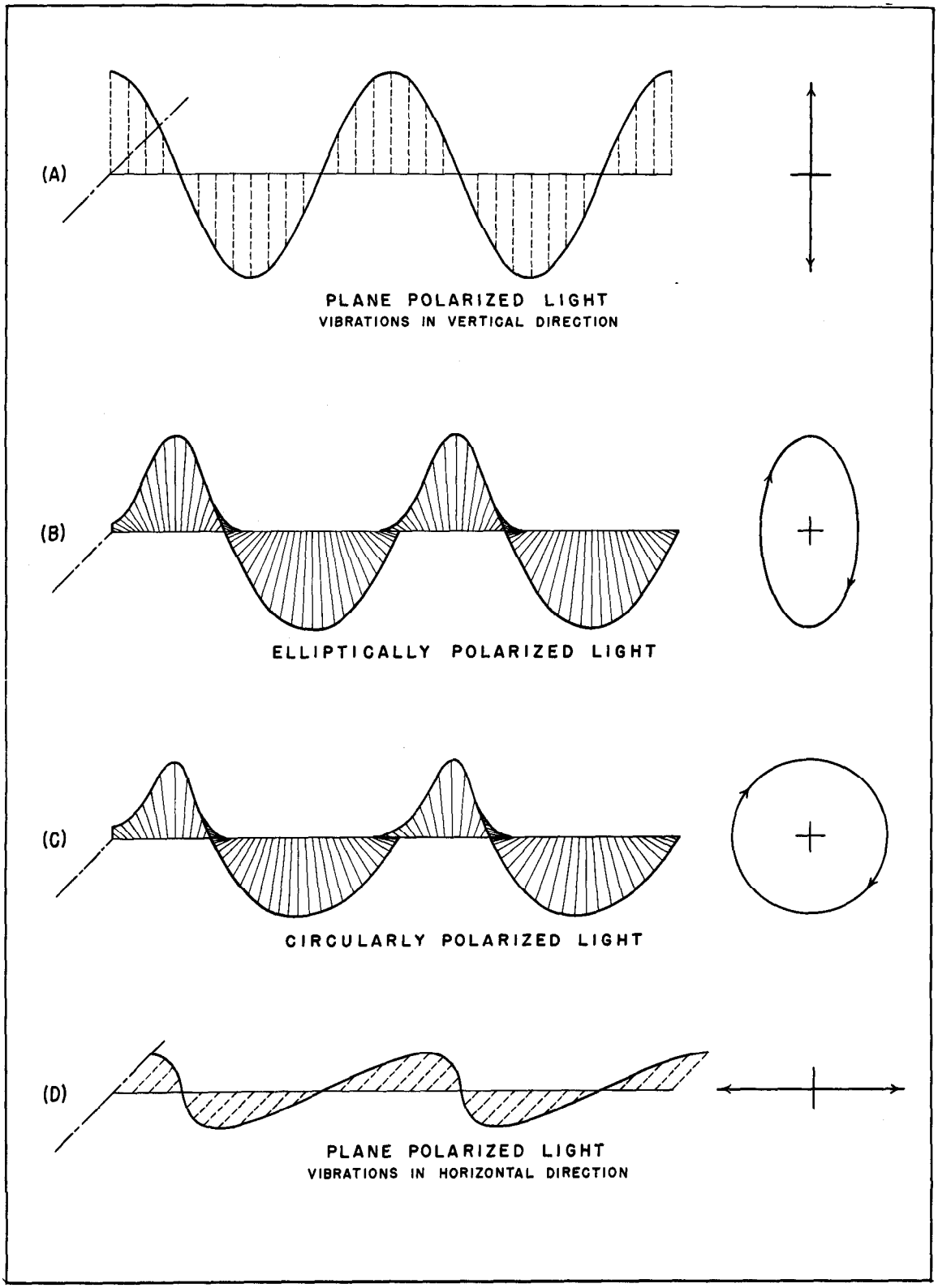

FIGURE 2 -- Representations of polarized light.

it will become light. The first dark band to appear, after the initial darkness, corresponds to the first complete cycle of interference and is referred to as fringe order number one. Fringe order number two exists at all points where there have been two complete cycles and so on through all the fringe orders.

Monochromatic Light--Each frequency of light makes a complete fringe cycle at a different stress increment. Therefore, it is important for sharp definition of fringes to limit the frequencies or wave lengths of the light emitted by the light source to a narrow band of the spectra. By using a well-designed filter in conjunction with a mercury vapor lamp, it is possible to isolate the green line of mercury, which has a wave length of 5461 Angström units.

Circular Polarization of Light--It is necessary that the planes of polarization of the beam passing through the model be at angles of 45 degrees with the principal stress directions for clarity of fringes. This results from the requirement that the light, in passing through the model, must be in mutually perpendicular plane-polarized components of equal amplitude. Since the light will pass through a stressed model only along planes parallel to the principal stress directions, 45 degrees is the only angle between the plane of the polarized incident beam and the principal stress directions that will divide the incident beam into equal components.

It is impossible to adjust the model so that its principal stress directions at all points are at 45 degrees with the plane of polarization of the light. In fact, there are places in the model where the principal stress planes and the polarization plane coincide. Under such conditions, the light passes through the model with no change of polarization of any sort.

The requirement that the plane of polarization be, at all points in the model, at 45 degrees to the principal stress directions is met by the introduction into the optical system of mica or other quarter-wave plates between the model and the polaroids. Mica is doubly-refractive or birefringent in a manner similar to the model material except that this is due to certain crystalline properties of the mica rather than to the application of stress as is the case of the model material. When the mica is set with its optical axis at 45 degrees with the plane of polarization of the light from the first polaroid, the light that emerges from the mica plate will, in general, be elliptically polarized. With the mica split to such a thickness that the relative displacement of one light component with respect to the other is one-quarter wave length of the light being used, the two components will have equal magnitudes. This is a special case of elliptically polarized light known as circularly polarized light. This is shown at (C) on Figure 2. Circularly polarized light has the desired property that, regardless of the direction of the principal stresses, an incident beam of such light always divides itself, when passing through the model, into two mutually perpendicular plane-polarized components of equal magnitudes. The second mica plate merely compensates for the insertion of the first mica plate and returns the light beam to a state of plane polarization.

Isoclinic Fringes--When plane-polarized rather than circularly polarized light is used in the photoelastic polariscope, i.e., no quarter-wave plates are in the optical path, two sets of fringes are developed in the model. Further, if white rather than monochromatic light is used, one set of fringes will be colored and the other set will be black. The colored fringes are the isochromatics previously discussed and they represent equal differences of principal stresses along any one fringe or contour of maximum shear. When monochromatic light is used, these fringes will, of course, be black.

The second set of fringes is called isoclinics. They are formed at those points where the light passes through the model with no change in polarization; in other words, the plane of the stress direction is the same as the plane of polarization. The isoclinic fringes, therefore, provide a method of determining the directions of the principal stresses throughout the model. However, since other instruments are available in the Bureau of Reclamation which permit a more rapid and accurate determination of the principal stress directions, the photoelastic polariscope is used only for the determination of boundary stresses and areas of stress

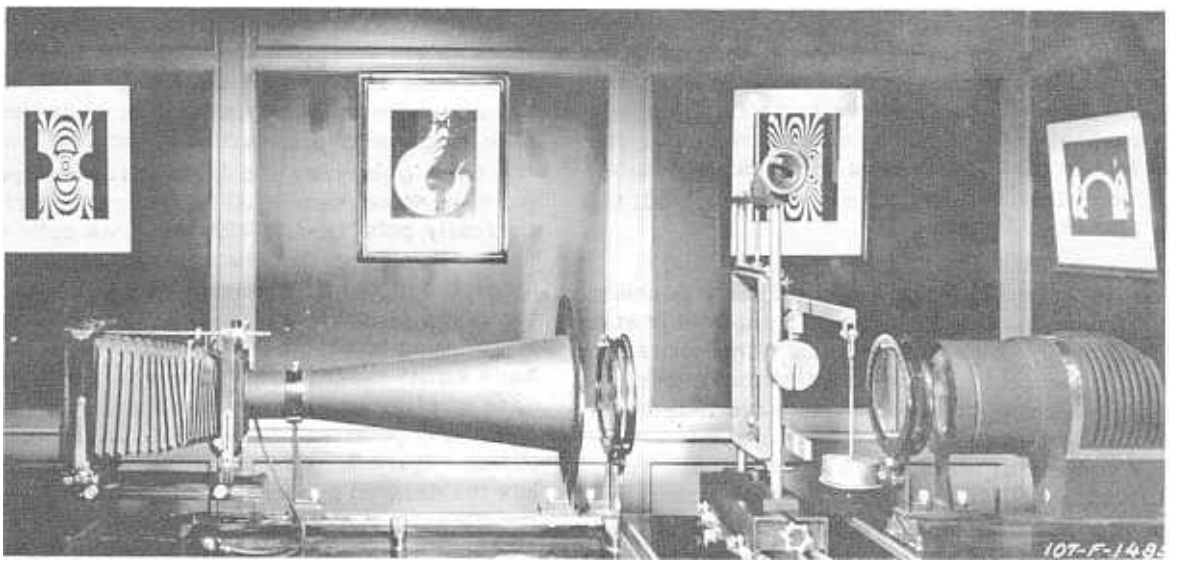

FIGURE 3 -- General view of photoelastic polariscope

concentration. Therefore, no further discussion will be made as to the theory and use of the isoclinic fringe pattern. For additional information on the isoclinic fringe pattern see any standard text on photoelasticity [10,11,12] The remainder of this section on the photoelastic polariscope will be concerned only with the interpretation and use of the isochromatic fringe pattern for determination of boundary stresses.

Construction and Installation

The photoelastic polariscope now in use by the Bureau of Reclamation is a commercial instrument with field 8-1/2 inches in diameter. A general view of the instrument is shown in Figure 3. A schematic diagram of the arrangement is given in Figure 4.

The light source consists of a 250-watt high-intensity mercury vapor bulb (Mazda AH5, 250 watts, air-cooled, Mogul base clear bulb), a diffusing heat absorbing filter, and a filter for isolation of the green line of mercury light (5461 Ångstrom units).

The optical system is composed of two parts; a 10-inch compound condensing lens unit which refracts the diverging light rays from the light source into parallel rays, and a compound projection lens unit which projects the parallel rays on to the ground glass or the film. Each element is enclosed to exclude interfering light. Within the limits required for practical considerations, the optical system is corrected for spherical and chromatic aberration, and is free of distortion and astigmatism.

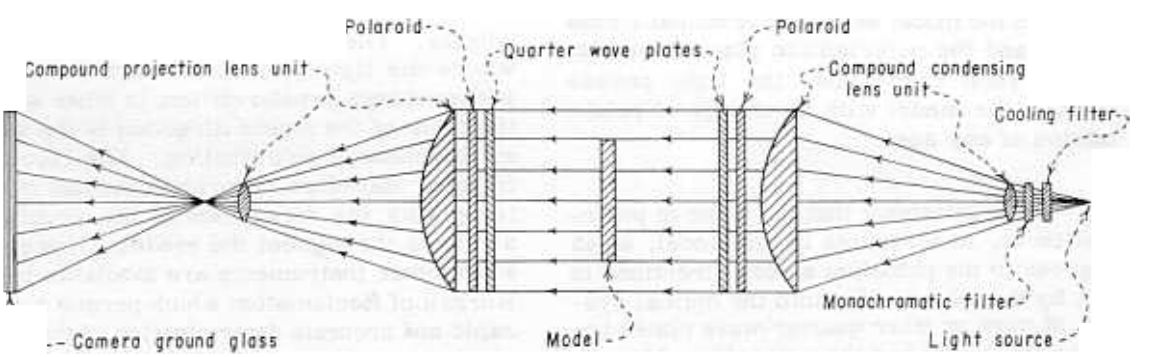

FIGURE 4 -- Optical path of photoelastic polariscope.

The polaroid disks and the quarter-wave plates are set in circular rotating mounts; each rotating independently of the other. Each mount is graduated in degrees from 0^{o} to 90^{o} to 0^{o}. This applies to both the polarizer assembly and the analyzer assembly. The quarter-wave plates can be swung in and out of the light path without affecting the polaroid disks. Each assembly is mounted on optical rails by a single rider support.

A camera, with no lens, follows the projection lens on the same optical rails. The camera is equipped with a shutter, an extendable bellows, and a ground glass for viewing the model. A small auxiliary aperture is provided at the shutter to give sharp definition when taking the photograph.

Adjustment

The component parts of the photoelastic polariscope are arranged as indicated in Figure 3 and Figure 4. With the parts mounted on supports of fixed height and on optical rails, the alignment of the polariscope is limited to adjustment of the light source to produce parallel rays of light between the polarizer and analyzer and adjustment of the final condensing or projection lens for proper focus.

The two units should be placed on their respective tables and leveled. By measurement, the focal lengths of the various lenses can be determined, and the light source and the lenses located in their approximate positions. The level should again be checked, and the two units securely fastened to the tables. Final adjustment for parallel rays and a uniform intensity of light over a circular field on the ground glass then can be made by minor adjustment of the light source and the projection lens.

The next step is the adjustment of the polaroid disks and the quarter-wave plates. The polarizer should be set first, preferably to pass vertically polarized light. This may be done by use of a Nicol prism equipped with level bubbles to indicate orientation of the plane of polarization. The analyzer should then be inserted and crossed with the polarizer so that the field, as viewed on the camera ground glass, is at maximum darkness. The first quarter-wave plate is then installed between the two polaroids next to the polarizer. Rotation of the quarter-wave plate will cause the field to vary from light to dark on the ground glass. The quarter-wave plate is rotated until extinction or maximum darkness is obtained on the ground glass. In this position, the axis of the quarter-wave plate is parallel to the axis of the polarizer, and the light passes through the quarter-wave plate without change. From this position, the quarter-wave plate should be rotated 45 degrees, in which position the light emerging from the quarter-wave plate will be circularly polarized, and the field will be at maximum brilliance. As a check, if the analyzer is rotated, there should be no change in the intensity of the light field on the ground-glass for any position of the analyzer. With the analyzer in its original position, the second quarter-wave plate should now be placed in the light path and rotated independently until the position of maximum darkness is observed on the ground glass of the camera. At this position, any rotation of this quarter-wave plate simultaneously with the analyzer should produce no change in the intensity of the field. Some very slight variation in intensity may be noted due to imperfection of the quarter-wave plates, but this is relatively unimportant in the determination of the isochromatic fringe pattern.

It has been found convenient to adjust all the indicators on the mounts to read 90 degrees when the polaroids and quarter-wave plates are properly oriented. This places all the indicators in a vertical position and facilitates checking the instrument for proper adjustment.

Calibration

In order to evaluate the model stresses, it is necessary to determine the constant C of equation (1). The method usually used is to construct a beam of rectangular cross-section from the model material and subject it to a uniform bending moment. The loaded beam, see Figure 5, is placed in the photoelastic polariscope and photographed. Figure 6 is an isochromatic photograph of such a beam. By counting from the zero fringe, the fringe order is determined at both the top and bottom boundaries of the beam, and the average recorded. The next step is to determine accurately the dimensions of the beam and the magnitude of the applied

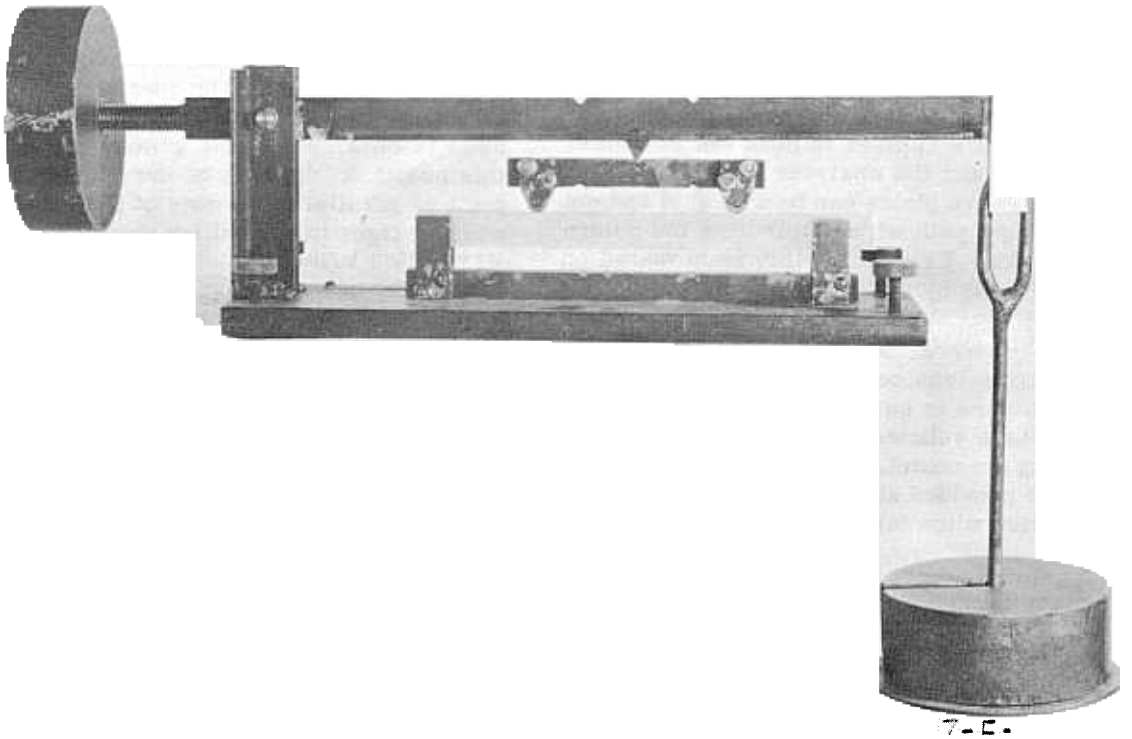

FIGURE 5 -- Loading device for photoelastic polariscope calibration.

load; then the extreme fiber stress is computed by the equation

$$s = \sigma_1 = \frac{Mc}{I} \qquad (2)$$

where

$s = \sigma_1$ represents extreme fiber stress,

M, bending moment,

I, moment of inertia, and

c, distance from the neutral axis of the beam to the extreme fiber.

From equation (1) with $\sigma_2 = 0$

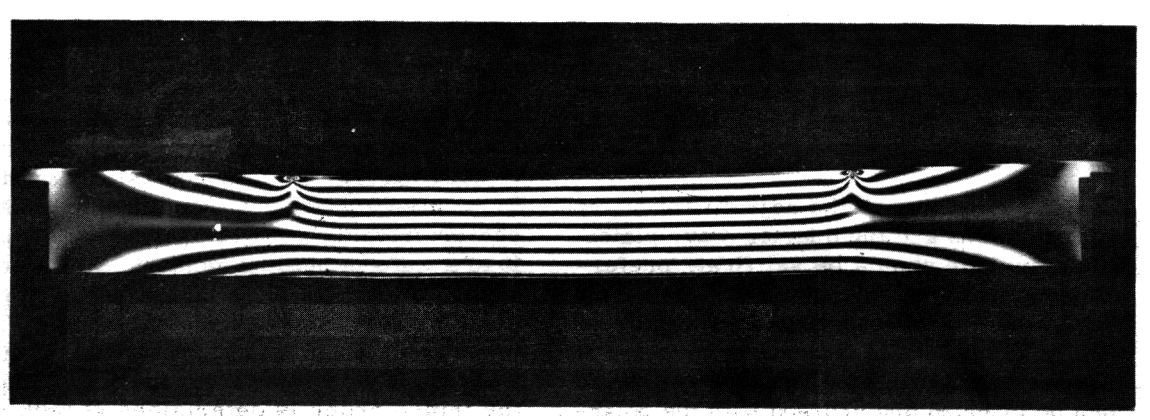

FIGURE 6 Isochromatic photograph of calibration beam.

$$\sigma_1 = NC \text{ or}$$

$$C = \frac{\sigma_1}{N}$$

but from equation (2) $\sigma_1 = \frac{Mc}{I}$

and so $$C = \frac{Mc}{IN} \quad . \quad . \quad . \quad (3)$$

Another method of calibration is to use a tensile specimen cut from the same plate as the model. A direct pull, P, is applied to the specimen and the fringe order determined at the center cross-section where the area is A, then

$$s = \sigma_1 = \frac{P}{A} \quad . \quad . \quad . \quad . \quad (4)$$

and in this case

$$C = \frac{P}{AN} \quad . \quad . \quad . \quad (5)$$

Operation

Since the photoelastic polariscope is used by the Bureau of Reclamation principally for the determination of boundary stresses, the only datum required is the isochromatic fringe pattern.

A model of the structure being analyzed is prepared, mounted in the loading frame, and placed in the photoelastic polariscope between the polarizer and the analyzer. The monochromatic filter is removed from in front of the light source. Then using the large aperture in the camera, the image is focused on the ground glass of the camera by adjusting the camera bellows. The pattern of the model on the ground glass should be uniformly dark over its entire area when the model is unloaded. As load is applied to the model, the fringe pattern will develop. This pattern will be colored, except for the zero fringe order, which will be black. When the entire load is on the model, the fringe pattern is observed, and the zero fringe order noted. If the observed stress pattern is complicated, it is advisable to place a piece of transparent paper on the ground glass and trace and label enough fringes to provide data for proper interpretation of the photograph of the fringe pattern. This operation is unnecessary if the location of the zero fringe order is obvious. The monochromatic filter is inserted into the light path, and the focus carefully checked. A smaller aperture is then inserted in the camera, and the photograph taken.

Exposure time for full-scale photographs is 15 seconds using Royal Panatomic film and an auxiliary aperture 1/4-inch in diameter. For maximum enlargement which will give an image approximately fifty percent larger than the model, the exposure time, using the same type film, is 60 seconds with an aperture of 1/4-inch diameter.

The boundary stresses and the maximum shear stress in the prototype can be determined from the photograph of the fringe pattern with proper use of the calibration factor for the fringe value of the model material and the ratio of the model to prototype loading.

Figure 7 is a photoelastic data sheet that has been printed to provide a convenient, uniform method of recording pertinent data regarding the loading mechanism, the loads applied, and the model dimensions. It is applicable to both the photoelastic polariscope and the photoelastic interferometer and provides space for computing and recording conversion factors and fringe values for prototype stresses.

Figure 8 presents the results of an actual photoelastic polariscope and photoelastic interferometer stress analysis. The results presented for the photoelastic polariscope are based on the isochromatic fringe pattern shown as Figure 1. The computations are recorded on the data sheet, Figure 7.

The model was prepared using Columbia Resin, CR-39, 0.375 inch thick. The base width was 6 inches and the opening was 4-1/2 inches in diameter. Prototype dimensions were based on an internal opening radius of r and the load was for a uniform foundation reaction intensity of v.

Various fringe orders have been numbered on the isochromatic photograph, Figure 1. It is obvious, from inspection of the model and its loading, where the boundaries are in tension and where they are in compression. By multiplying the fringe order,

PHOTOELASTIC DATA SHEET

Single Barrel Conduit with Circular Opening $t = r/3$ Concentrated Vertical Loading

Computer H.B.P.
Checker
Date May 8, 1962

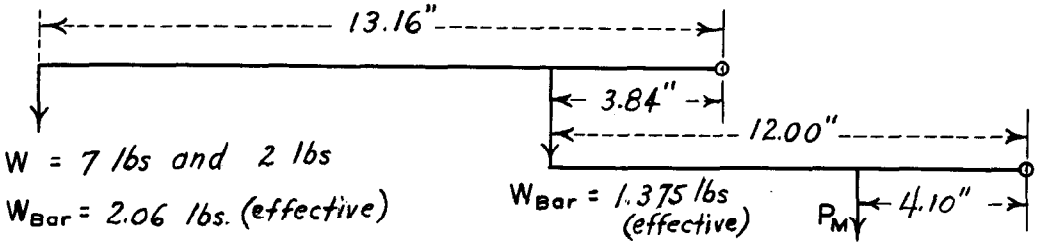

W = 7 lbs and 2 lbs
W_{Bar} = 2.06 lbs. (effective)
W_{Bar} = 1.375 lbs (effective)

Polariscope:

$$P_M = \left[9.06\left(\frac{13.16}{3.84}\right) + 1.375\right]\frac{12.00}{4.10} = 94.90 \text{ lbs}$$ ✓

Interferometer:

$$P_M = \left[4.06\left(\frac{13.16}{3.84}\right)\right]\frac{12.00}{4.10} = 40.72 \text{ lbs}$$ ✓

		Model	Prototype
Thickness (inches)		T_M = 0.375" ✓	T = r ✓
Any length (inches)		L_M = 6"	L = (8/3) r ✓
Load (pounds)	Polariscope	P_M = 94.90 lbs ✓	P = (8/3) vr^2 ✓
	Interferometer	P_M = 40.72 lbs ✓	P = (8/3) vr^2 ✓

Fringe value for thickness T_M, f.v = 254.5 lb/in³ ✓

$$K = \left(\frac{L_M}{L}\right)\left(\frac{T_M}{T}\right)\left(\frac{P}{P_M}\right) = \begin{cases} 0.0237 \text{ v in}^2/\text{lb (Polariscope)} \checkmark \\ 0.0553 \text{ v in}^2/\text{lb (Interferometer)} \end{cases}$$

Fringe value for prototype = (K)(f.v.) = 6.03 v ✓

v = intensity of load on prototype
r = internal radius of opening
Consistent units of v and r must be used.

FIGURE 7 -- Photoelastic data sheet.

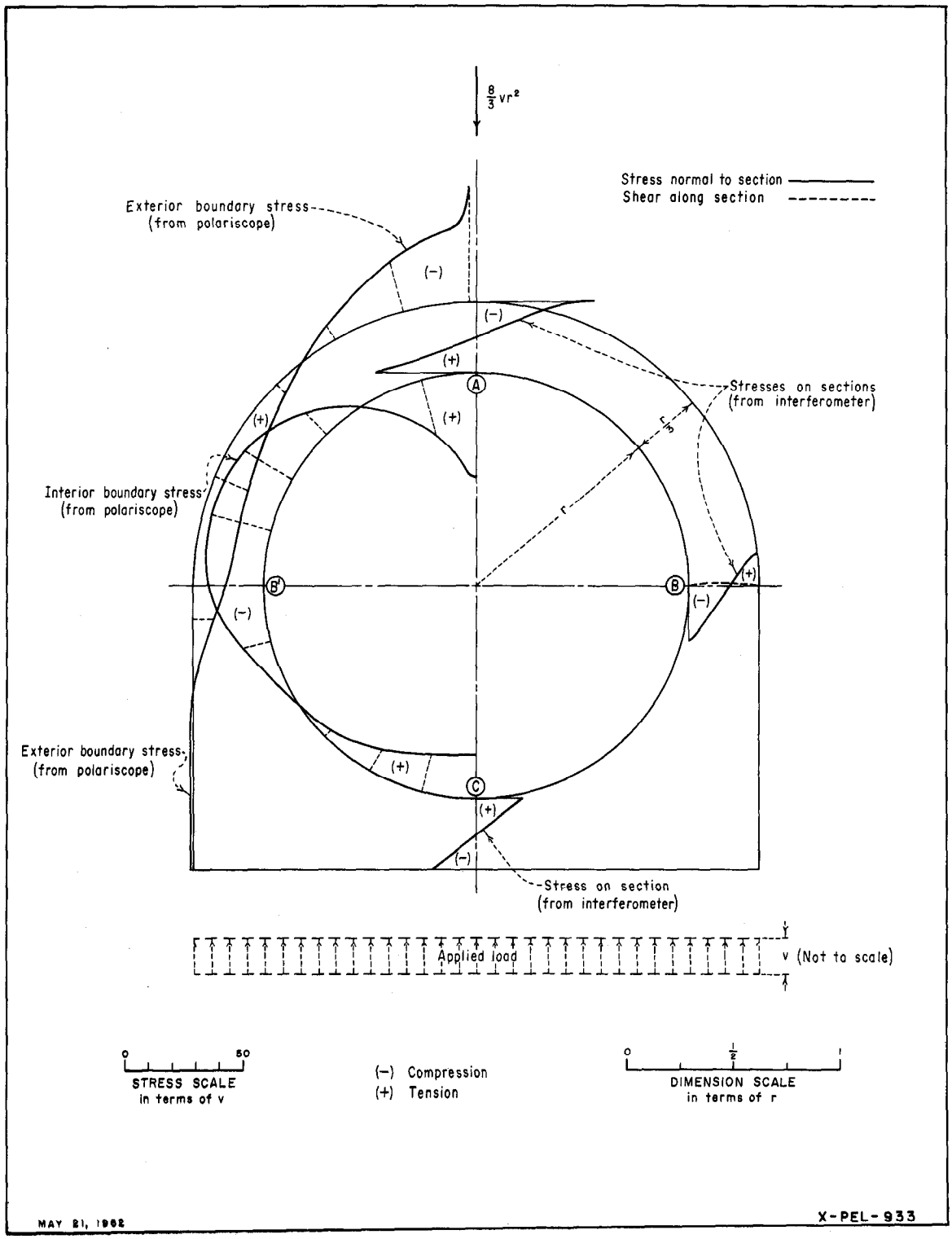

FIGURE 8 -- Stress analysis of single barrel conduit--photoelastic polariscope and photoelastic interferometer.

where it intersects a boundary, by the fringe value for prototype loading (6.03 v) given by the data sheet (Figure 7), the prototype stress at that point is obtained. These stresses are plotted normal to the boundaries at all points where isochromatic fringes intersect the boundaries. The curve drawn through these plotted values represents the boundary stress in the prototype. By observing the spacing of the fringes it is possible to estimate fractional fringe orders at critical points around the boundary, such as at the inside crown of the conduit.

The conduit and its loading are symmetrical about the vertical centerline. Therefore, the stresses for both the interior and the exterior boundaries have been plotted only for the half of the conduit to the left of the vertical centerline.

THREE-DIMENSIONAL PHOTOELASTICITY

General

The photoelastic polariscope and the photoelastic interferometer are ideally suited for the experimental solution of two-dimensional problems where analytical or other methods do not exist or would be too cumbersome or time-consuming to be applicable. In two-dimensional stress studies the models consist of plates with parallel faces, loaded at the edges so as to conform to the requirements of generalized plane stress conditions. Thus, any plane, parallel to the faces of the model, is a principal plane; and further, at all points on the path of any light ray normal to the face of the model, the directions of the principal axes are the same. Consequently, a ray of plane-polarized light entering the model at any point is divided into two rays oriented in the two principal stress directions. These two rays pass through the model unchanged except for the relative retardation between them resulting from the effect of the thickness of the model plate. This relative retardation provides the method of calculating the mean stress-difference in the thickness of the plate when proper loading has been applied to provide uniformity of load across the thickness of the plate.

In a great many problems, however, it is not sufficient to reduce or simplify them to a condition of plane stress. Therefore, some procedure must be devised to account for the three-dimensional effect. In the general case of three-dimensional stress, the conditions stated above for plane stress no longer exist. A ray of light, in passing through a stressed model, will pass successively through points at which the three principal axes of stress will have different inclinations, and the magnitudes of each principal stress will vary throughout the model. There will be a fringe pattern formed when polarized light is passed through a stressed three-dimensional model, but the relative retardation of the two light ray components which produce the fringes will be a function of the directions and the magnitudes of the principal stresses at the different points through the thickness of the model that the light ray traverses; and, generally speaking, the fringe pattern will give no indication of either magnitude or direction of the stresses or stress-differences at any particular point.

In order to find the stresses at a particular point or on a particular plane in a three-dimensional model, it is necessary to have some means of observing and measuring the changes produced by the light as it passes through that particular point or plane in the model. Two general methods have been used in adapting photoelasticity to three-dimensional studies. These methods are: The Freezing Method, and The Scattered Light Method.

The Freezing Method

Theory--When some photoelastic plastic materials* are heated to a certain critical temperature, loaded, and cooled slowly while still loaded, the fringe pattern developed in the plastic persists even when the load is removed after the material has cooled.

This phenomenon is explained rather fully in several of the references at the end

*See Section on Photoelastic Materials and Model Preparation for data on physical and optical properties of various photoelastic materials.

of this monograph, but a brief discussion will be included here for the sake of completeness.

Most photoelastic plastics can be classified as heat-hardening resins. As such, they have a strong primary molecular network which is the polymerized phase; and, within this primary network, a fusible phase. At ordinary room temperatures any applied load is carried almost entirely by the fusible phase. As the temperature is raised, however, the fusible phase becomes less viscous; and, when a certain critical temperature is reached, the applied load is carried entirely by the primary network. Thus, when the resin is heated, loaded, and cooled while still loaded, the fusible phase again becomes effective and holds or "freezes" the stresses in the primary network.

The internal forces involved are of molecular dimensions. Therefore, it is possible to cut the model material without disturbing the frozen stress pattern if care is taken that no heat stresses are induced by the cutting process. From this it follows that a three-dimensional model of a structure can be built, heated, loaded, and cooled under load, and the stress condition in the model will be truly three-dimensional. Then, by carefully slicing the model, the stress condition at specified points or on specified planes can be evaluated.

Evaluation of the stresses in a three-dimensional model is somewhat more complicated than in the two-dimensional case. The following conditions must hold for each parallel slice cut from the model.

1. The directions of the principal stresses in the plane of the slice must, at any point in the slice, be approximately constant throughout the thickness of the slice.

2. The magnitude of the stress-difference must be approximately constant throughout the thickness of the slice.

In order to obtain useful information directly from a slice cut from the model, the slice must be cut perpendicular to one of the principal stress axes. Therefore, the direction of one principal stress at the point or plane being investigated must be known. From the loading conditions and the construction of the model, there are two regions where this is known directly. They are: (1) An unloaded boundary, and (2) a plane of symmetry of the model and loading.

At all points on a surface on which no stress acts, one principal axis is normal to the surface. For the frozen model this is true at all points on a surface at which no external load is applied. It is not true for the surfaces of a cut made after freezing, since the internal frozen stresses extend throughout the model. At a plane, unloaded boundary a thin slice is at all points a principal plane and is a close approximation to the requirements for a condition of generalized plane stress. As such it can be treated exactly as a two-dimensional stress case for both the isochromatic and isoclinic fringe patterns; i.e., the difference between the principal stresses in the plane of the slice and the directions of the stresses will be known at all points in the slice.

A principal stress plane exists in a model when the loads applied to the model and the geometric shape of the model are symmetrical about that plane. If a thin slice be cut so that such a principal stress plane is at the mid-plane of the slice, then a two-dimensional stress condition will exist in such a slice. Again, however, this is true only if the conditions previously imposed are met; that the magnitude of the stress-difference and the directions of the stresses are approximately constant through the thickness of the slice.

It is possible to obtain the three principal stress-differences and in some cases the principal stresses themselves by means of additional measurements. However, the theory and procedures are complex, and it is beyond the scope of this discussion to consider them. Should a problem arise in which boundary stresses or stresses in planes of symmetry give insufficient information, then reference should be made to some of the publications listed in the bibliography.

Procedure--Since each study made will present different problems, only a general procedure can be outlined here.

The materials best suited to three-dimensional models are: (1) Fosterite; (2)

Kriston; and (3) Catalin 61-893. Physical and optical properties of these materials are discussed in the section on "Photoelastic Materials and Model Preparation." Each has advantages and disadvantages, and the selection of a material for any particular study should be governed by the conditions of the problem.

Columbia Resin, CR-39, the photoelastic material used for two-dimensional work, is not particularly suitable for three-dimensional work. This material exhibits considerable creep at the temperatures required for stress freezing and the frozen stresses change appreciably with time.

The fabrication of a three-dimensional model will, in general, follow the same procedure as for a two-dimensional model. An exception to this may be where the deformations induced by the loading are so great as to distort the final shape of the model. In such cases it may be necessary to construct the model so that the final shape, after heating, loading, and cooling, will be a close approximation of the desired shape. This is necessary, since the frozen stress pattern in the model is for the final shape and not the initial shape of the model.

The loading of a three-dimensional model will usually be somewhat more complicated than that required for a two-dimensional model. However, since only constant loading is required with no provision necessary for removal of the load until completion of the freezing cycle, it does not present some of the difficulties encountered in loading models for photoelastic interferometer studies. A large electric oven, thermostatically controlled, is used for heating the model. With the shelves removed, it is possible to place an entire loading frame in the oven. Therefore, if the model is such as will permit it, the loading mechanism can be built on the standard loading frame. For special cases, it may be necessary to construct individual frames and loading mechanisms for each case depending on the nature of the problem.

The procedure currently being used for freezing the stress pattern is to place the unloaded model in the oven and bring the temperature up to the recommended value for the plastic material being used. This temperature should be maintained for a sufficient length of time to insure that the entire model is at a uniform temperature. The time required is a function of the mass of model and of the model material. The load is then applied to the model, and the temperature continued at the recommended maximum value for a length of time sufficient to insure that the entire load is effective. The temperature is then gradually reduced and the load remains on the model until room temperature is reached.

Table I lists the recommended values to be used in the heating and cooling cycle for three plastics being used for three-dimensional analysis.

After the model has cooled to room temperature, it is unloaded and removed from the oven. Slices are then made at previously selected sections in accordance with the information desired and obtainable. Depending on the shape and size of the model, the slices can be cut on a band saw, scroll saw, or milling machine. The thickness of the slice may be governed somewhat by the configuration of the model. However, the thickness of slices should be kept to 1/4 inch or less. The minimum thickness will depend upon the machinability of the plastic and the number of fringes in the slice. Care must be taken while slicing the model that no heat is generated by the cutting as this will distort the

Table I

Plastic	Rate of heating degrees C/hr	Load temperature degrees C	Time for uniform temperature hr	Time for load uniform temperature hr	Rate of cooling degrees C/hr
Catalin 61-893	20	110	1 to 2	1	15
Fosterite	5	70	1 to 2	2	2
Kriston	30	134	1 to 2	1	30

frozen stress pattern.

In most cases the slice will not be sufficiently transparent after the machining operation to give a clear fringe pattern. Consequently, it is necessary to either immerse the slice in a fluid having the same refractive index as the model material or else coat the surfaces of the slice with such a fluid. Polishing will ordinarily not be feasible or satisfactory due to the time required and the tendency of the polishing process to round the edges of the slice, thus reducing the clarity at the boundaries. The usual procedure will be immersion of the slices. Suitable immersion fluids are:

Catalin 61-893	Halowax Oil No. RD 11-1
Fosterite	Halowax Oil No. 1000
Kriston	Halowax Oil No. RD 11-1

Further discussion on immersion fluids will be found in the section on "Photoelastic Materials and Model Preparation."

An alternative method to slicing the model into thin plates, consists of gradually reducing the model in thickness. The difference of fringe order between successive fringe patterns at a particular point will be the fringe order in a plate of thickness equal to that of the material removed.

Theoretically, the difference method should give more accurate results than slicing into thin plates, since it can be thought of as a slice or plate made with a cutter of zero thickness. Also, higher fringe orders may be obtained in the model with less stress. However, in actual practice, edge effects and shadows are so pronounced in the difference method that the boundary stresses are difficult to determine. Since this condition does not exist with the slices or plates, it is fairly easy, in such cases, to obtain sharp boundaries and clear stress patterns.

Interpretation of the fringe patterns obtained in the photoelastic polariscope will be dependent on the location in the model of the slice being studied. For the studies made to date, the slices have been taken on planes of symmetry or parallel to unloaded boundaries, and, therefore, the stresses have been relatively easy to evaluate. It is beyond the scope of this paper to outline the procedure necessary to evaluate the stresses on other planes. If, in the future, more complex models are studied, recourse should be had to some of the cited references for a method of evaluating stresses in such cases.

The Scattered Light Method

Theory--It is a known physical phenomenon that a light beam is scattered in all directions transverse to its path when passing through any material medium. If the light source is unpolarized, then the scattering will be of equal intensity in all directions transverse to the beam, and the scattered light will be plane-polarized. If, however, the material is birefringent or doubly refractive and the light beam is plane-polarized, it will be resolved into two components at 90^{o} to each other moving at different velocities through the material. The apparent amplitude of these components will depend upon the point of observation in the plane normal to the direction of the light beam.

Since the two components do travel at different velocities, they will alternately strengthen and weaken each other along their scattered light beams. For the condition where the two components have equal amplitudes there will be cancellation of all light when the two components are completely out of phase and a doubling of intensity when they are in phase. Thus, when the scattered light is observed in or normal to the plane of polarization, alternate light and dark fringes will be visible.

If the birefringence of the material being considered is due to a condition of stress, then the relationship between principal indices of refraction and principal stresses may be written as follows:

$$\begin{aligned} K(n_o - n_1) &= S_1 \\ K(n_o - n_2) &= S_2 \\ K(n_o - n_3) &= S_3 \end{aligned} \quad \ldots\ldots\ldots \quad (6)$$

where

K represents a constant characteristic of the material,

n_o, index of refraction of unstressed material,

n, index of refraction,

S, principal stress, and

subscripts 1, 2, and 3 directions at right angles to each other in space.

For the condition $S_1 < S_2 < S_3$, the maximum shear, τ_{max}, is:

$$\tau_{max} = \frac{K}{2}(n_1 - n_3). \quad . \quad . \quad . \quad . \quad . \quad . \quad . \quad . \quad (7)$$

Thus, the maximum shear can be found at any point in the stressed model by a measurement of the indices of refraction and evaluation of the constant K. In actual practice, however, the differences between the indices of refraction are so small that it is difficult to obtain even approximate results by the use of equation (7). However, the relationship between the indices of refraction can be used to evaluate the difference between principal stresses.

Let the polarized light beam pass through the model in the direction of S_2 with the plane of polarization at 45° to S_1 and S_3. The relative velocities of the two light components are a function of the ratio of n_1 to n_3 and retardation will take place at the rate:

$$dR = (n_1 - n_3)\, ds \quad . \quad . \quad . \quad . \quad . \quad . \quad . \quad . \quad (8)$$

or, if the relative retardation is expressed in terms of wave length, with

$$R = N\lambda \quad . \quad . \quad . \quad . \quad . \quad . \quad . \quad . \quad . \quad . \quad . \quad . \quad (9)$$

then

$$\frac{dN}{ds} = \frac{1}{\lambda}(n_1 - n_3) = \frac{1}{K\lambda}(S_3 - S_1) = \frac{1}{C}(S_3 - S_1) \quad . \quad (10)$$

where

R represents relative retardation,

λ, wave length, in air, of the light source,

N, amount of relative retardation in wave lengths,

ds, fringe spacing,

C, stress-optical coefficient of material,

other symbols as defined previously.

If the stresses remain approximately constant over a small increment of the light path, then equation (10) may be written

$$S_3 - S_1 = C\frac{\Delta N}{\Delta s} \quad . \quad . \quad . \quad . \quad . \quad . \quad . \quad . \quad (11)$$

And, if the increment is such that $\Delta N = 1$, then Δs determines the value of $S_3 - S_1$. If Δs is replaced by d then equation (11) becomes

$$S_3 - S_1 = \frac{C}{d} \quad . \quad . \quad . \quad . \quad . \quad . \quad . \quad . \quad . \quad . \quad (12)$$

Where d also represents fringe spacing.

It was stated previously that the polarized light should be passed through the model along the direction of S_2. If this direction is unknown it can be found by passing the light in various directions until dN/ds is a maximum; i.e., where the fringes are the most closely spaced. With the light passing along the direction of S_2, fringes will be seen with maximum visibility at 45° to S_1 and S_3. Directions S_1 and S_3 can be determined from the positions where minimum fringe intensities occur.

The principal stresses at a free boundary may be individually measured, since the stress perpendicular to a free boundary vanishes, and the other two stresses lie in the plane tangent to the boundary. If the direction of the light is made parallel to this tangent plane, and the model rotated until the maximum and minimum fringe spacings occur, these spacings will give the separate principal stress values.

Apparatus--A special polariscope has been constructed for use in the analyses by the scattered light method, because the direction of observation is at right angles to the direction of passage of the light and observations must be made at different positions around the model. A photograph of the apparatus is shown in Figure 9.

The light source is a high-intensity, water-cooled, mercury-vapor lamp designated as a 1000 watt, AH-6 lamp by the manufacturer. The water jacket of the lamp

FIGURE 9 -- Apparatus for scattered light method of analysis.

has been silver-plated except for a 1/4-inch aperture for the light source. Monochromatic light is secured by placing a filter in front of the lamp. The two lenses in the system are so arranged as to provide a parallel field of light emerging from the second lens. The polarizer follows the lens system, and provision is made for a quarter-wave plate, which can be inserted or removed, as desired. A slit of adjustable width is the final component in the cabinet. An immersion tank to contain the fluid, model, and loading device is placed on top of the cabinet.

The immersion tank was built from stress-free plate glass. An attempt was made to purchase fused glass tanks of a suitable size to hold model and loading frame, but the cost of a stress-free tank was prohibitive. Therefore, sheets of stress-free plate glass were used, and the corners joined using brass channels with aquarium cement as a sealer. This method is not entirely satisfactory, because over a long period of time the immersion fluid reacts with the aquarium cement. Further work is contemplated on preparing a more suitable immersion tank.

The polarizer, the quarter-wave plate, and the immersion tank are all mounted in rotatable, graduated rings so that it is possible to adjust the model and the plane of polarization as required.

Procedure--The general procedure should be readily apparent from the previous discussions concerning the theory and the apparatus for the scattered light method.

Suitable model materials for use in the scattered light method are Catalin 61-893 and Kriston (see section on Photoelastic Materials and Model Preparation). Columbia Resin, CR-39, has the same limitations for

use in the scattered light method as cited in the freezing method and Fosterite is optically insensitive at ordinary room temperatures. The size of the model to be analyzed is governed by the size of the immersion tank and the required loading frame.

Fabrication of the model, in general, follows the methods used for two-dimensional models and models for the freezing method. A detailed discussion of model preparation is included in section on Photoelastic Materials and Model Preparation. Usually the model will have faces which are not polished and which are not normal to the line of observation and/or light beam. As a result, it must be immersed in a fluid to improve light transmission through the unpolished faces and to eliminate reflections and refraction.

With the model loaded and immersed, the light is passed through it in the desired planes, and the fringes observed and photographed. Directions of principal stresses can be determined as outlined previously. The thickness of the sheet of light can be varied by means of the adjustable slit until the proper plane is illuminated and the intensity is sufficient to provide a good fringe pattern.

It is impossible to outline a precise procedure for photographing the pattern. The exposure time will be a function of the intensity of the fringe pattern, and this is dependent upon the initial light intensity, the thickness of the light sheet, the shape of the model, and other variables. Experience will provide a guide as to proper exposure time.

As shown in the development of the theory, the stresses are a function of the fringe spacing. Therefore, the measurement of the fringe spacing is critical. No precise apparatus is available, at present, for this purpose. Measurements have been made with a precise scale and magnifier. Other experimenters have used a micrometer comparator or made a microphotometric trace of the variation in the density of the negative.

Summary

Each method of three-dimensional stress analysis possesses certain advantages and disadvantages. Some of the factors influencing the method to be used are:

1. Distortion of model. Deformations at the temperatures required for freezing the stress patterns in the freezing method are about 25 times as great for bakelite and 12 times as great for Fosterite as at ordinary room temperatures. This can result in excessive change from the original model shape unless care is exercised.

2. Apparatus. The freezing method utilizes the same polariscope as the usual two-dimensional studies, whereas the scattered light method requires an entirely new type of apparatus.

3. Interpretation of stresses. Stress patterns in the slices cut from models using the freezing method have the same general meaning as the familiar two-dimensional stress patterns. With the scattered light method the pattern has an entirely different meaning and requires additional apparatus to evaluate.

4. Models. In the freezing method the model is destroyed by slicing at the planes of interest, while in the scattered light method the model can be annealed and used again for the same or a different loading. In the freezing method the model may be observed in any direction without interference from a loading frame, and the immersion tank required need be only large enough to accommodate the slices being studied.

5. Area of analysis. In the scattered light method the sheet of light can usually be made thinner than it is possible to machine a slice for the freezing method. Also, there is always the possibility, when cutting the slice, of disturbing the frozen stress pattern by the machining operation. However, in the scattered light method the intensity of light is low, especially in thick sections and in regions distant from the point of entry of the light.

Three-dimensional stress analysis is still a very new experimental tool. Much work must be done on both materials and

techniques before it becomes a common procedure for the photoelastic laboratory. On the basis of the small amount of work that has been done to date, three-dimensional photoelasticity appears to hold much promise of providing methods which will permit solutions of problems which previously have been unsolvable.

THE PHOTOELASTIC INTERFEROMETER

General

The photoelastic polariscope permits the determination of the maximum shear at any point or series of points in a model, the directions of the principal stresses at all points, and the extreme fiber stress. However, this is not sufficient information for many design problems. It often becomes necessary to know both the magnitude of each principal stress and its direction throughout the entire structure before a suitable design can be effected.

Although several methods are available, the problem of finding the individual principal stresses and their directions at interior points in a structure is not as simple as finding boundary stresses. To obtain the principal stresses σ_1, σ_2, and their direction θ separately, most procedures involve a combination of the three sets of values of $\sigma_1 - \sigma_2$, $\sigma_1 + \sigma_2$, and θ. The difference between principal stresses and the directions of such stresses can be obtained with the photoelastic polariscope. However, the sum of the principal stresses must be obtained by other means. One method is to employ one of the several forms of graphical integration [24, 25]. Another method is to make use of some auxiliary experiment by which the sum of the principal stresses is measured at all points. Examples of the equipment for this type of experiment are the lateral extensometer, membrane analogy, and electrical analogy tray. The latter two, as well as the graphical method, have been used by the Bureau of Reclamation with only moderately good results. Each method has its own limitations and sources of error, such as the fact that the use of the membrane and electrical analogs presupposes a knowledge of the sum of the principal stresses at all points on the boundary and also that it is possible to construct a boundary which will represent the sum of the principal stresses. It is evident, then, that if there is a concentrated load at any point on the boundary, the analogy breaks down. The delicate manipulation and close control of room temperature necessary in using the lateral extensometer precludes the use of this instrument unless adequate physical facilities are available.

The method used by the Bureau of Reclamation for determining the individual principal stresses and their directions at any point in a structure is based on the use of the photoelastic interferometer. This instrument determines each principal stress and its direction separately without need of information from other methods of analysis.

A method of measuring the absolute retardation of a beam of light passing through a transparent model when subjected to a change in stress was brought to the attention of the scientific world by Henry Favre [26] in 1929. The principal optical instrument used by Favre for measuring this retardation, from which he was able to obtain the individual principal stresses, was a precise interferometer of the Mach-Zehnder or Jamin type.

An instrument patterned after the one built by Favre was designed by engineers of the Bureau of Reclamation and constructed in the shops of the Bureau. This instrument has been called a photoelastic interferometer and has been in continuous use since 1936. Figure 10 is a photograph showing a general view of the instrument. This instrument should not be confused with lateral extensometers [27,28] employing the interferometer principle in their operation.

Theory

General--In presenting the theory of the photoelastic interferometer it is assumed that terms and concepts such as plane-polarized light, monochromatic light, and rotation of plane of polarization by means of half-wave plates are well understood [29]. However, a brief explanation of the phenomenon of interference is given.

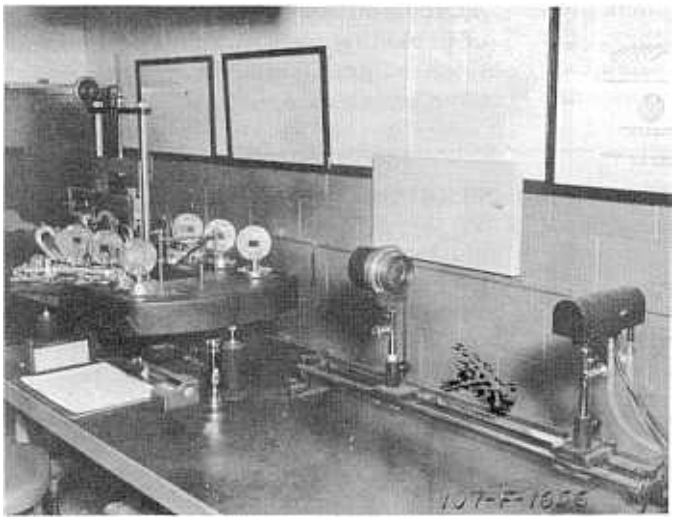

FIGURE 10 -- General view of photoelastic interferometer.

Description--Figure 11 is a photograph showing the details of the photoelastic interferometer. Figure 12 is a diagrammatic sketch showing its optical paths. This sketch will be referred to frequently in the following discussion.

The principal optical parts are the two optical flats L_3 and L_4 and the four optical parallels L_1, L_2, L_5, and L_6: L_3 and L_4

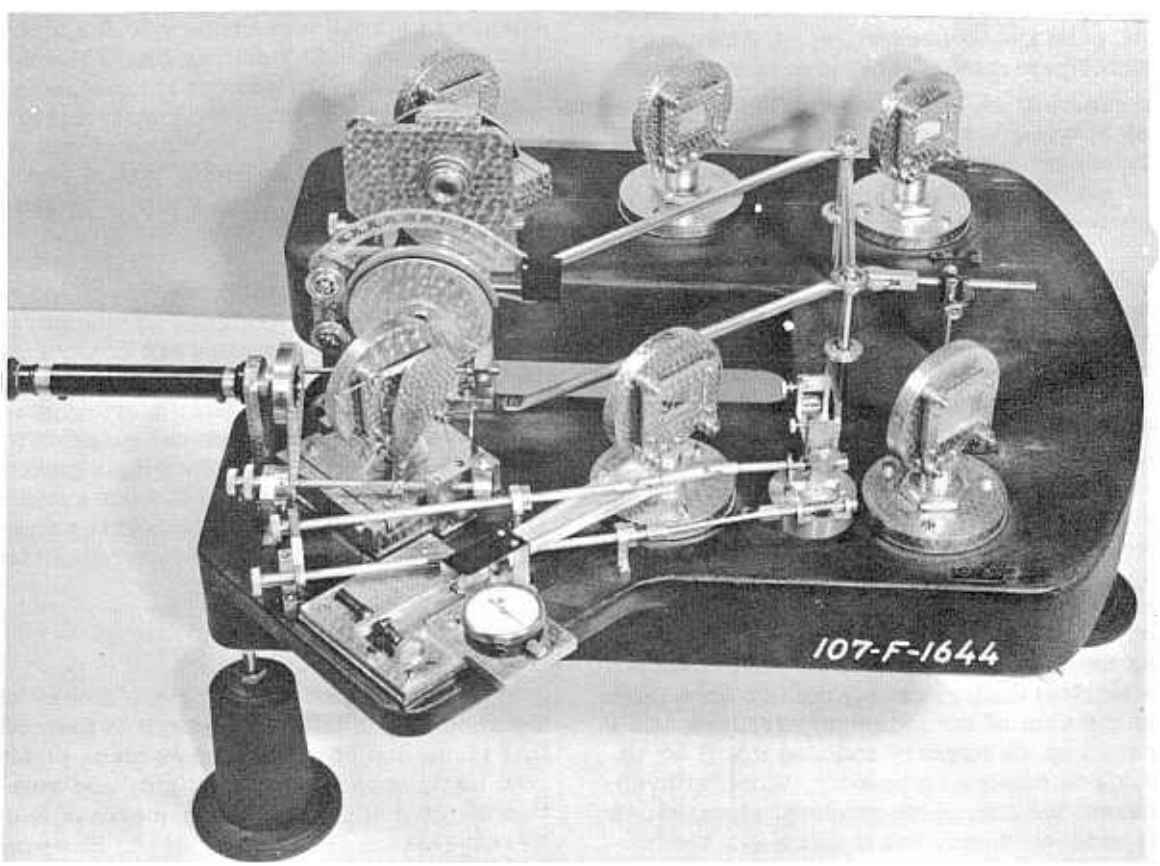

FIGURE 11 -- Detailed view of photoelastic interferometer.

are given a full first-surface aluminum plating. L_2 and L_5 are clear glass with no plating. L_1 and L_6 are given a thin plating of aluminum on one face. The plating is such that light is both transmitted and reflected in equal intensities when the angle of incidence is 45 degrees. The light beam that starts at the point source, S , is, therefore, split into a double path at L_1 and is brought together again at L_6. That part of the light which goes around the model is referred to as the outside path, while the part which goes through the model is referred to as the inside path. The interference phenomenon is developed at L_6, where the two paths converge, and is visible as a series of alternate light and dark bands or interference fringes. The fringes are visible in the telescope and are entirely different from the isochromatic fringes associated with the photoelastic polariscope. Also, the interference fringes are visible both before and after loading the model. The interference fringes are merely shifted by a change of stress within the model, and the change of stress is linearly related to the number of interference fringes that cross a fixed point in the field of the telescope.

Interference Phenomenon--In order that the phenomenon may be better understood, temporarily lay aside the common concept regarding a beam of light as a sine curve and instead visualize it, as shown at (A) in Figure 13, as resembling a corrugated sheet; in other words, a sine curve with the additional dimension of depth. Looking downward on this corrugated sheet, the valleys are represented as dashed lines and the ridges as solid lines. This convention is shown at (B) in Figure 13. At (C) in Figure 13 is shown the condition at L_6 where the inside and outside paths converge. It is physically impossible to adjust the position of the optical parallel, L_5, in such a manner that the direction

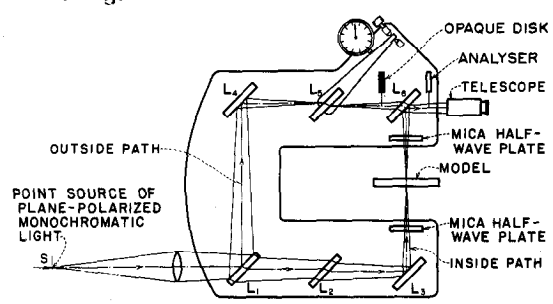

FIGURE 12 -- Optical paths of the photoelastic interferometer.

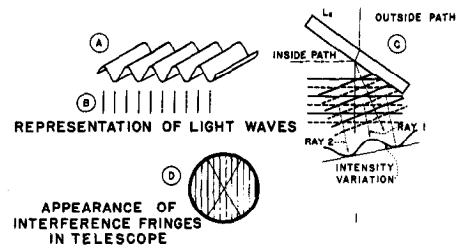

FIGURE 13 -- Representation of light waves and the development of interference fringes.

of propagation of the inside path upon reflection coincides exactly with the direction of the transmitted or outside path. The divergence of the two paths is shown in an extremely exaggerated condition but permits a visualization of the interference phenomenon. With the eye looking in the direction of the two emerging beams (see Figure 13(C)), it is evident that, along ray 1, the valleys for one system coincide with the valleys for the other system. Similarly, the ridges of the two systems coincide along this ray. Therefore, along ray 1, the illumination is built up from both sources. For ray 2, the valley points are nullified by the ridge points and illumination will be extinguished along this ray. For sections between ray 1 and ray 2, the intensity will vary from bright to dark. This variation in illumination is visible in the telescope as a series of light and dark bands called interference fringes. Their general appearance in the telescope is shown at (D) of Figure 13. The two heavy diagonal lines are the fixed cross-hairs in the telescope. It can be seen from an examination of (C) in Figure 13 that if, for any reason, either the inside path or the outside path undergoes a change in effective length relative to the other path, there will be an accompanying displacement of interference fringes across the field of view in the telescope. Furthermore, this change in length will be equal to the product of the number of fringes that pass the cross-hair intersection times the wave length of the light source. The wave length of the light source now being used is 5461 Ångström units (the green line of the mercury spectrum), or 0.000,021,5 inch. Since it is possible to estimate fractional fringe displacements as small as one-tenth fringe, it follows that the instrument is capable of detecting optical length changes with a precision of about a two-millionths of an inch. Be-

cause of this extreme sensitivity, the photoelastic interferometer is ideally suited to the problem of measuring changes in refractive indices of transparent models undergoing a change in stress; and, since each principal stress is a linear function of the change in refractive index in the two principal stress directions, the photoelastic interferometer may be used to measure individual principal stresses.

Requirements--Before the photoelastic interferometer can be applied directly to the problem of stress measurements, several essential requirements must be fulfilled. First of all, since the state of stress in general varies from point to point within the model, it is necessary that the beam of light that traverses the model come to a focus within the model. This is approximated by starting with as small a point source of light as possible and choosing the focal length and location of the lens in the optical path in such a manner that a real image of the point source falls within the model as shown in Figure 12. For most problems, it will be sufficient if the width of the beam within the model is less than one millimeter. The optical measurements can, at best, give the average state of stress over the small area of the model through which the light beam passes.

Another essential feature is that the beam of light that penetrates the model must be plane-polarized and vibrating in a principal stress direction. Since there are two principal stress directions at every point and the directions vary from point to point, there must be some convenient provision made to rotate the plane of polarization into the principal stress directions. In addition, there must be a means of quickly determining when the plane of polarization coincides with a principal stress direction. These conditions are fulfilled by making use of two small polarizing disks ("Polaroids") and two mica half-wave plates. The first polarizing disk is mounted in a fixed position on the optical rail immediately in front of the light source. It is oriented in such a position that the transmitted light is polarized in a vertical plane. Thus, the light will be vertically polarized in the remainder of the optical system with the exception of the small interval between the two mica half-wave plates. Figures 11 and 12 show the location of the half-wave plates and their mountings. The two mica plates are split to be half-wave plates for the green line of mercury and are linked mechanically to rotate in unison. The two plates are cut from the same sheet of mica, but the second plate is set in reverse position with respect to the first plate. When the first plate causes a rotation of the plane of polarization into some position other than vertical, the second plate produces the reverse effect. This insures that the light emerging from the second plate is always polarized in a vertical plane, regardless of the plane of polarization of the light in the interval between the half-wave plates. This fulfills the requirement of rotating the plane of polarization of the light beam that penetrates the model.

Orienting Light Beam in Principal Stress Direction--In order to determine when the plane of polarization of the light beam that penetrates the model coincides with a principal stress direction, an auxiliary polarizing disk called the analyzer, which is oriented to pass only horizontally polarized light, is placed in front of the telescope at the same time that the light beam in the outside path is cut off. Since the analyzer passes only horizontally polarized light and only vertically polarized light emerges from the second half-wave plate, the light field in the telescope will be extinguished. If a stressed, doubly-refractive model is now placed between the mica plates, the light that emerges from the model will not, in general, be plane-polarized. The emerging light vector may, however, be resolved into two components, one coplanar with the incident beam and one perpendicular to it. The second half-wave plate will rotate the coplanar component into a vertical plane, and the perpendicular component into a horizontal plane which will pass unchanged through the analyzer and will appear in the telescope as a light field. As the mica plates are rotated in unison, the intensity of illumination in the telescope will vary from extinction to full illumination. Extinction occurs when the plane of polarization of the light beam incident upon the model coincides with a principal stress direction.

Relation Between Refractive Indices and Principal Stresses--At this point, it would be well to review the laws relating changes in refractive indices to principal stresses as investigated by such men as Maxwell[30], Neumann[31], Favre[26], Filon[32], and

others. For plane stress, these relations are:

$$\delta_1 = C_1\sigma_2 + C_2\sigma_1$$
$$\delta_2 = C_1\sigma_1 + C_2\sigma_2 \quad \ldots\ldots\ldots (12)$$

where

δ represents change in refractive index,

σ, principal stress,

C, stress-optical coefficient, and

1, 2, subscripts denoting principal stress directions.

Solving equation (12) for the principal stresses:

$$\sigma_1 = A\delta_1 + B\delta_2$$
$$\sigma_2 = B\delta_1 + A\delta_2 \quad \ldots\ldots\ldots (13)$$

where the constants A and B, are defined by:

$$A = \frac{C_2}{C_2^2 - C_1^2}$$
$$B = \frac{C_1}{C_1^2 - C_2^2} \quad \ldots\ldots\ldots (14)$$

Since A and B can be evaluated by a simple calibration experiment (which will be outlined later), the principal stresses, σ_1 and σ_2, can be determined by equation (13) in terms of the changes in refractive indices, and the latter are linearly related to the number of interference fringes that pass the cross-hairs in the telescope while the model is undergoing a change of stress. The individual principal stresses are, therefore, linear functions of the fringe displacements.

Construction and Installation

As stated previously, the photoelastic interferometer being used by the Bureau of Reclamation was designed and constructed by Bureau personnel. Detailed shop drawings are not included in this monograph but they have been prepared to cover all details of construction.

Figure 10 shows the over-all appearance and arrangement of the component parts of the apparatus.

The light source, shown at the extreme right in Figure 10, is a water-cooled, high-intensity, mercury-vapor lamp. The housing for the light source is of special design to provide a small aperture and holders for the required filter and polaroid. Auxiliary equipment for operation of the light source, such as transformer, flow switch, and solenoid, is mounted on the table directly under the lamp housing.

The condensing lens, shown at the center of Figure 10, is a compound lens with a focal length of approximately one meter.

Both the light source and the lens are mounted on movable carriages which, in turn, are mounted on a pair of optical rails. The light source can be adjusted vertically, laterally, and along the rails, and the lens can be moved vertically and along the rails.

Figure 11 is a close-up view of the photoelastic interferometer showing details of construction.

A darkened, ventilated room is required for proper and efficient operation of the photoelastic interferometer. Further, since the instrument is sensitive to movements of the order of the wave length of light, it is necessary that the temperature remain nearly constant while readings are being taken. Therefore, in selecting a location for installing the instrument, care must be taken to see that the above requirements are met. In addition a water supply of not less than four gallons per minute, with waste facilities, a constant-voltage electrical source suitable for the mercury light, and a source of compressed air for use in loading the models must be available.

A substantial table must be provided on which to mount the component parts of the instrument. It must have sufficient stability to provide a vibration-free stand for the photoelastic interferometer. Since such a table is heavy and is not likely to be moved once the installation has been made, it has been found convenient to have the water, electricity, and compressed air supplies terminate on the table.

Adjustment

Aligning Flats--The first step in obtaining fringes in the telescope is the adjustment of the optical flats and parallels

(hereafter all are called flats) of the instrument. This alignment can be done by using an indoor target method or by utilizing some distant object visible from the place where the adjustment is being made. The following discussion of this step in the adjustment of the photoelastic interferometer is based on the use of targets. However, if use of a distant object is more feasible, then the procedure should be modified by replacing the targets by the distant object.

Necessary facilities and equipment required are:

a. A room with a clear area about 50 feet or more square, which can be darkened. Two aisles 50 feet in length at right angles to each other would be satisfactory

b. A surveyor's transit

c. A precision bench level

d. A precision 12-inch scale

e. A fifty-foot tape

f. Extension cords and flood lamps for illuminating the targets

g. Screwdrivers and wrenches for adjusting mounts on the photoelastic interferometer base

h. Flashlight

i. C-clamps

j. 24-inch straight-edge

k. Large 45° triangle

l. Plumb bob

m. Two inserts containing vertical and horizontal cross-hair centerlines. When inserted in the optical flat frame the cross-hairs must be in the plane of the reflecting surface of the optical flat. Figure 17 shows the shape and dimensions of these inserts.

n. Two targets: One with two centers a distance apart equal to L_1L_4, on the same horizontal centerline, and one with three centers spaced distances apart equal to L_1L_2 and L_2L_3 or L_4L_5 and L_5L_6, all located on the same horizontal centerline.

Figure 14 shows the numbering of the optical flats. Targets suitable for use in this adjustment are shown in Figure 15. These should be made on heavy show card stock or bristol board. Dimensions should be based on actual measurements of the spacing of the flats of the photoelastic interferometer being adjusted.

Figure 14 also shows schematically the steps to be taken in the adjustment. Figure 16 shows the positions of the flats in their mounts for the completed adjustment.

The photoelastic interferometer should be set up on a table near one corner of the room with L_4 nearest the corner. The setup should be rigid and free from vibration and movement. The base should then be leveled. Remove all flats from their frames on the base. Align all frames at approximately 45° with a line between centers of the mounts, and adjust them so that their horizontal centerlines are all at the same elevation. It will also be found convenient to remove the complete half-wave plate assemblies and the telescope support while the adjustment is being made.

Set up the transit 8 or 10 feet in front of L_1 in line with L_1L_4. Place the inserts containing vertical and horizontal centerline cross-hairs in frames L_1 and L_4. Adjust the transit so that the vertical and horizontal centerline cross-hairs of the inserts in L_1 and L_4 are on the cross-hairs of the transit. Remove insert from L_4, replace flat L_4, and place insert in L_6. Adjust flat L_4 until centerlines of the insert in L_6 are on cross-hairs of the transit, and remove both inserts. Locate center of target A on line L_4L_6 and level the horizontal centerline of target A and target B by moving the targets. Using the plumb bob establish a point on the floor on line L_4L_6, 8 to 10 feet in front of L_6 to be used as the second position of the transit.

To make the first adjustment place flat L_1 in position and adjust the capstan nuts so that the centerlines of the image of target B are on the cross-hairs of the transit. Now plunge the transit and locate the center of target C on L_1L_4 and level the horizontal centerline of targets C, D, and E. The transit is now moved to the position previously established in front of L_6 on the line

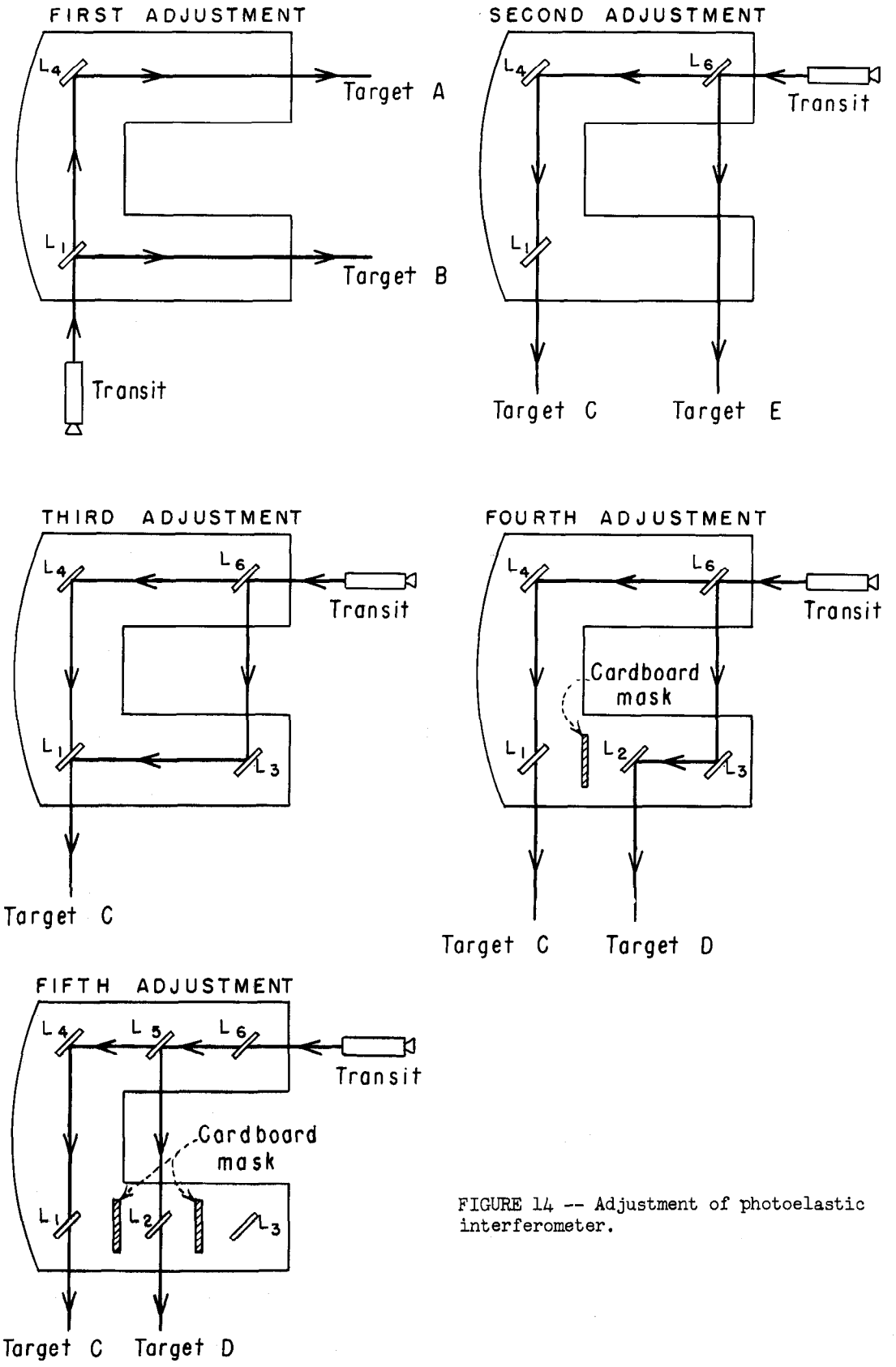

FIGURE 14 -- Adjustment of photoelastic interferometer.

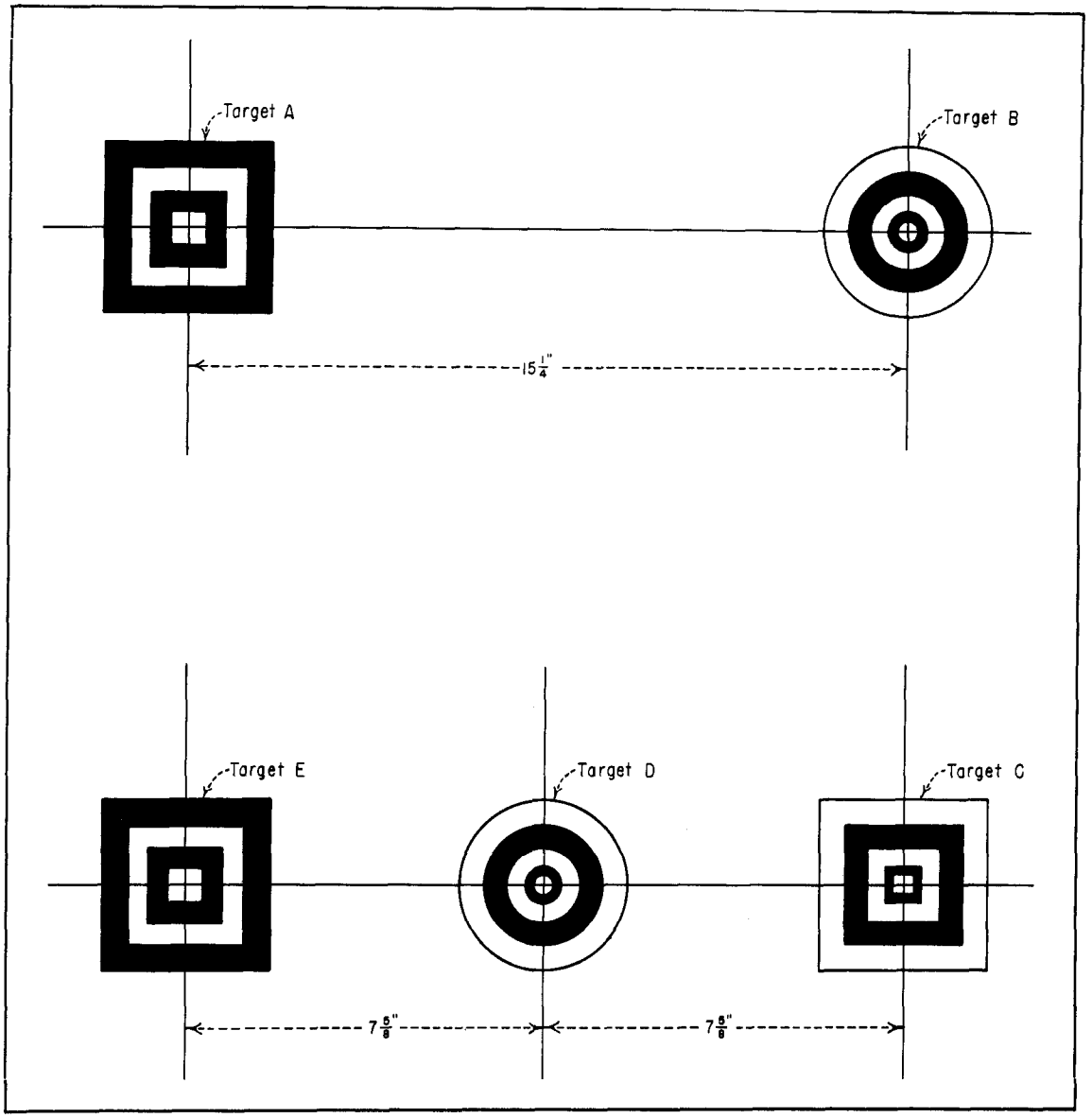

FIGURE 15 -- Alignment targets for adjusting interferometer.

L_4L_6 and adjusted to the horizontal plane through the centerlines of the targets. Align the transit on line L_4L_6 by rotating it about its vertical axis so that the vertical centerline of target A is on the vertical cross-hair of the transit. Plunge the telescope or rotate the transit 180° about its vertical axis.

The second adjustment is made by placing flat L_6 in position and adjusting the capstan nuts so that the centerlines of the image of target E is on the cross-hairs of the transit. The images of targets C and E should be coincident.

For the third adjustment place flat L_3 in position and adjust the capstan nuts to obtain coincident images of target C by the two separate paths $L_1L_4L_6$ and $L_1L_3L_6$.

To make the fourth adjustment place flat L_2 in position and obtain coincident images in the transit of targets C and D through the two separate paths $L_1L_4L_6$ and $L_2L_3L_6$ using a cardboard mask as required.

Finally, for the fifth adjustment, place L_5 in position and make adjustments similar to those on L_2. Coincident images must be

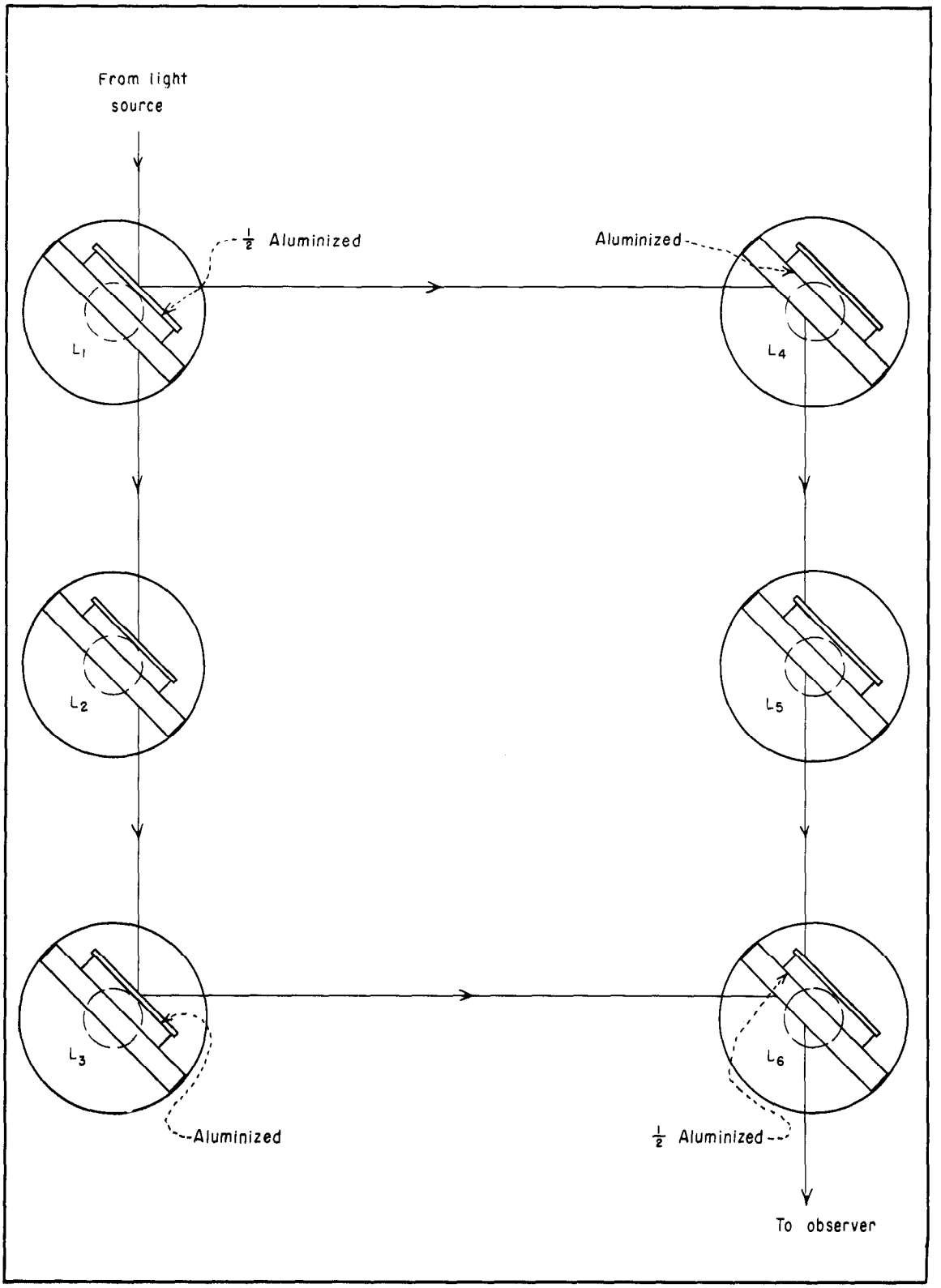

FIGURE 16 -- Position of flats in mounts during adjustment of photoelastic interferometer.

obtained from targets C and D through paths $L_1L_4L_6$ and $L_2L_5L_6$, using cardboard masks as required.

The transit must be placed far enough away from the optical flats and the targets to permit proper focusing. Also, the greater the distance that the targets can be placed away from the flats, the less critical will be the spacing between the targets in relation to the actual spacing between the flats. Double images may be present due to reflection from both surfaces of flats L_1, L_2, L_5, and L_6. Care must be taken to insure that the proper reflection is being used. Here again, the greater the distance the transit and targets are placed from the flats, the less apparent will be the double-image effect.

If the photoelastic interferometer has been removed from its permanent installation for this phase of the adjustment, it should now be returned to its supports and leveled carefully. The transit should be set up and the light source and the condensing lens adjusted in elevation to bring them into the same horizontal plane with the centerlines of the optical flats. The support for the telescope should be replaced.

Adjustment of Light Path--The next step is the adjustment of the light path. Reference

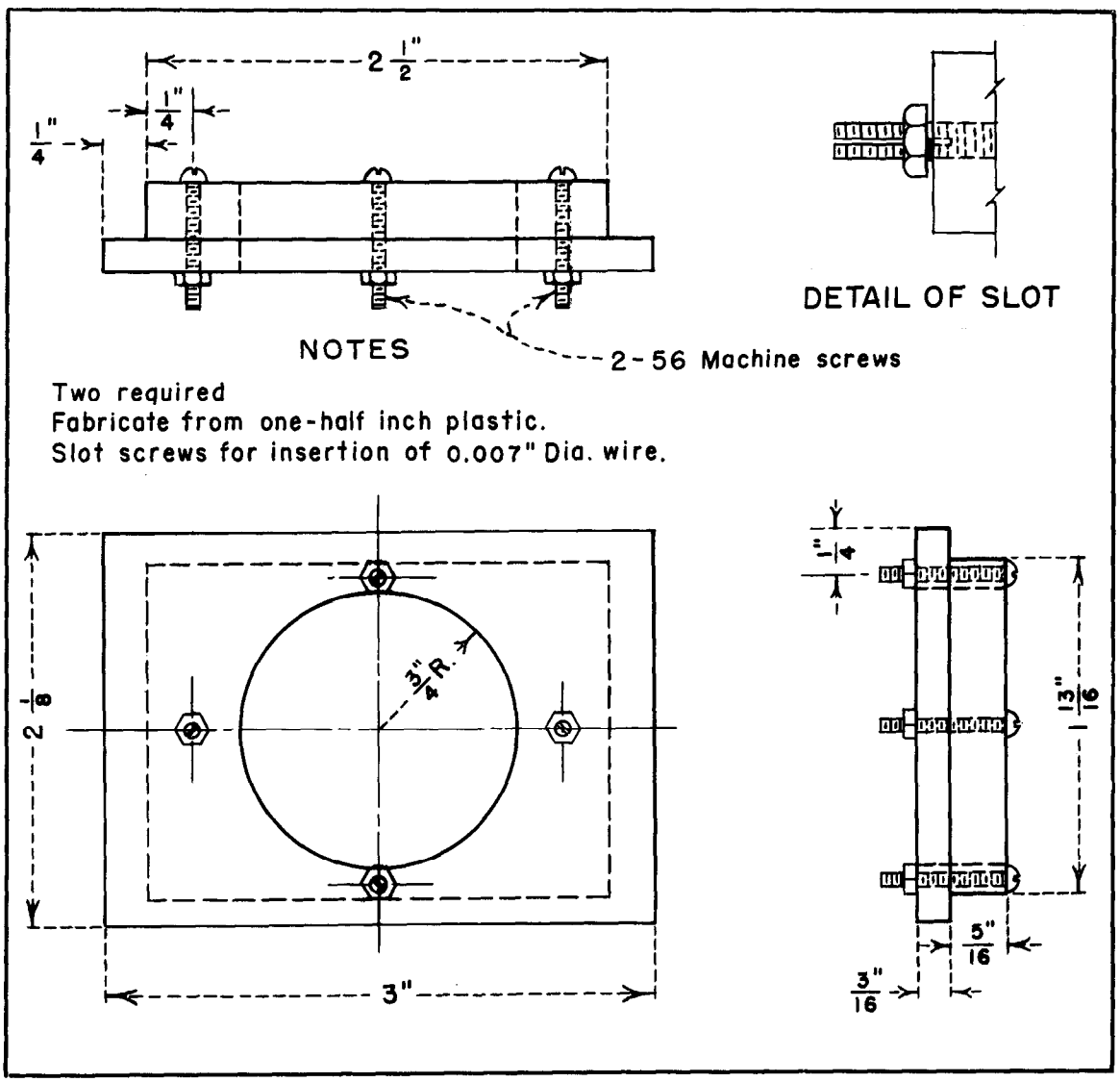

FIGURE 17 -- Insert for aligning optical flats during adjustment of photoelastic interferometer.

to Figure 10 will show the relative positions of the light source, the lens, and the photoelastic interferometer. With the light operating, the optical rails, on which are mounted the light source and the lens, should be adjusted until the aperture of the light source and the center of the lens are on the line $L_1L_2L_3$. Move the lens along the optical rails until the light beam is focused approximately midway between L_3 and L_6. The light going around the outside path should be checked to see that the beam is approximately centered in the flats. When this is accomplished, the optical rails should be secured to the table. Minor adjustment of the light path can be made by means of the sliding base support of the light source. A large and a small aperture are provided for the light source. It will be more convenient if the initial adjustment of the light path is made with the larger opening in front of the light, but for final checking of the alignment and observation of the field in the telescope, the smaller opening should be used. With the telescope in place and focused approximately on L_6 the field should be large and uniform for both the inside and outside paths when viewed through the telescope.

The polaroid and the monochromatic filter should be installed in the light housing, and the polaroid adjusted to pass vertically polarized light. This is done by use of a Nicol prism which is placed on the optical rail between the lens and light and set to pass horizontally polarized light. The polaroid is rotated until extinction of the light occurs and then locked in this position. After the polarizer has been adjusted the Nicol prism is removed from the light path. The analyzer directly in front of the telescope is then placed in position and rotated until extinction occurs when viewed through the telescope. The analyzer is locked in this position in its mount.

The half-wave plate assemblies, with the half-wave plates removed, are now installed on the base and adjusted until the beam of light is passing through the center of the opening on the assemblies. After they are in position they should be fastened securely in place and the drive wire, which moves them simultaneously, installed. The indicator scales on both assemblies are set at zero and the assemblies locked to prevent rotation. With both the polarizer and the analyzer in the light path, insert the half-wave plate nearest the light source into its mount. The half-wave plate is then rotated without disturbing the zero setting of the indicator scales until extinction occurs. The second half-wave plate is then put in its mount and rotated until extinction occurs. After this adjustment is completed, the half-wave plates are locked in position by means of their locking nuts. The half-wave plate assemblies are unlocked and rotated simultaneously and extinction observed. If the adjustment is correct the extinction will be complete and uniform over the whole range of motion of the half-wave plates. If extinction is relieved due to rotation of the plates, the second plate is removed and turned over, and the adjustment of that plate repeated.

The final step in the adjustment of the photoelastic interferometer is the obtaining of interference fringes at flat L_6. Initially, the fringes are obtained without a model or compensating piece of material being used. The adjustment is made by means of the three capstan nuts on mount L_6. The adjustment consists of a very careful movement of L_6 until the fringes are obtained. There can be no precise method outlined here because the procedure is essentially cut and try. A sharp pin point inserted in the light path immediately after the first polaroid and the filter may prove helpful. Adjustment of L_6 should be made to bring the two images of the pin together. Interference fringes should occur when the images are coincident.

Calibration

As shown previously the individual principal stresses are given by the equations:

$$\sigma_1 = A\delta_1 + B\delta_2$$
$$\sigma_2 = B\delta_1 + A\delta_2 \qquad \ldots\ldots\ldots\ldots (13)$$

Numerical values for A and B are determined by a simple calibration experiment. A calibration test specimen is cut from the same plate as the experimental model, placed in the photoelastic interferometer, and subjected to stress. The principal stress directions are determined by the method outlined. These directions are set, in succession, on the half-wave plates. The dial gage readings, L and R, are obtained, in turn, by noting the fringe movement between the po-

sition of load and no load for each principal stress direction at the point being analyzed in the test specimen. In equations (13) let L be a measure of δ_1, expressed in terms of dial gage readings, and let R be a measure of δ_2, also expressed in terms of dial gage readings. In the specimen $\sigma_2 = 0$ and $\sigma_1 = P/a$; therefore, by inserting values of L , R , σ_1, and σ_2 into equations (13) the numerical values of A and B can be determined. The values are functions of the model material, the model thickness, and the wave length of the light being used.

Figure 18 shows the arrangement for calibration. The test specimen in this figure is one-half inch thick, one inch wide, and four inches long. The width-to-length ratio must be kept sufficiently small so that the σ_2 stress can be considered as zero. In this case the test piece is being loaded in compression although a tensile test would be satisfactory provided proper care is taken in assigning sign conventions to the stresses, the deflections, and the constants.

Readings are taken across a section at the mid-length of the test piece. Usually five points across the width will be sufficient to provide a satisfactory average.

The calibrating is done at three or four load increments for load intensities in the region of those expected in the model of the structure. An average value for all loads is determined and used.

Operation

Reference has been made previously to the fact that the individual principal stresses are linear functions of the fringe displacements and are measured by the number of fringes that pass by the cross-hairs in the telescope while the model is undergoing a change in stress. In actual operation, however, it is not necessary to count the number of fringes that pass the cross-hairs in the telescope. The operation is much more rapid and more accurate if the outside path is changed in length by an amount equal to the refractive change of the inside path by using the clear glass optical parallel, L_s, which is mounted on a spindle and equipped with a tangent arm and a tangent screw. As the tangent screw is turned, the effective length of glass through which the outside path of light must travel is changed. Therefore, the change in length of the outside light path may be made equal to the change of the inside path. A micrometer measuring dial bears against an insert in the tangent arm, and changes in length of the outside path are indicated on the micrometer dial.

The procedure to be followed in preparation of photoelastic models is discussed in a Section under that title. Also discussed are the loading frame and the air piston and their use. Therefore, it will be assumed that the photoelastic interferometer is in adjustment, the model of the structure has been prepared and mounted in the loading frame, the model material has been calibrated, and the experiment is ready to proceed.

The model is loaded with dead weight and unloaded by means of an air piston which removes the dead weight. The air to the piston is controlled by a valve system on the top of the interferometer table. This valve system provides a method of supplying air to the piston and exhausting the air from the piston.

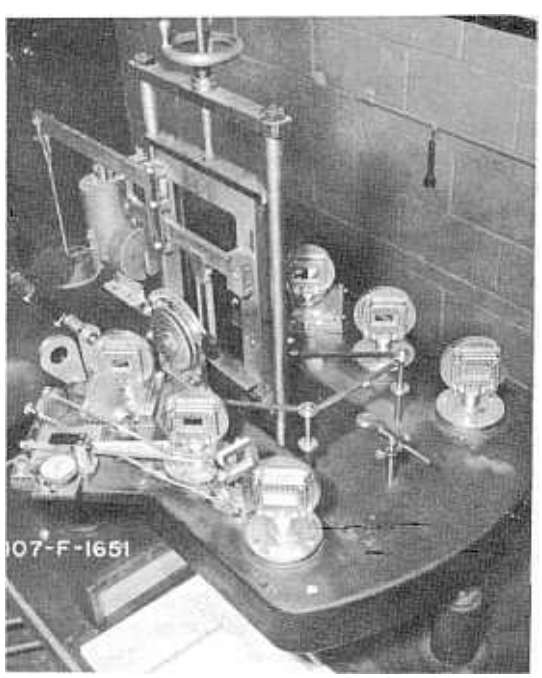

FIGURE 18 -- Calibration specimen in photoelastic interferometer.

The operation of the photoelastic interferometer normally requires an operator and a recorder. The operator controls the loading and unloading of the model, the half-wave plates, and the measuring dial. The recorder reads the angle of rotation of the half-wave plates and the measuring dial and records these readings.

The first step is to adjust the focus of the inside light path so that the light has its minimum diameter spot in the model. This is accomplished by sliding the lens on the optical rails until the minimum spot of light exists in the model.

The next step is the orientation of the model with respect to the scales on the loading frame. The outside path of light is blocked by means of the single shutter which is controlled by the small inner knob of the two which control the shutters and the analyzer polaroid. The telescope is adjusted until it is focused on the model. The model is then loaded and moved vertically by means of the screw feed of the loading mechanism until the point of light is on the edge of the model, or other such point, which is to be used as a horizontal reference line. The scale and vernier are adjusted to some arbitrary reading selected for easy use in a coordinate system. The same procedure is repeated for the lateral orientation. Due to the backlash in the traversing mechanism, the screw feed should always be turned in the same direction, when approaching a point for reading, as was used in orienting the model.

Next, the shutter is removed from the outside light path, and the telescope is again focused approximately on L_8. The model is moved to the first point at which a reading is to be taken. A compensating piece of material, cut from the same sheet of plastic as the model, is inserted in the compensator holder in the outside light path to compensate for the model being placed in the inside light path. The compensator holder is then adjusted until fringes are obtained. In some cases, minor adjustment of flat L_8 may be necessary.

The next step is the determination of the principal stress directions. The analyzer polaroid and the shutter which blocks the outside light path are moved into position in front of the telescope by turning the large outer knob of the two which control the shutters and analyzer polaroid. The operator then rotates the half-wave plates until extinction is observed. This is done with the load on the model. There are two positions of the half-wave plates that give extinction. These are the two principal stress directions and the two settings of the half-wave plates will be 45 degrees apart. The recorder reads and records these angles in the proper columns on the data sheet (see Figure 19).

After the half-wave plates are set so that the light is passing through the model in a principal stress direction, the analyzer polaroid and the shutter are removed from the light paths, and the operator is ready to take readings. The operator uses his left hand to operate the valve system which controls the loading of the model, and with his right hand he operates the screw which controls the movement of the tangent arm and the micrometer measuring dial for measuring the movement of the fringes. The dial is set on zero by the recorder and the operator removes the load from the model by means of the valve system. The operator selects some fringe with reference to the cross-hairs of the telescope. As he releases the air from the piston and the load is applied to the model, he keeps this reference fringe in the same position with respect to the cross-hairs of the telescope. This is accomplished by turning the tangent motion screw which rotates L_5 and also moves the micrometer measuring dial. When the entire load is on the model the recorder reads the dial and returns it to zero position. The observer repeats the procedure; and, if the two readings check, the recorder enters the reading in the proper column on the data sheet. The recorder then turns the half-wave plate to the other principal stress direction which has been previously determined. The procedure for taking readings is then repeated at this new direction. After the readings have been taken in both principal stress directions, the model is moved to a new point by means of the screw feeds on the loading frame, and the entire procedure of determining principal stress directions and fringe movements is repeated. This is continued until all points necessary for the stress study have been read.

Reference has been made to the data sheet, Figure 19. This sheet provides a

INTERFEROMETER STRESS ANALYSIS DATA SHEET

Sheet No. _____

Single Barrel Conduit with Circular Opening
t = r/3
Conc. vertical load with uniform foundation reaction

K = 0.0553 v in²/lb
A = -5.40 lb/in²
B = +7.08 lb/in² σ_L = KAL + KBR
KA = -0.299 v
KB = +0.392 v σ_R = KBL + KAR

$\sigma_x = \sigma_L \cos^2 \Phi_R + \sigma_R \sin^2 \Phi_R$
$\sigma_y = \sigma_R \cos^2 \Phi_R + \sigma_L \sin^2 \Phi_R$
$\tau_{xy} = (\sigma_R - \sigma_L) \frac{1}{2} \sin 2\Phi_R$

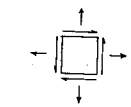

+ Sign Convention

Observer R.W.C.
Recorder I.O.
Computer HBP v IFA
Date May 8, 1962

Line	D/r	X (in.)	Y (in.)	Angles ½Φ_L	½Φ_R	Φ_R	Dial Readings L	R	Principal Stresses σ_L/v	σ_R/v	Φ_R sin²Φ_R	cos²Φ_R	½ sin 2Φ_R	Component Stresses σ_x/v	σ_y/v	τ_{xy}/v	Ave. Ⓑ & Ⓑ' * σ_x/v	σ_y/v	τ_{xy}/v
Ⓐ	.022	5.00	7.30	45	0	0	+163	+214	+35.2	-0.1	0	1.0	0	+35.2	-0.1	0			
	.089	5.00	7.45	45	0	0	+ 71	+ 96	+16.4	-0.9	0	1.0	0	+16.4	-0.9	0			
	.156	5.00	7.60	45	0	0	- 15	- 7	+ 1.7	-3.8	0	1.0	0	+ 1.7	-3.8	0			
	.222	5.00	7.75	45	0	0	-129	-130	-12.4	-11.7	0	1.0	0	-12.4	-11.7	0			
	.289	5.00	7.90	45	0	0	-288	-287	-26.4	-27.1	0	1.0	0	-26.4	-27.1	0			
Ⓑ	.022	7.30	5.00	1	44	88	-103	-134	-21.7	-0.3	.9988	.0012	.0349	-0.34	-21.7	+0.7	-0.4	-21.8	+0.4
	.089	7.45	5.00	3	42	84	- 70	- 88	-13.6	-1.1	.9891	.0109	.1040	- 1.26	-13.5	+1.3	-1.0	-13.6	+1.1
	.156	7.60	5.00	8	37	74	- 34	- 40	- 5.5	-1.4	.9240	.0760	.2650	- 1.67	- 5.2	+1.1	-1.5	- 5.0	+1.1
	.222	7.75	5.00	41	4	8	+ 18	+ 11	- 1.1	+3.8	.0194	.9806	.1378	- 0.98	+ 3.7	+0.7	-1.2	+ 3.8	+0.9
	.289	7.90	5.00	44	1	2	+ 64	+ 47	- 0.7	+11.0	.0012	.9988	.0349	- 0.70	+11.0	+0.4	-0.4	+10.9	+0.4
Ⓒ	.022	5.00	2.70	45	0	0	+ 81	+106	+17.3	+0.1	0	1.0	0	+17.3	+0.06	0			
	.089	5.00	2.55	45	0	0	+ 50	+ 63	+ 9.7	+0.8	0	1.0	0	+ 9.7	+0.76	0			
	.156	5.00	2.40	45	0	0	+ 12	+ 14	+ 1.9	+0.5	0	1.0	0	+ 1.9	+0.52	0			
	.222	5.00	2.25	45	0	0	- 29	- 37	- 5.8	-0.3	0	1.0	0	- 5.8	-0.30	0			
	.289	5.00	2.10	45	0	0	- 65	- 83	-13.1	-0.7	0	1.0	0	-13.1	-0.66	0			
Ⓑ'	.022	2.70	5.00	45	0	0	-136	-105	- 0.5	-21.9	0	1.0	0	- 0.5	-21.9	0			
	.089	2.55	5.00	43	2	4	- 87	- 68	- 0.6	-13.8	.0049	.9951	.0696	- 0.7	-13.7	-0.9			
	.156	2.40	5.00	37	8	16	- 36	- 30	- 1.0	- 5.1	.0760	.9240	.2650	- 1.3	- 4.8	-1.1			
	.222	2.25	5.00	6	39	78	+ 10	+ 18	+4.1	- 1.5	.9568	.0432	.2034	- 1.3	+ 3.9	-1.1			
	.289	2.10	5.00	1	44	88	+ 49	+ 65	+10.8	- 0.2	.9988	.0012	.0349	- 0.2	+10.8	-0.4			

* The sign of the shear on Line Ⓑ' must be reversed before averaging with the shears on Line Ⓑ to give comparable results.

Note: For computing principal stresses from normal and shearing stresses use Form DG-583.

FIGURE 19 -- Interferometer stress analysis data sheet.

convenient form for recording all necessary data for computing the principal stresses. It includes space for computing and entering the stresses in rectangular coordinates as well as the necessary equations for computing the stresses. Space is also provided for recording pertinent data such as personnel, applied loading, calibration factors, project, and date.

Example

The photoelastic interferometer has been used to determine the distribution of stress across various sections of a single barrel conduit. This is the same conduit for which the boundary stresses were obtained using the photoelastic polariscope. Reference is made to Figures 7 and 8. Figure 7 gives data regarding loading and dimensions of the model and prototype structure. Figure 8 shows the results of the stress analysis.

Figure 19 presents the data from which the stresses were determined for lines (A), (B), and (C).

THE BABINET COMPENSATOR

General

The Babinet Compensator, see Figure 20, is an instrument designed for the precise measurement of the relative retardation of light due to double refraction. Magnitudes in the order of one-hundredth of a wave length can be measured with the Babinet Compensator. Thus, it is possible to determine with great accuracy fractional fringe order values in photoelastic models. This is of particular value when a small difference of principal stress exists in the region of interest in the model.

Theory

It can be shown analytically and verified experimentally[33,34,35] that the relative retardation of light in the two principal stress directions caused by double refraction, as a photoelastic model is subjected to stress, is a direct measure of the difference of the principal stresses. For a two-dimensional stress system this stress-optic law can be expressed as

$$R_t = Ct\ (\sigma_1 - \sigma_2) \quad \ldots\ldots\ldots \quad (15)$$

where:

R_t represents the relative retardation between the two light components,

C, the stress-optic constant,

t, plate or model thickness, and

σ_1 and σ_2, the principal stresses.

Since the Babinet Compensator also measures relative retardation, it is possible to compensate the relative retardation in a photoelastic model with the Babinet Compensator and thus determine the difference in principal stresses by proper calibration of the compensator.

Equation (15) is valid not only for applying the Babinet Compensator but is, in fact, the basis for all photoelastic stress analyses.

Construction

The basic elements of the Babinet Compensator are two right angle quartz prisms each with equal acute angles of approximately 2-1/2 degrees. However, the optical axes of the two prisms are perpendicular to each other. Also, one prism is fixed and the other is movable relative to the first so as to make the combined thickness of the two prisms variable. The movement is accomplished with a fine screw with a graduated drum head so that the amount of movement can be accurately determined. Reference cross-hairs are fixed relative to the fixed prism. When

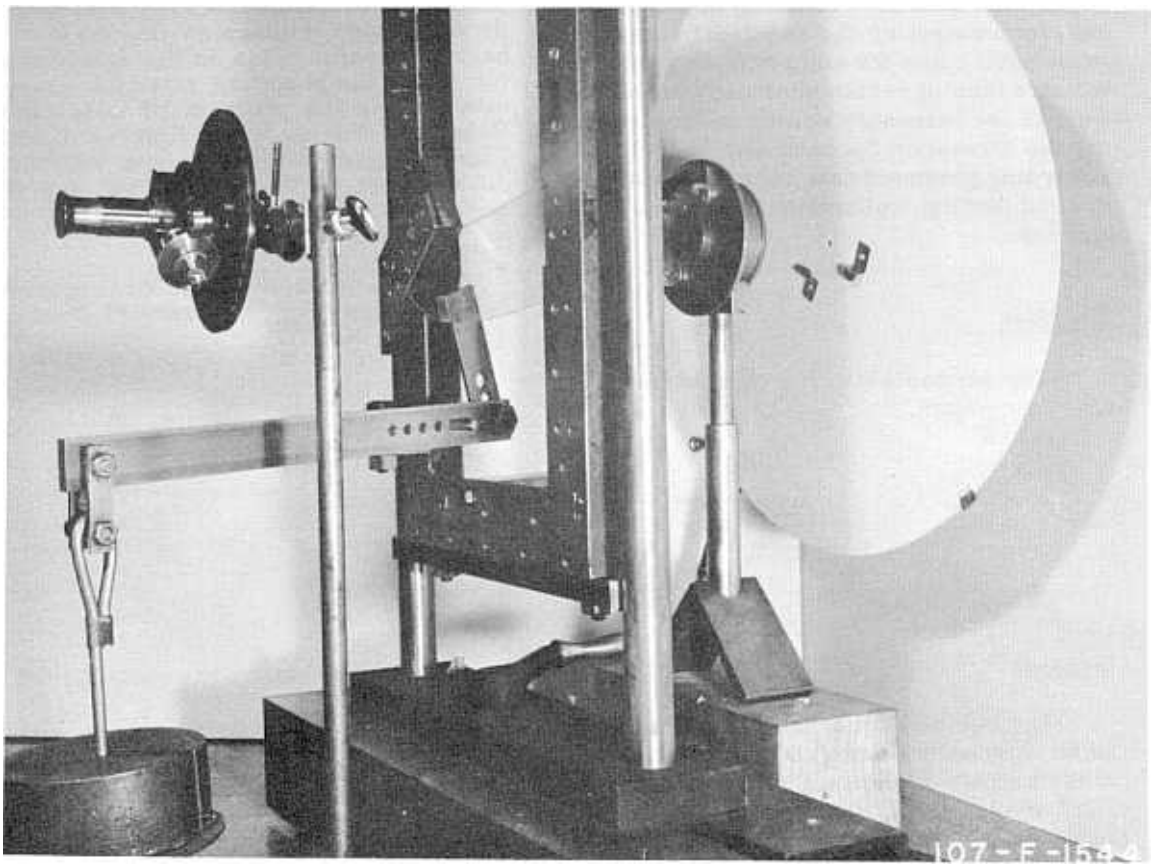

FIGURE 20 -- Typical arrangement of Babinet Compensator and model.

the graduated drum head is in zero position the two prisms have the same thickness at the cross-hairs.

When polarized light passes through the prisms of the Babinet Compensator, it is resolved into rectangular components and emerges with a relative retardation caused by the passage through different thicknesses in the two prisms. Only at the zero position will there be no retardation. When a stressed model which is doubly refractive is placed in the polarized light beam a relative retardation will be produced by the model. This can be compensated with the Babinet Compensator by moving the prism until the zero position occurs at the point under investigation. By proper calibration the amount of movement can be used to measure the difference in principal stresses at the point in question.

It is necessary that the light source be polarized. However, the analyzer is contained in the eyepiece of the Babinet Compensator. A small aperture must be provided between the light source and the model to restrict the area covered to a small enough region that the stress difference will be essentially constant over the area illuminated.

Application

The Babinet Compensator is used in conjunction with a source of monochromatic light which is plane-polarized by means of a polaroid. The light source and polarizer are set up on one side of the model and the compensator on the other. The compensator eyepiece contains the analyzer. The polarizer is set, by using the Nicol prism equipped with spirit levels, to polarize the light in a vertical plane. This is not strictly necessary as any plane of polarization may be used so long as it is known. The eyepiece of the compensator has a mark on it which shows the plane of polarization of the analyzer. The analyzer is then "crossed" with

the polarizer. If the eyepiece is held in this position and the compensator is rotated, it will be found that there are two positions where there is maximum brilliance of fringes and two positions of extinction where no fringes exist. These positions are 90 degrees apart. The correct reading of the compensator is where the maximum movement of the fringes is obtained, and the maximum movement of the fringes occurs when the axes of the wedges are in a principal-stress direction. It has been found by experimentation that, if the procedure is as outlined above, the maximum movement occurs where the maximum brilliance of the fringes occurs. Therefore, by holding the analyzer and polarizer "crossed" and rotating the wedges until maximum brilliance is obtained, the compensator is immediately put in operating position. The load may then be applied to the model and readings taken. Readings are taken by setting the cross hairs of the instrument on a fringe and then measuring the movement of the fringe between conditions of load and no load. The movement is measured by means of the micrometer screw which moves the wedges. If the directions of the principal stresses are desired, they may be determined by use of the protractor scale attached to the compensator.

Model Materials

As with the other methods of photoelastic analysis, the model material must be doubly refractive. Thus, the usual photoelastic model materials, such as Columbia Resin, CR-39, and Catalin 61-893 can be used with the Babinet Compensator. It is possible also to use materials which are much less sensitive optically than the usual materials used for the photoelastic polariscope and photoelastic interferometer since the Babinet Compensator measures very small changes of stress. Because of this, it is sometimes possible to make built-up models using Pyralin, cementing the joints with acetone.

THE BEGGS DEFORMETER

General

The Beggs Deformeter[36,37] is an apparatus, devised by the late Professor George E. Beggs of Princeton University, for the mechanical solution of statically indeterminate frame structures. Small elastic scale models of structures are deformed by a special set of plugs and gages, and the resulting deformations in the model are accurately measured by means of micrometer microscopes.

The Beggs Deformeter method automatically takes into account the work in a structure due to moment, thrust, and shear, as well as the effect of haunches, sharp corners, brackets, and other shape changes. In the usual analytical methods only work due to moment is considered and odd shapes are difficult to evaluate. Further, the Beggs Deformeter apparatus has the advantage over other types of deformeter model methods because it uses micrometer microscopes which require only small deformations in the models, so that the distortion of the model is not great enough to introduce any error.

Theory

The basis of the deformeter method of stress analysis comes from a direct application of Maxwell's Law of Reciprocal Displacements which states: If a force P, applied at point A in direction θ_A, causes a deflection δ at point B in direction θ_B, then a force kP, applied at point B in direction θ_B, will cause a deflection $k\delta$ at point A in direction θ_A.

There is shown at (A) of Figure 21 an indeterminate frame structure composed of a beam and a column. It is fixed at points a and b and loaded at point c with a force P. This structure is equivalent to the structure shown at (B) where the restraint at the base of the column has been replaced by the reactions S, T, and M. These reactions, as yet undetermined, are such that there is no displacement or change of slope at the base of the column. The structure will be statically determinate when the magnitudes of these three reactions have been determined.

To determine the magnitude of the horizontal force S, assume that the column base is on frictionless rollers and therefore free to displace laterally. Under the action of the force P, the structure will assume the shape shown at (C) of Figure 21, and at point b the column will move outward a distance d. Now assume the structure to be loaded not with the force P but only with the horizontal force S at the column base as shown at (D). The value of S is such that at point b the column moves inward a distance d. Simultaneously, the unloaded point c moves upward a distance e. When these two systems are superimposed, the result is the original structure with its original loading.

Applying Maxwell's Law to the structures and loads shown at (C) and (D) gives the relation

$$\frac{d}{P} = \frac{e}{S}$$

or

$$S = P\frac{e}{d} \quad \ldots\ldots\ldots\ldots \quad (16)$$

The force S is therefore equal to the product of the known force P and the ratio of the deflections e and d. The deflections e and d exist simultaneously on the structure shown at (D), and, regardless of the force S required to produce the deflection d in this structure, the ratio of e to d will remain unchanged. The magnitude of d is therefore quite arbitrary. Furthermore, the ratio of e to d is independent of the size of the structure. This is the basis of the Beggs Deformeter analysis.

By similar reasoning it can be shown that the vertical force T is expressed by the equation

$$T = P\frac{g}{f} \quad \ldots\ldots\ldots\ldots \quad (17)$$

where g is the deflection at the load point c caused by the displacement f acting at the point b as shown in Figure 21 (E).

The moment M acting at b is given by the relation

$$M = P\frac{j}{h}n \quad \ldots\ldots\ldots\ldots \quad (18)$$

where j is the deflection at the load point c caused by the angular rotation h (measured in radians) as shown in Figure 21 (F), and n is the scale factor. The scale factor is the ratio of prototype dimensions to corresponding model dimensions.

Construction and Installation

The Beggs Deformeter apparatus is manufactured commercially. The one in use by the Bureau of Reclamation was purchased in 1938 directly from the inventor. Some minor modifications have been made in later models[38] but they are unimportant and affect only the appearance and not the theory or operation of the apparatus. Figure 22 shows a typical arrangement of the instrument and a model. The model is a representation of a frame section of the Grand Coulee Pumping Plant.

The standard Beggs Deformeter set includes six gage blocks, with normal plugs; three micrometer microscopes complete with stands; one set each of deformeter plugs for moment, thrust, and shear; and minor miscellaneous accessories.

Models are usually mounted on a plane sheet of 3/4-inch thick plywood which in turn is securely clamped to a small table of such a height as to allow the personnel normally to be seated while taking the readings. Adequate illumination of the model must be provided, but care should be taken that no deflections due to temperature stresses are induced in the model by heat from the light source. Fluorescent lamps, of the type used on drafting tables, have been found to be the most satisfactory means of illuminating the model.

Figure 23 shows the method of applying the displacements and rotations to the model by means of the gage block. The gage block is made of two notched steel bars. Accurately ground, hardened steel plugs are inserted in the notches, and the two steel bars are held snugly against these plugs by means of two small coil springs. Each of the three types of displacement requires a separate set of plugs. These are all illustrated in Figure 23. Now consider the model of Figure 21 and the group of gage blocks on Figure 23 labeled "Column fixed at base." For the angular displacement employed in determining the moment M, one set of plugs is

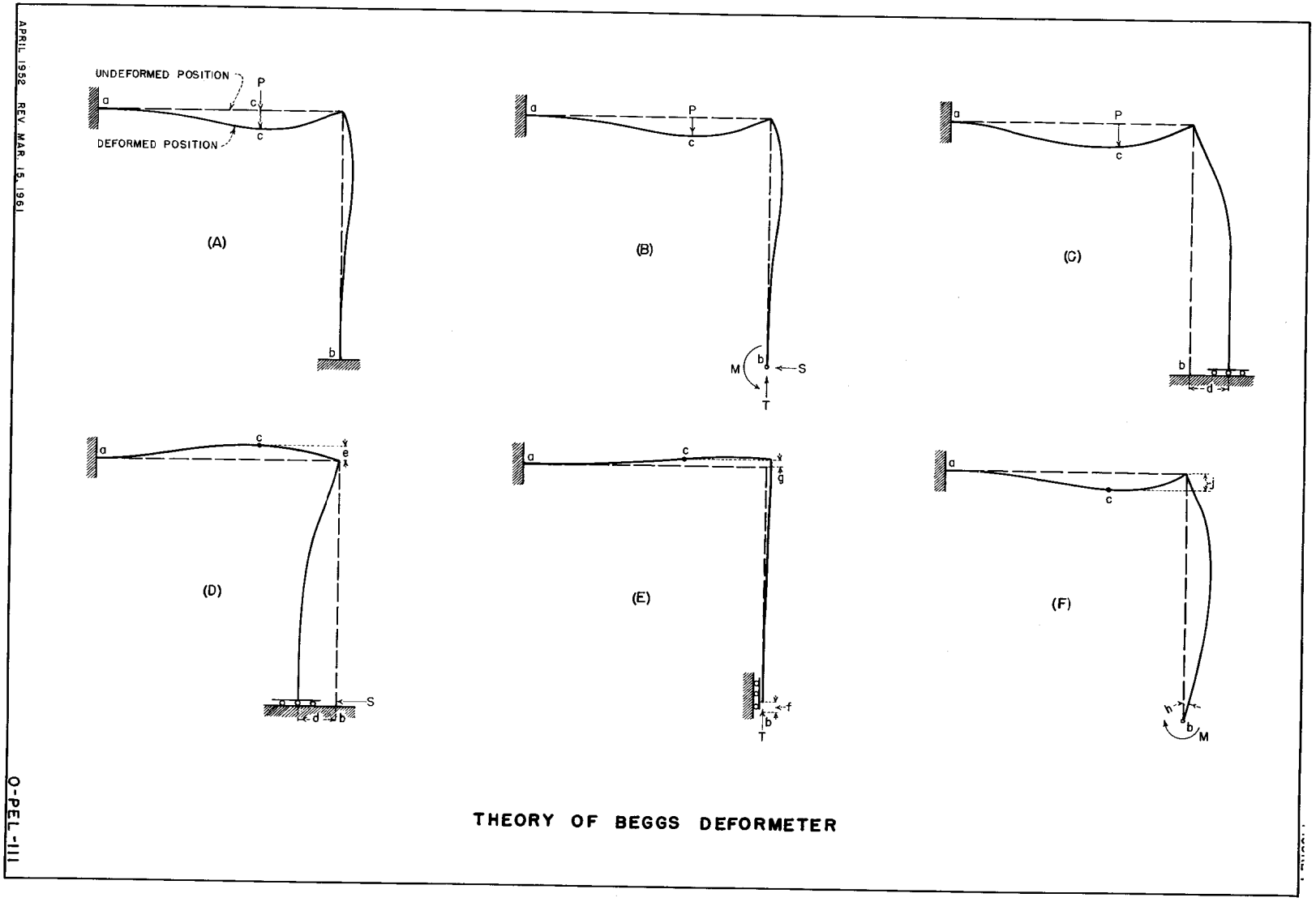

FIGURE 21 -- Theory of Beggs Deformeter.

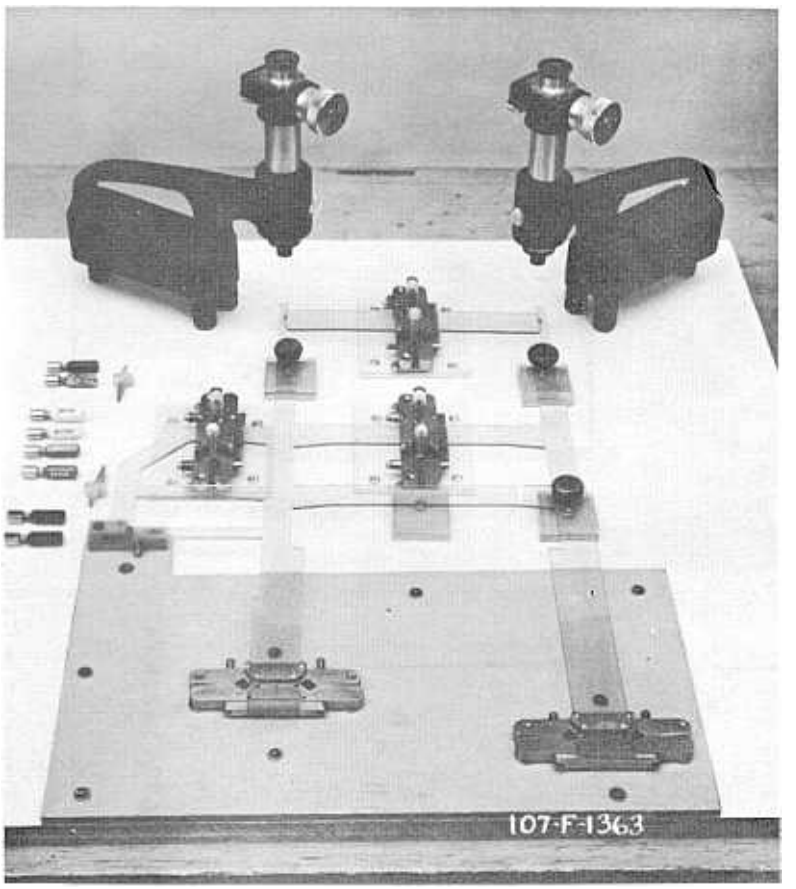

FIGURE 22 -- Typical arrangement of Beggs Deformeter and model.

used. These are of circular cross-section; but one is of larger diameter than the other.

For the first position the large plug is in the left notch, and the small plug is in the right notch. For the second position the plugs are reversed. The net effect is an angular displacement in a clockwise direction. For the displacement used to determine the thrust, T, two sets of plugs are used. For the first position the two plugs used are of equal diameter and slightly larger in diameter than the normal plugs. For the second position, the plugs used are of equal diameter and slightly smaller in diameter than the normal plugs. The net effect is a thrust along the axis of the member to which the gage is clamped. For the displacement used to determine the shear, S, only one set of plugs is used. These were originally of circular cross section but have an accurately ground flat side or facet, as shown in the figure. In the first position these facets face the upper left. In the second position they face the upper right. The net effect is a shear displacement of the model to the right.

Microscopes equipped with filar eyepieces are used to read the model displacements at points corresponding to the load points of the actual structure. Displacements must be read in the direction that the applied loads act on the actual structure. However, instead of actually applying loads to the model, only known displacements at the gage blocks are applied. The difference in micrometer readings measures the model displacement induced by the displacement at the gage block from the first position of the plugs to the second position of the plugs.

Calibration

As stated previously, accurately ground plugs are inserted in notched gage blocks to produce, separately, pure moment, thrust, and shear deflections on the model. These plugs are machined to a tolerance of $\pm$ 0.00005 inch. Deformations of the model at various

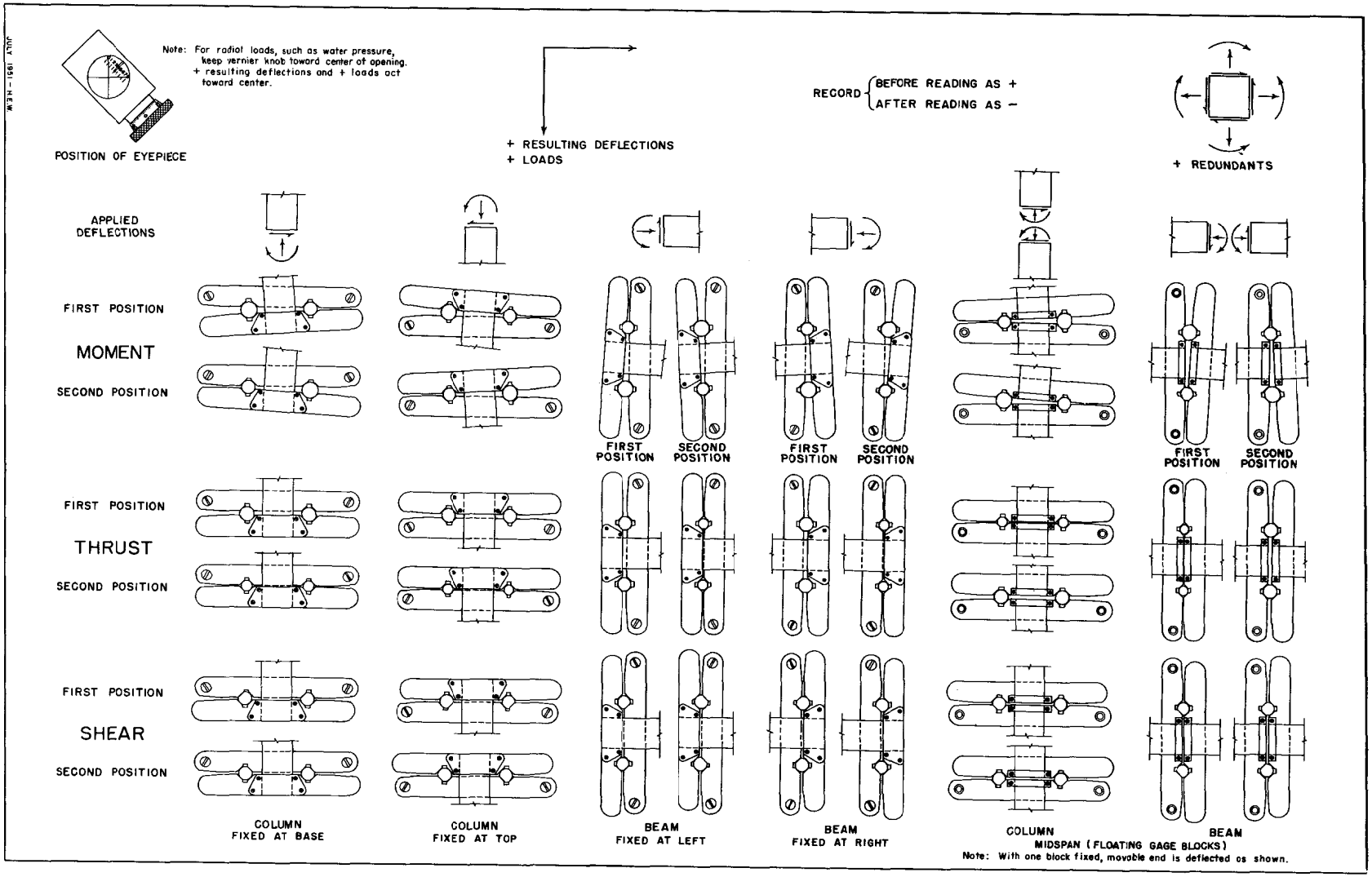

FIGURE 23 -- Beggs deformeter deflection and sign conventions.

load points are observed by means of 10X micrometer microscopes equipped with filar eyepieces.

Calibration factors, which are a function of the plug diameters and the micrometer microscopes, are used to simplify the application of the Beggs Deformeter. When calibration factors are multiplied by the microscope readings, the product is the ordinate of an influence diagram. The magnitude of the moment, thrust, or shear at the gage block for a traveling unit load is given by the corresponding influence diagram.

The calibration of the micrometer microscopes consists of the determination of a factor which relates the value of one unit of movement of the reticle or cross-hairs to a unit of length. The microscope should be assembled and mounted in its support stand. In the assembling of the microscope, care must be taken that the micrometer is firmly seated on the optical tube and that the objective at the other end of the optical tube is screwed completely into position. Another requirement is that the unit be properly focused. The eyepiece should be first focused on the reticle by screwing the eyepiece inward or outward until the reticle is most clearly visible. While doing this the microscope should be directed toward a broad source of illumination such as a sheet of white paper rather than being focused on any external object. After the reticle is in sharp focus the microscope should be focused on the object by sliding the optical tube up or down until a sharp focus is achieved. When the eye is moved from side to side of the eyepiece, there must be no apparent relative motion or parallax effect between the reticle and the object. If such motion exists, adjustment must be repeated until it has been eliminated. A calibrated micrometer microscope will be in proper calibration only when it is in proper focus[39].

A stage micrometer, with a glass object slide and a 2 mm scale, subdivided into units of 0.01 mm, is used to calibrate the microscopes. The micrometer microscope is focused on the stage micrometer, and a reading taken across the 2 mm scale. Repeat readings should be taken until a consistent value is obtained. This procedure should be followed for all microscopes of the apparatus.

In the most recent calibration (September 1950) made of the three microscopes now being used by the Bureau of Reclamation the calibrations were found to be

$$1 \text{ microscope unit} = 19.66 \times 10^{-6} \text{ inch} \quad \text{(No. 4829)}$$

$$= 19.63 \times 10^{-6} \text{ inch} \quad \text{(No. 4836)}$$

$$= 19.58 \times 10^{-6} \text{ inch} \quad \text{(No. 4835)}$$

$$\text{or an average of} \qquad 19.62 \times 10^{-6} \text{ inch}$$

The calibration of the plugs is somewhat more complicated. It is possible to calibrate directly by using the dimensions indicated on the plugs, or by reading actual displacements produced by the various plugs and gage blocks. Calibration using the plug dimensions is indicated by Figure 24. Figure 25 outlines the procedure to be followed when actual deflections caused by the plugs are used as a basis for determination of the calibration constants. In this method there is no need to know the absolute values of either the plug dimensions or the micrometer units. All that is required are deformations in micrometer units. Since the deflections at the various load points are also read in micrometer units the requirement, as discussed in the theory of the instrument, of knowing the ratio of the two readings rather than actual values is satisfied. Also indicated on Figure 25 are the deflections in micrometer units and the constants now being used as calibration factors for the Beggs Deformeter apparatus.

Operation

The principal material used for models in the Beggs Deformeter is sheet plastic such as Lucite, Lumarith, or Plexiglas. The usual thickness is 0.1 inch, but for relatively rigid models the thickness may be reduced to 0.06 inch or less. Other materials that have been used include cardboard and sheet cork.

The model is laid out on the plastic material to scale. Boundary lines are made with a sharp-pointed scriber. Members of the model structure should be made with the same proportions of stiffness as those of the actual structure by making the width

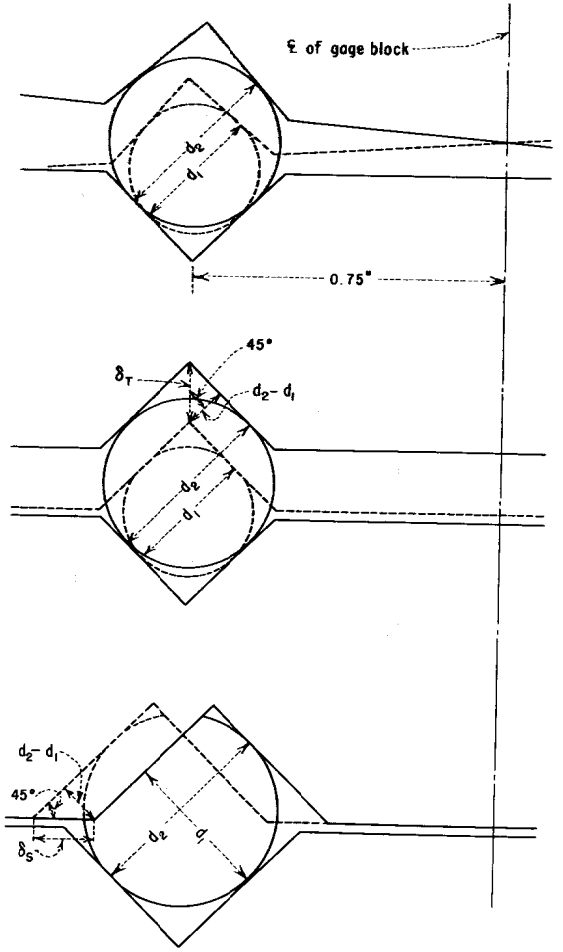

$d_2 - d_1$ = Difference in plug dimensions

δ_M = Displacement per inch

$$\delta_M = \frac{d_2 - d_1}{0.75 \times \cos 45^\circ} \text{ (approximately)}$$

$$= \frac{0.32773 - 0.32228}{0.73 \times 0.70711} = \frac{0.00545}{0.53033}$$

$$= 0.010277$$

$$\text{Moment Calibration Factor} = \frac{\text{Micrometer Calibration Factor}}{\delta_M} \times \text{Scale Factor}$$

$$= \frac{0.00001962}{0.010277} \times \text{Scale Factor}$$

$$= 0.0019091 \times \text{Scale Factor}$$

$d_2 - d_1$ = Difference in plug dimensions

δ_T = Vertical movement or thrust

$$\delta_T = \frac{d_2 - d_1}{\cos 45^\circ}$$

$$= \frac{034302 - 0.307015}{0.70711}$$

$$= 0.050919$$

$$\text{Thrust Calibration Factor} = \frac{\text{Micrometer Calibration Factor}}{\delta_T}$$

$$= \frac{0.00001962}{0.050919}$$

$$= 0.0003853$$

$d_2 - d_1$ = Difference in plug dimensions

δ_S = Horizontal movement or shear

$$\delta_S = \frac{d_2 - d_1}{\sin 45^\circ}$$

$$= \frac{0.34302 - 0.30700}{0.7071l}$$

$$= 0.050940$$

$$\text{Shear Calibration Factor} = \frac{\text{Micrometer Calibration Factor}}{\delta_S}$$

$$= \frac{0.00001962}{0.050940}$$

$$= 0.0003852$$

FIGURE 24 -- Beggs deformeter calibration using plug dimensions.

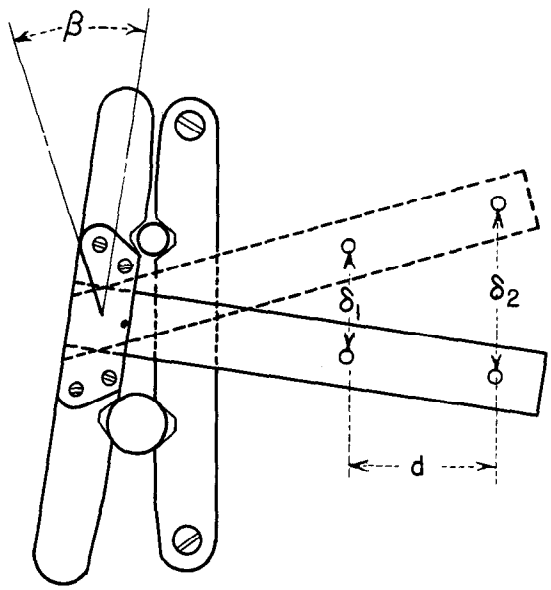

Units:

β is expressed in radians,
δ_1 and δ_2 as micrometer units,
d as inches,
m as micrometer units per inch,
n scale factor – dimensionless

$$\beta = \frac{\delta_2 - \delta_1}{md}$$

$$\text{Moment Calibration Factor} = \frac{\frac{1}{m}}{\beta} n = \frac{\frac{1}{m}}{\frac{\delta_2 - \delta_1}{md}} n = \frac{d}{\delta_2 - \delta_1} n$$

$$= \frac{4}{2060} n = 0.001942\, n$$

$$\text{Thrust Calibration Factor} = \frac{1}{\text{Deflection at gage block caused by thrust plugs (micrometer units)}}$$

$$= \frac{1}{2572} = 0.0003888$$

$$\text{Shear Calibration Factor} = \frac{1}{\text{Deflection at gage block caused by shear plugs (micrometer units)}}$$

$$= \frac{1}{2572} = 0.0003888$$

FIGURE 25 -- Beggs deformeter calibration using measured deflections.

of the model members proportional to the cube root of the moment of inertia of the prototype members. For continuous structures, such as conduits or tunnels, this will result in the model width being proportioned to the thickness of the prototype section.

Deflection readings are taken at the load point in the direction the applied load is acting on the actual structure. To accomplish this for externally acting loads, the members should be subdivided into short increments of length. The centers of these increments should be located, and a fine reference line, made with either a very sharp-pointed scriber or a corner of a razor blade, drawn on the model in the direction the load is acting. The length increments should be sufficiently small so that any significant change in the readings will be apparent when they are evaluated. Because of the resulting simplification in computations, it is best, when possible to use equal increments of length along any one member. For boundary loads, these reference lines should be drawn from the boundary toward the center of the member. They should be sufficiently long to allow for accurate orientation of the micrometer microscope. For dead load effects, the model should be divided into small sections and the centers of gravity of these sections located. A reference line should be drawn through the center of gravity in the direction of the force of gravity. It is important that the microscope be oriented in the exact direction that the load is acting.

When the model has been laid out to scale and the load points located, it should be carefully cut to line by some means such as a scroll saw, rotary sanding drum, and file. Care should be exercised to make the layout and the cutting as accurate as possible, since small errors in the model will be greatly magnified in the actual structure. Figure 27 is a photograph of a model showing the method of locating the reference lines for external and internal loads on the boundary.

The next step involves fastening the model to the gage block and mounting the gage block on the board. For the purpose

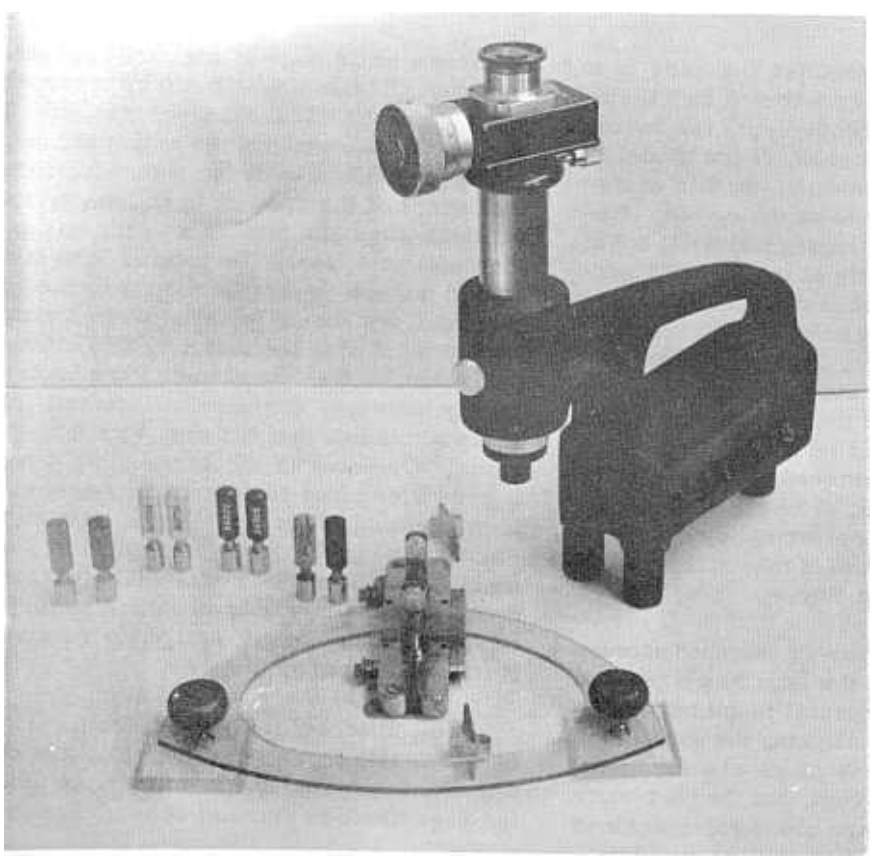

FIGURE 26 -- Beggs deformeter model of single barrel conduit.

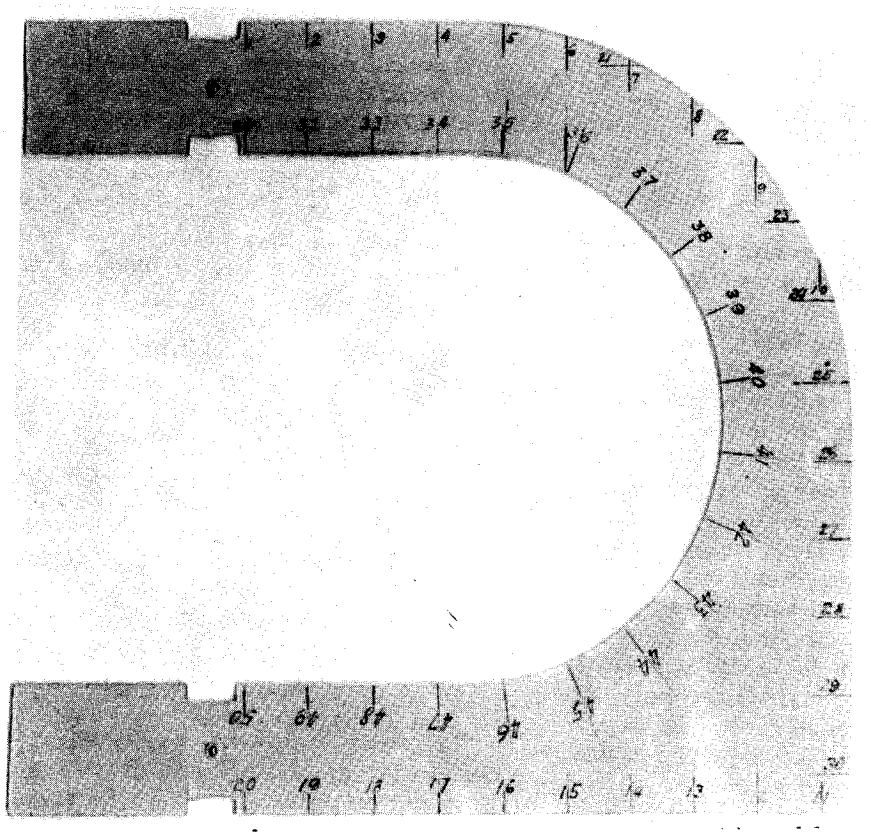

FIGURE 27 -- Beggs deformeter model showing load points and pinned-end joints.

of this explanation consider the case of a single barrel conduit as shown in Figure 26. It will be found convenient, for saving work and providing checks, if the model is cut on an axis of symmetry. In this example, let the cut be made at the crown. Before making the cut, locate and drill a No. 70 drill size pivot hole at a point 1/8 inch from the line on which the cut will be made on the normal to this line through the centerline of the member. That is to say, the hole should be so located that it will make the model pivot about the center point of the cut. This hole should be on the side of the model that will be fastened to the movable half of the gage block. The cut can then be made. It should be approximately 0.03 inch wide with equal amounts of material removed from each side of the line.

The model may now be fastened loosely to the gage block and the gage block secured to the board. Two special plugs have been fabricated for use in aligning the gage block and the model. These plugs are the same diameter as normal plugs, but the part which projects above the gage block was machined to form a knife edge at the exact center of the plug. These plugs should be inserted in the gage block. Place a steel straight-edge across the knife edges and adjust the model in the gage block until the reference line at the invert of the conduit is in line with the straight-edge and thus is a prolongation of the reference line at the crown. The model should now be clamped securely to the gage block. Care should be taken that no distortion is induced in the model by this clamping operation. After the clamps have been securely fastened, check the alignment. Two sizes of clamps are included with the apparatus. One size is the same width as half a gage block and is attached by means of four screws. This size should be used for relatively rigid models such as fixed end members. The other size clamp is much narrower and has only two screws for attachment. It is better suited for relatively flexible members.

The fixed end is the most frequent type of end condition encountered. For this condition the member is securely clamped to the gage block as outlined above. However,

a pinned-end member often occurs. In this case the gage block must transmit only thrust and shear deflections to the model. This is accomplished by the use of a small steel ball inserted in the model at the point where the pinned joint is to be. The ball should be slightly larger in diameter than the thickness of the model and should be press fitted into the hole in the model. The pivot pin should be removed from the gage block by pressing it out from the under side. This will leave a small hole as a seat for the steel ball. There is a similar hole in the clamp which provides a seat for the top of the ball. The screws holding the clamp should be drawn up sufficiently tight to prevent displacement of the steel ball but still allow for rotation. A check should be made at the gage block to see that this condition exists. Figure 27 shows a model with pinned-end connectors of this type.

The model must be supported at a sufficient number of points to restrict all deformation to the plane of the model. This is accomplished by supporting the model on small steel balls and placing small lead weights on top of the model to hold it down. These supports and weights can be seen in Figures 22 and 26.

In certain structures end conditions or arrangement of members may require that the entire gage block be allowed to float. Figure 22 illustrates this condition. The figure also shows that a new model is not required as the different cuts are made to reduce the structure to one that is statically determinate. Normal plugs are inserted in the gage block after all the readings at that particular cut are completed, and the entire gage block is allowed to float.

An alternate procedure is to make all the required cuts at one time and use gage blocks with normal plugs inserted in all cuts except the one at which the deformations are being introduced. After completing the readings at one cut it is only necessary to place normal plugs in the gage block at that cut and apply the deformations at another cut, repeating this procedure until deformations have been applied at all cuts.

Other end conditions can be accounted for by proper construction of the model and clamping devices to induce the end conditions desired.

With the model mounted on the board, the micrometer microscopes are assembled and focused on the model using the procedure outlined previously. Depending upon the size of the model and the number of load points to be read, one, two, or three micrometer microscopes may be used. Figure 23 presents a method for securing consistent results from a Beggs Deformeter stress analysis. Shown on the figure are the procedures to be followed for (1) fastening the model to the gage block for various types of members; (2) orienting the micrometer microscope; (3) applying the deflections; (4) determining positive sign convention for deflections, loads, and micrometer readings; and (5) determining positive sign convention for redundants.

To secure consistent, accurate results the following precautions, in addition to those previously mentioned, should be observed:

1. The micrometer microscopes must be oriented with the normal plugs in the gage blocks.

2. The microscopes must be oriented so that the cross-hair falls exactly along the reference line so the reading will be in the direction the load is acting.

3. The plugs, particularly the shear plugs, should be checked to see that they are properly and firmly seated in the notches in the gage blocks when the deflections are read.

4. The model must be properly supported and weighted down sufficiently to prevent any buckling, especially with stiff members.

5. The movable half of the gage block must bear solidly on its slides.

6. The ends of the model between the clamps must not touch when the small thrust plugs are in place in the gage blocks.

Figure 28 is the data sheet used for recording the readings obtained. Space is provided for three readings at each point with an additional space for an average of the readings. However, readings must be taken until consistent values are obtained. Readings are recorded on the data sheet in ac-

PAGE NO.________

BEGGS DEFORMETER DATA SHEET

FEATURE ____

DETAIL ____ DATE ______________

POINT		BEFORE	AFTER	DIFF.	AVERAGE	POINT		BEFORE	AFTER	DIFF.	AVERAGE
	M						M				
	T						T				
	S						S				
	M						M				
	T						T				
	S						S				
	M						M				
	T						T				
	S						S				
	M						M				
	T						T				
	S						S				

FIGURE 28 -- Beggs deformeter data sheet.

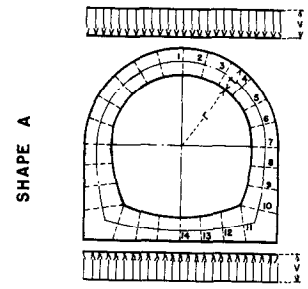

SHAPE A

POINT	$t = \frac{r}{2}$			$t = \frac{r}{3}$			$t = \frac{r}{6}$		
	$\frac{M}{vr^2}$	$\frac{T}{vr}$	$\frac{S}{vr}$	$\frac{M}{vr^2}$	$\frac{T}{vr}$	$\frac{S}{vr}$	$\frac{M}{vr^2}$	$\frac{T}{vr}$	$\frac{S}{vr}$
1	+0.357	+0.033	0	+0.317	+0.030	0	+0.274	+0.031	0
2	+0.308	+0.132	+0.366	+0.274	+0.119	+0.325	+0.236	+0.108	+0.284
3	+0.175	+0.403	+0.633	+0.155	+0.360	+0.562	+0.132	+0.318	+0.490
4	-0.006	+0.773	+0.727	-0.006	+0.688	+0.645	-0.008	+0.605	+0.562
5	-0.185	+1.141	+0.621	-0.165	+1.015	+0.551	-0.147	+0.890	+0.479
6	-0.312	+1.408	+0.343	-0.279	+1.252	+0.304	-0.246	+1.096	+0.262
7	-0.352	+1.500	-0.033	-0.314	+1.333	-0.030	-0.276	+1.167	-0.031
8	-0.327	+1.495	-0.132	-0.292	+1.328	-0.120	-0.256	+1.162	-0.110
9	-0.273	+1.483	-0.230	-0.244	+1.317	-0.209	-0.213	+1.152	-0.190
10	-0.190	+1.464	-0.328	-0.169	+1.300	-0.297	-0.147	+1.136	-0.268
11	+0.042	+0.157	-0.947	+0.004	+0.156	-0.915	-0.031	+0.153	-0.882
12	+0.261	+0.051	-0.633	+0.216	+0.052	-0.612	+0.174	+0.050	-0.590
13	+0.394	-0.012	-0.317	+0.345	-0.010	-0.307	+0.298	-0.010	-0.296
14	+0.439	-0.033	0	+0.388	-0.030	0	+0.340	-0.031	0

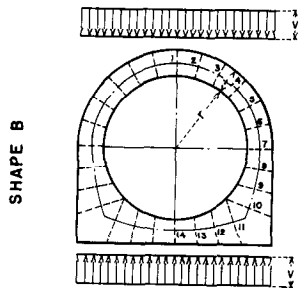

SHAPE B

POINT	$\frac{M}{vr^2}$	$\frac{T}{vr}$	$\frac{S}{vr}$	$\frac{M}{vr^2}$	$\frac{T}{vr}$	$\frac{S}{vr}$	$\frac{M}{vr^2}$	$\frac{T}{vr}$	$\frac{S}{vr}$
1	+0.353	+0.028	0	+0.311	+0.030	0	+0.265	+0.038	0
2	+0.304	+0.127	+0.368	+0.268	+0.118	+0.326	+0.227	+0.115	+0.282
3	+0.170	+0.399	+0.636	+0.149	+0.359	+0.563	+0.125	+0.325	+0.486
4	-0.012	+0.770	+0.730	-0.012	+0.688	+0.646	-0.015	+0.610	+0.556
5	-0.192	+1.139	+0.625	-0.172	+1.015	+0.552	-0.152	+0.894	+0.472
6	-0.321	+1.407	+0.348	-0.285	+1.252	+0.305	-0.249	+1.098	+0.255
7	-0.362	+1.500	-0.028	-0.321	+1.333	-0.030	-0.277	+1.167	-0.038
8	-0.330	+1.487	-0.198	-0.291	+1.321	-0.186	-0.247	+1.153	-0.179
9	-0.248	+1.455	-0.366	-0.217	+1.290	-0.339	-0.180	+1.123	-0.318
10	-0.119	+1.404	-0.529	-0.101	+1.241	-0.488	-0.076	+1.076	-0.452
11	+0.069	+0.305	-0.941	+0.044	+0.296	-0.890	+0.030	+0.279	-0.838
12	+0.260	+0.119	-0.634	+0.226	+0.113	-0.600	+0.202	+0.101	-0.566
13	+0.381	+0.008	-0.319	+0.341	+0.006	-0.302	+0.311	-0.004	-0.285
14	+0.423	-0.028	0	+0.380	-0.030	0	+0.348	-0.038	0

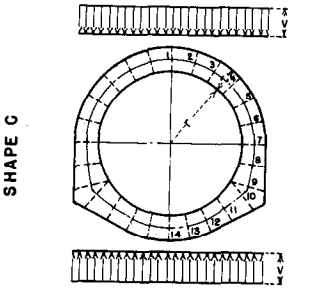

SHAPE C

POINT	$\frac{M}{vr^2}$	$\frac{T}{vr}$	$\frac{S}{vr}$	$\frac{M}{vr^2}$	$\frac{T}{vr}$	$\frac{S}{vr}$	$\frac{M}{vr^2}$	$\frac{T}{vr}$	$\frac{S}{vr}$
1	+0.368	-0.004	0	+0.328	-0.008	0	+0.286	-0.015	0
2	+0.318	+0.097	+0.376	+0.283	+0.082	+0.335	+0.246	+0.063	+0.296
3	+0.180	+0.372	+0.651	+0.160	+0.326	+0.581	+0.138	+0.278	+0.513
4	-0.008	+0.747	+0.753	-0.008	+0.661	+0.672	-0.011	+0.573	+0.594
5	-0.197	+1.123	+0.653	-0.177	+0.996	+0.584	-0.160	+0.867	+0.518
6	-0.335	+1.399	+0.379	-0.301	+1.242	+0.341	-0.271	+1.085	+0.306
7	-0.387	+1.500	+0.004	-0.348	+1.333	+0.008	-0.314	+1.167	+0.016
8	-0.360	+1.489	-0.179	-0.326	+1.324	-0.160	-0.296	+1.159	-0.137
9	-0.277	+1.456	-0.360	-0.253	+1.293	-0.326	-0.235	+1.131	-0.287
10	-0.187	+0.840	-0.974	-0.188	+0.779	-0.883	-0.195	+0.719	-0.789
11	+0.031	+0.542	-0.809	+0.014	+0.498	-0.729	-0.010	+0.455	-0.646
12	+0.209	+0.303	-0.598	+0.177	+0.274	-0.530	+0.138	+0.247	-0.460
13	+0.319	+0.083	-0.335	+0.274	+0.078	-0.296	+0.223	+0.076	-0.257
14	+0.359	+0.004	0	+0.309	+0.008	0	+0.253	+0.015	0

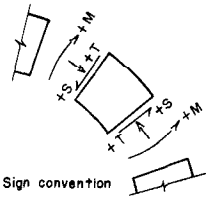

+ Sign convention

REV. JULY 9, 1953
REV. SEP. 28, 1954

SINGLE BARREL CONDUIT
BEGGS DEFORMETER STRESS ANALYSIS

COEFFICIENTS FOR MOMENT, THRUST, AND SHEAR

I. UNIFORM VERTICAL LOAD - UNIFORM FOUNDATION REACTION

SHAPES A, B, AND C

SEP. 8, 1950

X-PEL-372

FIGURE 29 -- Beggs deformeter stress analysis--coefficients for moment, thrust, and shear--uniform vertical load; uniform foundation reaction.

cordance with the convention given on Figure 23. In taking the readings it may be helpful in establishing a point on which to read if a soft-lead pencil is rubbed across the point. Placing a piece of black paper under the model at the point in question may accentuate the point. Readings should be taken as near to the actual load point as is possible.

As stated earlier, when the deflection readings are multiplied by the proper calibration factor the products are the ordinates of an influence diagram. The area under this diagram is the reaction at the cut for a uniform load of unit intensity. This will be either a bending moment, a thrust, or a shear depending upon the type of deformation introduced at the cut.

To avoid unnecessary calculating, it is convenient either to sum up or to plot and planimeter the deflection readings and to apply the calibration factor to the resultant sum or area. Plotting the readings may be helpful since it will disclose, in many cases, any obvious errors in reading or recording. If the load acting is of uniform intensity the readings may be used directly. If the load is variable, then the reading must be multiplied by the ordinate of the load diagram at the point where the reading was taken. If the length increments are equal it simplifies the computations in that the deflection readings may be summed, and the sum multiplied by the length increment and the calibration factor for the particular reaction being considered. If the readings are plotted then the planimetered area must be multiplied by the proper factor for vertical and horizontal scale used in the plotting and also multiplied by the calibration factor for the particular reaction being considered.

In the special case of the dead load of a structure, the readings are taken at the center of gravity of increments of area and are multiplied by the increment of area to give the load-deflection effect for that area. These may be summed and the sum multiplied by the calibration factor to give the reaction. If the increments of area are equal, the deflection readings may be combined and the sum multiplied by the increment and the calibration factor to obtain the desired reaction.

It is thus possible to determine the required magnitudes of the bending moment, thrust, and shear reactions at the cut or gage block to prevent any rotation, thrust, or shear movement due to the load considered. With these three values, a structure which was indeterminate to the third degree is determinate. If the structure is indeterminate beyond the third degree, additional cuts must be made to reduce it to a statically determinate structure.

With the structure statically determinate the moments, thrusts, and shears at various points throughout the structure can be determined by use of the equations of statics. These may be either stress coefficients for a unit load intensity, or they may be actual values for the particular load acting on the structure. These will be the reactions at the centerline of the structure, and the stresses across the section at the extreme fibers must be obtained in the usual manner. Figure 29 shows part of a typical Beggs Deformeter study with a tabulation of the moment, thrust, and shear coefficients for a unit uniform vertical load acting on a single-barrel conduit.

THE ELECTRICAL ANALOGY TRAY

General

The electrical analogy tray is used for experimentally solving certain types of problems arising in the field of hydraulics, particularly in the branch dealing with the slow subsurface seepage flow of water through earth masses. Essentially, the method consists of producing and studying an analogous arrangement or problem in which the actual flow of water is represented by the flow of electricity through an electrolyte in a tray or tank having the same relative dimensions as the prototype.

Theory

The analogy is permissible because Laplace's differential equation is valid for both the flow of electricity through the electrolyte and the flow of water through earth masses. Laplace's differential equation is

Darcy's Law	Ohm's Law
$Q = KA\frac{H}{L}$	$I = K'A'\frac{V}{L'}$
Q represents quantity of water,	I represents amount of current,
K, coefficient of permeability,	K', coefficient of conductivity,
A, cross-sectional area,	A', cross-sectional area,
H, head producing flow, and	V , voltage producing flow, and
L, length of flow path	L', length of flow path.

expressed as:

$$\frac{\partial^2 \phi}{\partial x^2} + \frac{\partial^2 \phi}{\partial y^2} = 0 \quad \ldots\ldots\ldots (19)$$

where

ϕ is a potential function, and

x and y, coordinates of points in the flow field.

The analogy can be seen at once by comparing Darcy's Law for the flow of water through an homogeneous granular material with Ohm's Law for the flow of electricity through a uniformly conductive medium.

Construction of Apparatus

The electrical analogy tray apparatus is basically a Wheatstone bridge circuit so arranged that the relative electrical potential at any point in the electrical analogy tray model may be determined. Figure 30A shows the conventional Wheatstone bridge circuit, and Figure 30B shows the simplified circuit of the electrical analogy tray apparatus. Corresponding points on the two diagrams are designated by the same letter, so the application of the bridge circuit to the electrical analogy tray apparatus may be easily understood. The bridge, as applied to the electrical analogy tray apparatus, is considered to be in balance when points B and D are at the same potential; i.e., no voltage exists between these points. For example, consider the potential selector unit set for a potential of 20 percent: the potential drop between points A and D is then 20 percent of the total potential that exists between points A and C, and the bridge will be in balance when point B is selected so that the potential drop between points A and B is 20 percent of the total potential that exists between points A and C.

The electrical components of the electrical analogy tray apparatus consist of three primary circuits based on their use. These are the selecting, the amplifying, and the indicating units. These components are indicated on the block diagram of Figure 30B and are readily separated on the circuit diagram of Figure 31. In the actual apparatus, the selecting and the indicating units are assembled in the same cabinet and have been called the control panel. An exterior view of this cabinet is shown as Part G of Figure 37, and detailed top and bottom views are shown in Figures 32 and 33. The amplifying unit, in conjunction with the power supply, has been called the chassis. These have been assembled in another cabinet which is located beneath the electric analogy tray table and connected to the control panel by a multistranded cable. Details of the chassis are shown in Figures 34 and 35. Figure 36 is a list of component parts required for the control panel and the chassis.

The potential selector unit, shown in Figure 30B as a variable tapped resistance, is actually, as will be noted by referring to Figures 31, 32, and 33, an assembly of locking type push-button switches (S_4 and S_5) and a potentiometer (R_{16}) connected as shown in the circuit diagram, Figure 31. Each switch assembly is made up of a bank of 10 locking type push-buttons so arranged that each button operates a double pole, sin-

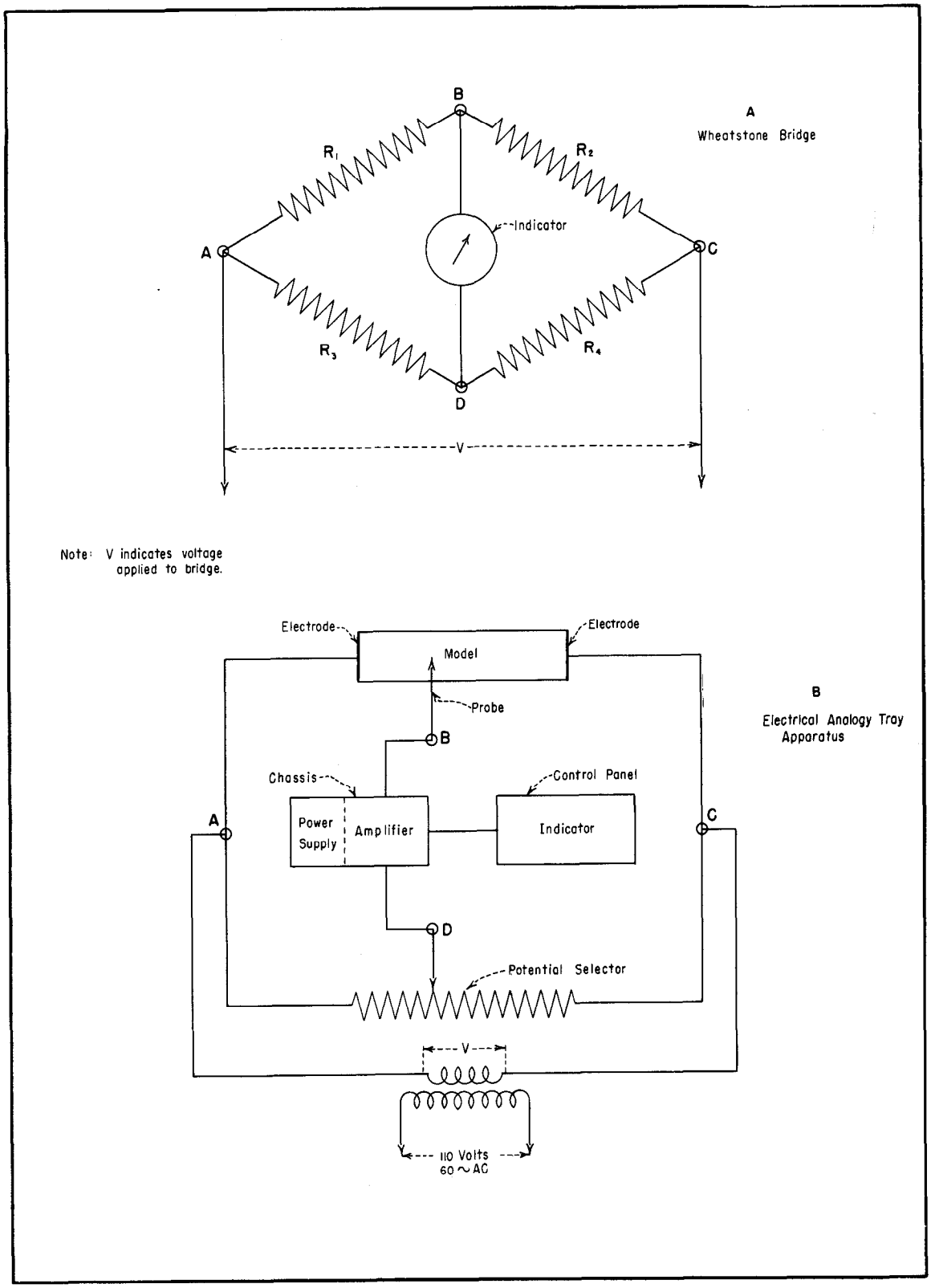

FIGURE 30 -- Electrical analogy tray apparatus--simplified diagrams.

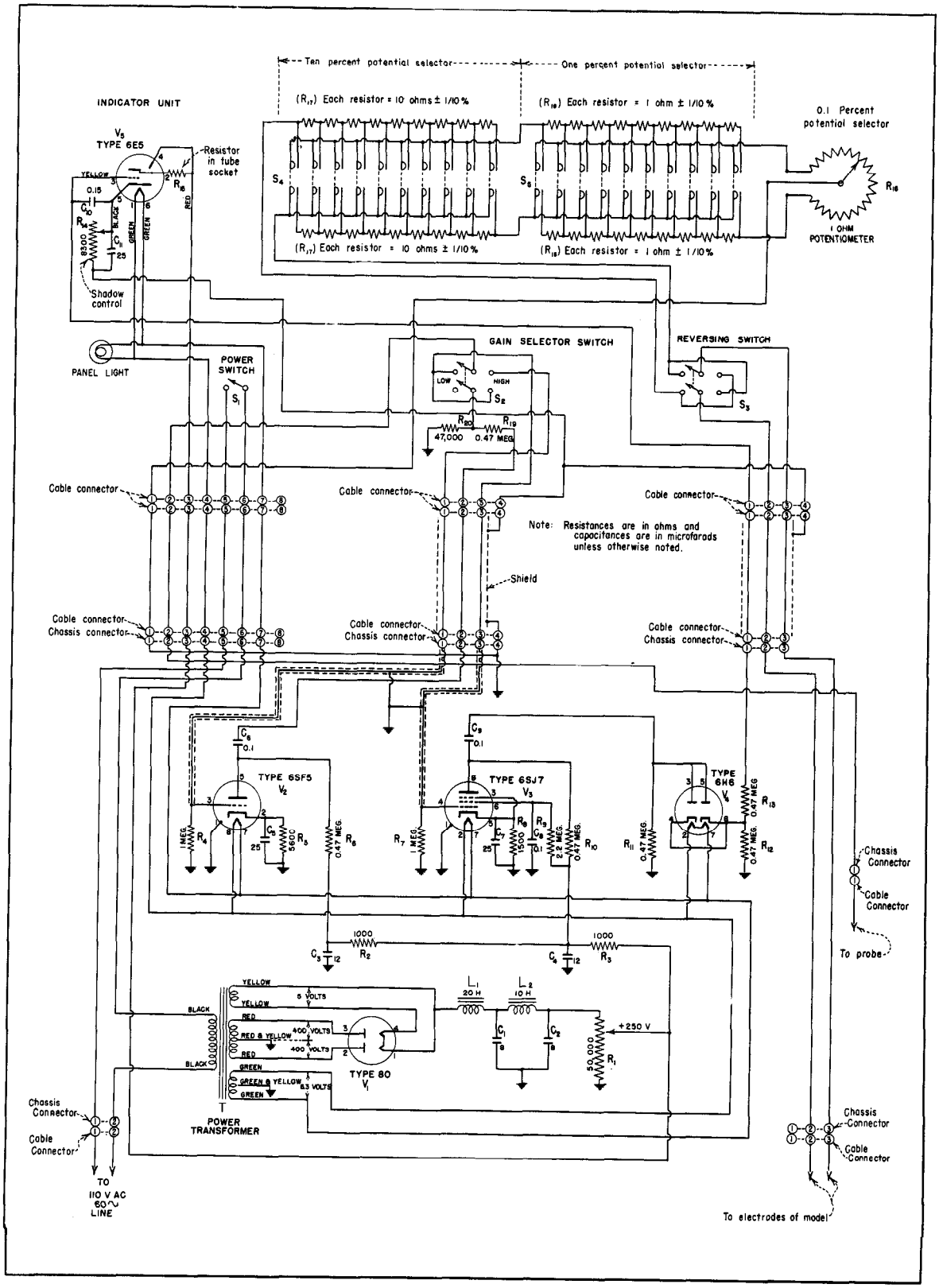

FIGURE 31 -- Electrical analogy tray apparatus--circuit diagram of selecting, amplifying, and indicating units.

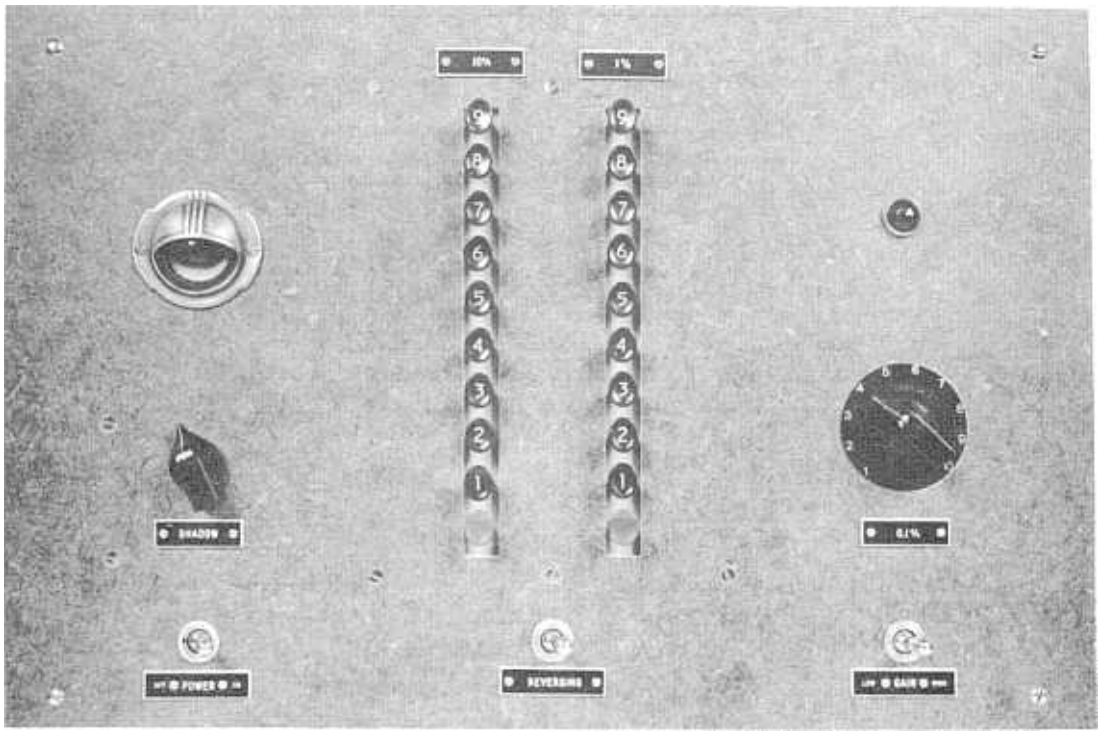

FIGURE 32 -- Electrical analogy tray apparatus--top view of control panel.

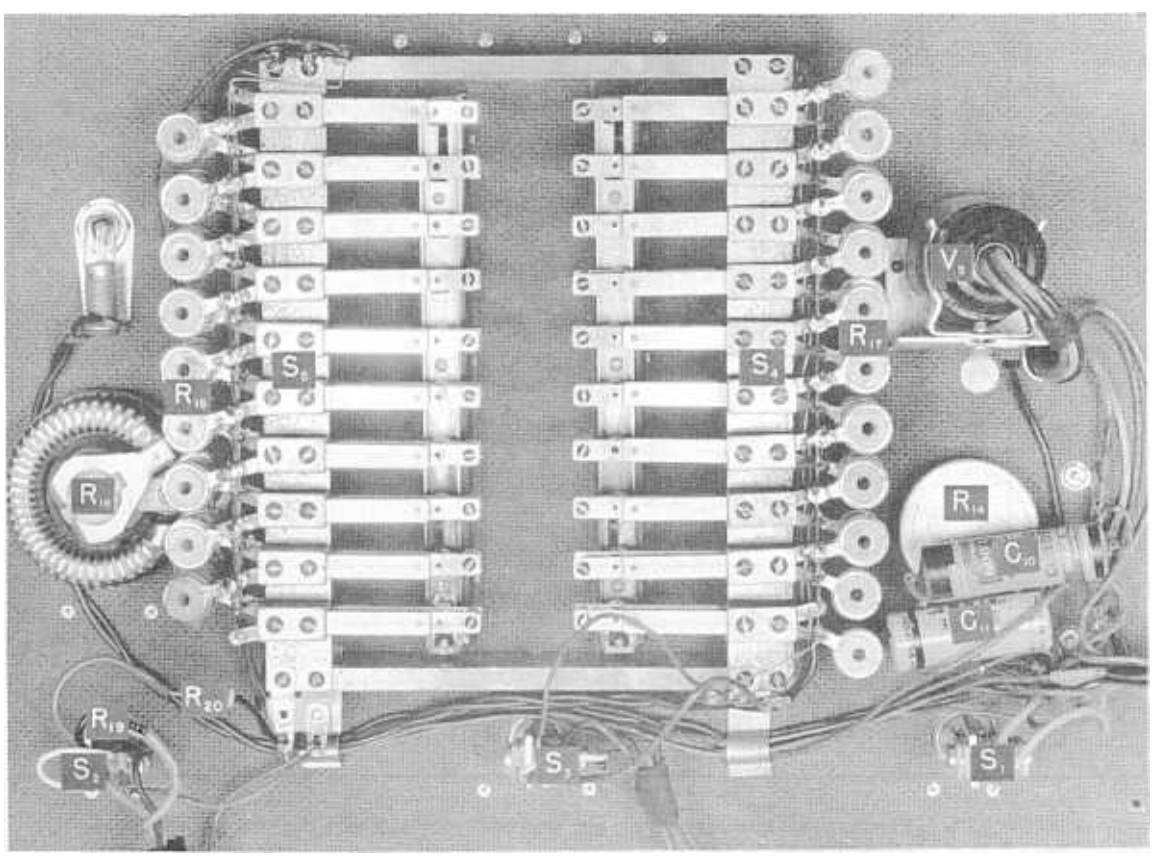

FIGURE 33 -- Electrical analogy tray apparatus--bottom view of control panel.

FIGURE 34 -- Electrical analogy tray apparatus--top view of chassis.

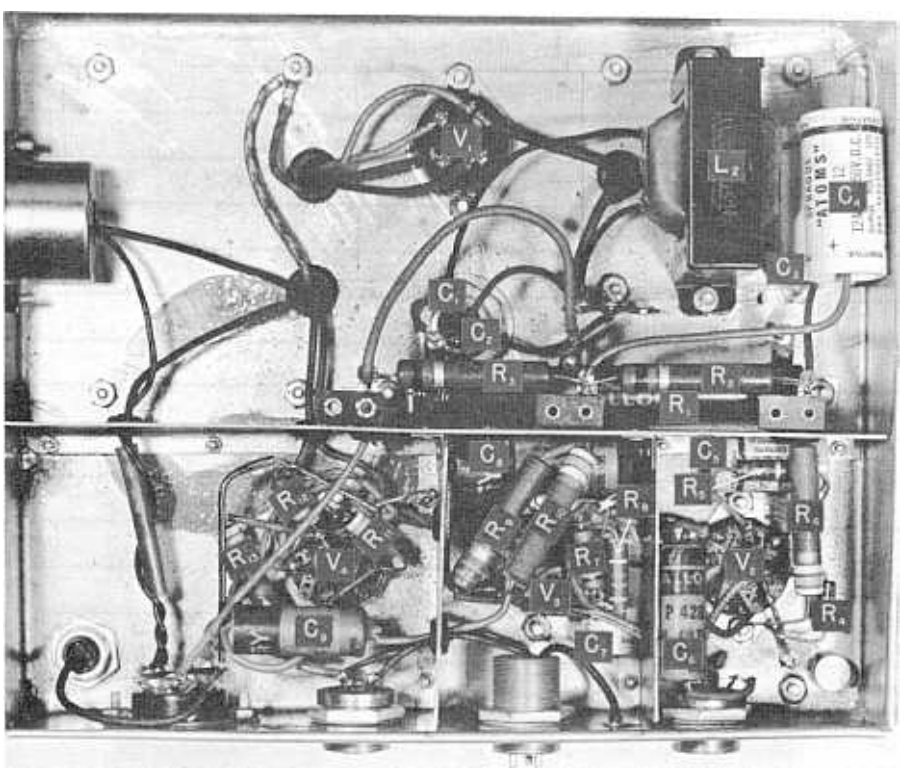

FIGURE 35 -- Electrical analogy tray apparatus--bottom view of chassis.

SYMBOL	COMPONENT PART
R_1	50,000 ohms, 50 watts, variable tap
R_2, R_3	1,000 ohms, 2 watts
R_5	5,600 ohms, 1/2 watt
R_4, R_7	1 megohm, 1/2 watt
R_6, R_{10}, R_{19}	0.47 megohm, 1 watt
R_8	1,500 ohms, 1/2 watt
R_9	2.2 megohms, 1 watt
R_{11}, R_{12}, R_{13}	0.47 megohm, 1/2 watt
R_{14}	8,300 ohms, potentiometer
R_{15}	1 megohm, 1/4 watt, (mounted in tube socket)
R_{16}	1 ohm, potentiometer
R_{17}	10 ohms, precision wire wound, (±0.1% of 1%)
R_{18}	1 ohm, precision wire wound, (±0.1% of 1%)
R_{20}	47,000 ohms, 1 watt
C_1, C_2	8-8 mfd, dry electrolytic, 600 V. D.C.
C_3, C_4	12 mfd, dry electrolytic, 450 V. D.C.
C_5, C_7, C_{11}	25 mfd, dry electrolytic, 25 V. D.C.
C_6, C_9	0.1 mfd, paper, 400 V. D.C.
C_8	0.1 mfd, paper, 600 V. D.C.
C_{10}	0.15 mfd, paper, 600 V. D.C.
T_1	Power transformer, 400-0-400 V., 6.3 V., 5 V.
L_1	Filter choke, 20 henries
L_2	Filter choke, 10 henries
V_1	Vacuum tube, type 80
V_2	Vacuum tube, type 6SF5
V_3	Vacuum tube, type 6SJ7
V_4	Vacuum tube, type 6H6
V_5	Vacuum tube, type 6E5
S_1	Switch, toggle, S.P.S.T.
S_2, S_3	Switch, toggle, D.P.D.T.
S_4, S_5	Switch assembly, potential selector
Panel Lamp	6-8 V., 0.15 amp.

FIGURE 36 -- Electrical analogy tray apparatus--component parts.

gle throw, leaf-type switch. These switches are normally open. One switch is mounted beneath each push-button so that depressing the button causes the switch to close. Switch assembly S_4 permits the selection of potentials in multiples of 10, i.e., 0%, 10%, 20%, 30% ... 80%, 90%. Switch assembly S_5 permits the selection of potentials in units, i.e., 0%, 1%, 2% ... 8%, 9%. The potentiometer R_{16} permits the selection of potentials in the range 0% to 1%. The potentiometer dial permits direct reading to 1/10 of 1%.

The voltage developed across the center arm of the bridge circuit (point B to D, Figures 30A and 30B), i.e., between the probe and the variable tap on the potential selecting unit (the center tap of potentiometer (R_{16}) is applied to the amplifier unit. This unit consists of a pentode (6SJ7) amplifier, V_3, used for low gain, and this in cascade with a triode (6SF5) amplifier, V_2, provides the high gain. The GAIN switch on the control panel permits the operator to select the amplifier stage most suitable for use with the model being surveyed. The High GAIN stage gives a voltage gain approximately twice that of the LOW GAIN stage. Both amplifier stages are conventional circuits.

The output of the amplifiers is rectified by the rectifier tube (6H6), V_4, before being applied to the null indicator V_5. This eliminates any shadow fluctuation and causes the shadow to show minimum angle at the balance point. The null indicator is a type 6E5 electron-ray tube (indicator type). This is a voltage indicating device which indicates visually, by means of a fluorescent target, a change in the controlling voltage. The visible effect is observed on the fluorescent target located in the end of the bulb. The pattern on the target varies from a shaded angle of approximately 90 degrees, when the bridge is out of balance, to a shaded angle of approximately 0 degrees when the bridge is balanced. The shaded angle (shadow) may be varied by the operator by means of the SHADOW control on the control panel. The action of this control is to vary the bias applied to the 6E5 tube by varying the resistance in the cathode circuit of the tube. Otherwise the indicating tube circuit is conventional.

The POWER switch on the control panel is a single pole, single throw, toggle switch connected in the primary circuit of the power transformer. In the operation of the electrical analogy apparatus the electrode of the model which is considered to be at 0% potential is connected to the 0% end of the potential selecting unit. The REVERSING switch provides a convenient means of reversing the connections to the model with respect to the potential selecting unit. The panel lamp is connected in the filament circuit and operates as an ON - OFF indicator. Figures 34 and 35 are photographs of the assembled amplifier unit.

For convenience in locating coordinates of points, a scanning device is used. The arrangement is shown in Figure 37. Two fixed parallel bars, A, which are adjustable in height for leveling purposes, carry a movable cross-assembly, B. In turn, the movable cross-assembly carries a mount, C, which holds the probe needle, D. Mount C is movable along the cross-assembly, B. The scale, E, forms a part of the cross-assembly B and provides a coordinate system for lateral movement. The scale, F, provides a measure of the coordinates in the direction normal to scale, E. The entire scanning device is mounted securely on a rigid table.

Construction of Models

Electrical analogy tray models are usually prepared of sheet plastics such as cellulose nitrate, cellulose acetate, plexiglas, or lucite. These materials are machined easily, and are welded together by wetting with acetone or other suitable solvents. Since the procedure for preparing models is more easily described for two-dimensional problems, the discussion will be confined to the procedure for such a problem. However, by proper consideration of boundary conditions, relative dimensions, and other related factors, three-dimensional models may be constructed. As an example, to simplify the discussion, consider an earth dam resting on an impervious foundation as shown in Figure 38.

To prepare the model, a thin sheet of the plastic (usually 1/10-inch thick) is cemented to a piece of plate glass or plywood. On this are erected vertical strips of the plastic (usually 1 to 2 inches high) along the

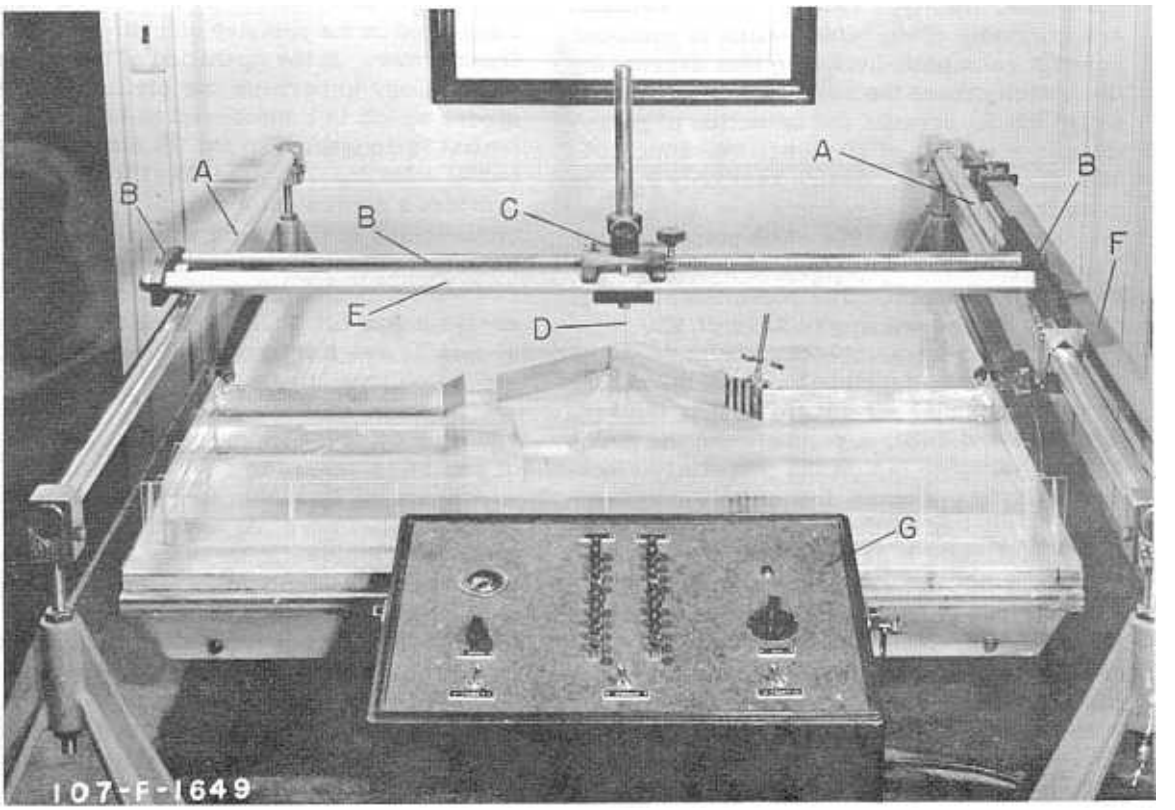

FIGURE 37 -- Arrangement of electrical analogy tray apparatus.

lines which define, to scale, the cross-section of the dam. The strips are cemented with solvent to the base sheet. Boundary conditions are satisfied by establishing electrical potentials corresponding to the hydraulic potentials. Since the actual potentials or voltages at specific points on the model are of no concern, the total potential in the system is represented as unity, and the potential at interior points is determined as a percent of the total.

The potential function, when a gravity field exists in the plane of the model, is

$$\phi = P \pm y \quad \ldots\ldots\ldots\ldots (20)$$

where

ϕ represents potential,

P, internal water pore pressure, and

y, vertical coordinate of the point.

Equation (20) is used to establish the boundary conditions for the model. A coordinate system as shown in Figure 38 is used; and, in the case under consideration, equation (20) must be used with the plus sign. Then along the upstream face of the dam, ϕ becomes equal everywhere to a constant (H in this case), since:

$$\phi = P + y = H$$

Along the downstream face of the dam $P = 0$; therefore;

$$\phi = + y$$

In this application, the upper line of saturation within the dam also must be established. This line, called the phreatic line, is both a streamline and a line of zero pressure. Then since $P = 0$ it again follows:

$$\phi = + y$$

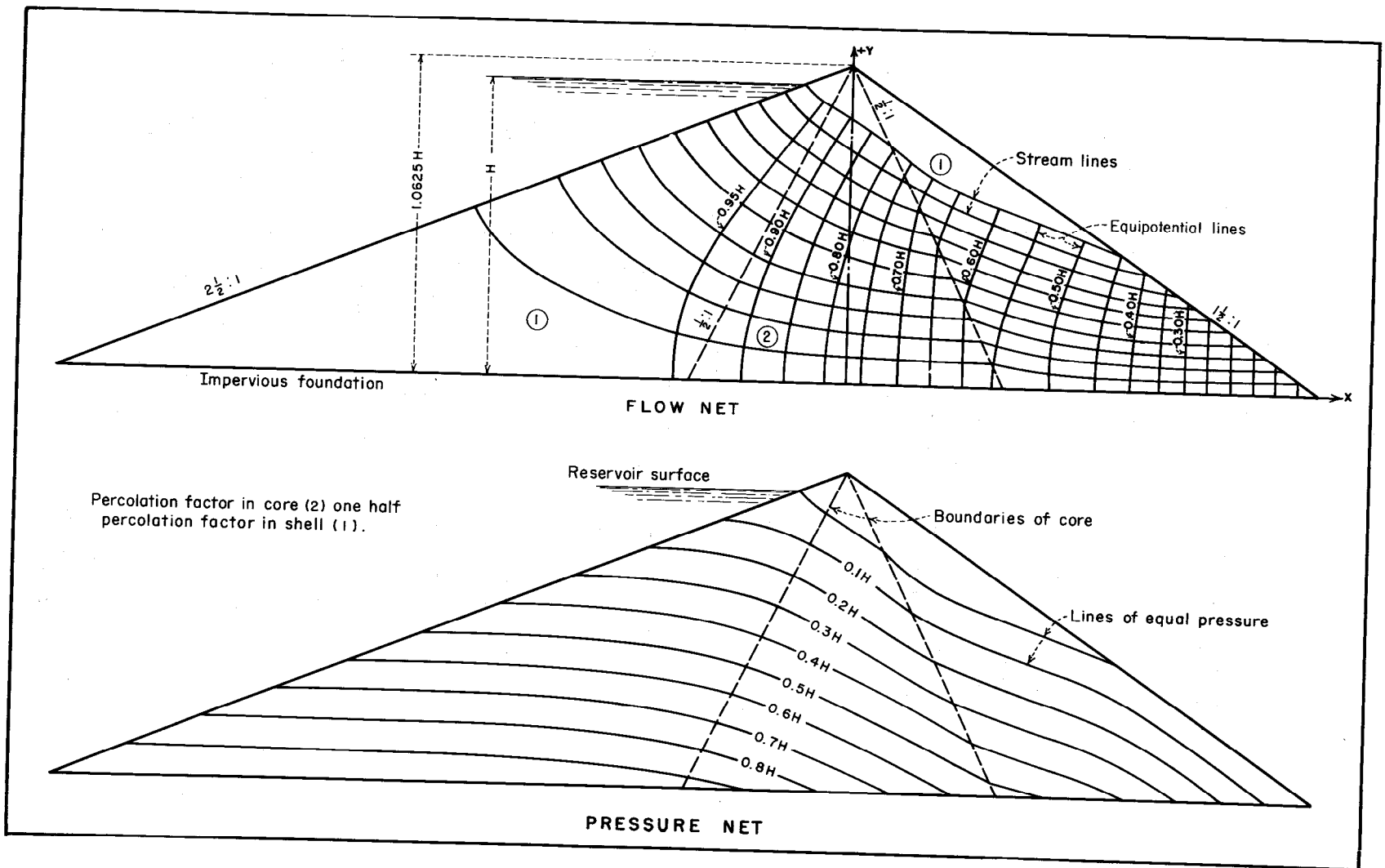

FIGURE 38 -- Electrical analogy tray study of earth dam.

The location of the phreatic line is usually found by a cut-and-try process which will be described later.

In the model, the constant-potential upstream boundary is represented by a strip of metal (either brass or copper may be used provided that the same metal is used throughout the model to prevent electrolysis) which is at a constant electrical potential. The base of the dam, which is a stream line, is represented by a nonconducting plastic strip. The varying potential which exists on the downstream face is approximated by a series of small metal strips attached to the plastic boundary. These strips are of equal width and are spaced uniformly along the boundary from the reservoir water level to the tailwater surface. The potential of each strip is controlled, from 100% on the strip at the elevation of the reservoir water surface to 0% on the strip at the tailwater surface, by means of a number of resistors of equal value connected in series. The strips are connected to the junctions of the resistors. Usually 20 resistors and an equal number of strips are used so that the potential will vary along the downstream boundary in 5% steps. The more strips used, the closer the downstream boundary will represent the theoretical uniformly varying potential boundary. Any strips which lie above the phreatic line may be omitted as shown in Figure 39; however, the equivalent resistance must still be included, but it may be done with a single resistor. The phreatic line, which is also a stream line, is represented by a nonconducting boundary made of modeling clay. Clay is used in order to facilitate the rapid change of the location of the phreatic line required in the cut-and-try procedure used to determine its final form and location. The clay for the phreatic line is placed in the model and trimmed approximately to shape. Details concerning the determination of the final shape and its location are given later. Experience and reference to previous studies will indicate the general shape of the boundary. Figure 39 shows a diagrammatic layout of the model and the electrical circuits.

Operation

The model, having been prepared as described previously, is placed under the scanning device and leveled in all directions. The model is oriented with respect to the coordinate system of the scanning device so that the probe needle, in being moved along some constant coordinate, traverses a selected reference line on the model. The electrodes of the model are connected to the leads from the potential selector unit. Usually it is desired that the upstream boundary be at 100 percent potential and the toe of the downstream boundary or tailwater at zero potential. If it is found that the opposite condition exists, it is only necessary to throw the reversing switch located on the control panel of the potential selector unit.

Ordinary tap water has been found to be a satisfactory electrolyte. The electrolyte is put in the model to the proper depth, and the probe needle lowered into the electrolyte until the tip is just under the surface. It should be kept in mind that the surface of the electrolyte is a plane on which the equipotential net is to be investigated and as such has no depth.

The clay boundary representing the phreatic line is now shaped so as to satisfy the boundary conditions. To do this a point is selected on the approximate phreatic line a distance y above the impervious foundation, and the potential is read at this point. As shown by equation (22), the potential here must equal y. Since the potentials are to be determined in percent, it may be stated: If, at the point in question, y equals 80 percent of H (where H is the depth of water in the reservoir) then ϕ also must equal 80 percent. If ϕ as read on the potential selector unit is not 80 percent, the clay boundary must be adjusted until $y = \phi$. Several values of ϕ must be checked in a similar manner until the complete phreatic line is located.

When the phreatic line has been established, the potentials throughout the model are then surveyed. In conducting the experiment, two persons are normally employed. One, the operator, controls the scanning device and the potential selector unit. The other, the recorder, prepares a plan of the model, superimposes thereon a coordinate system corresponding to that of the scanning device and plots readings given to him by the operator. Normally, the equipotential lines are surveyed at 5 percent intervals except where it is necessary to find intermediate lines due to excessive width between the 5 percent lines, or where the

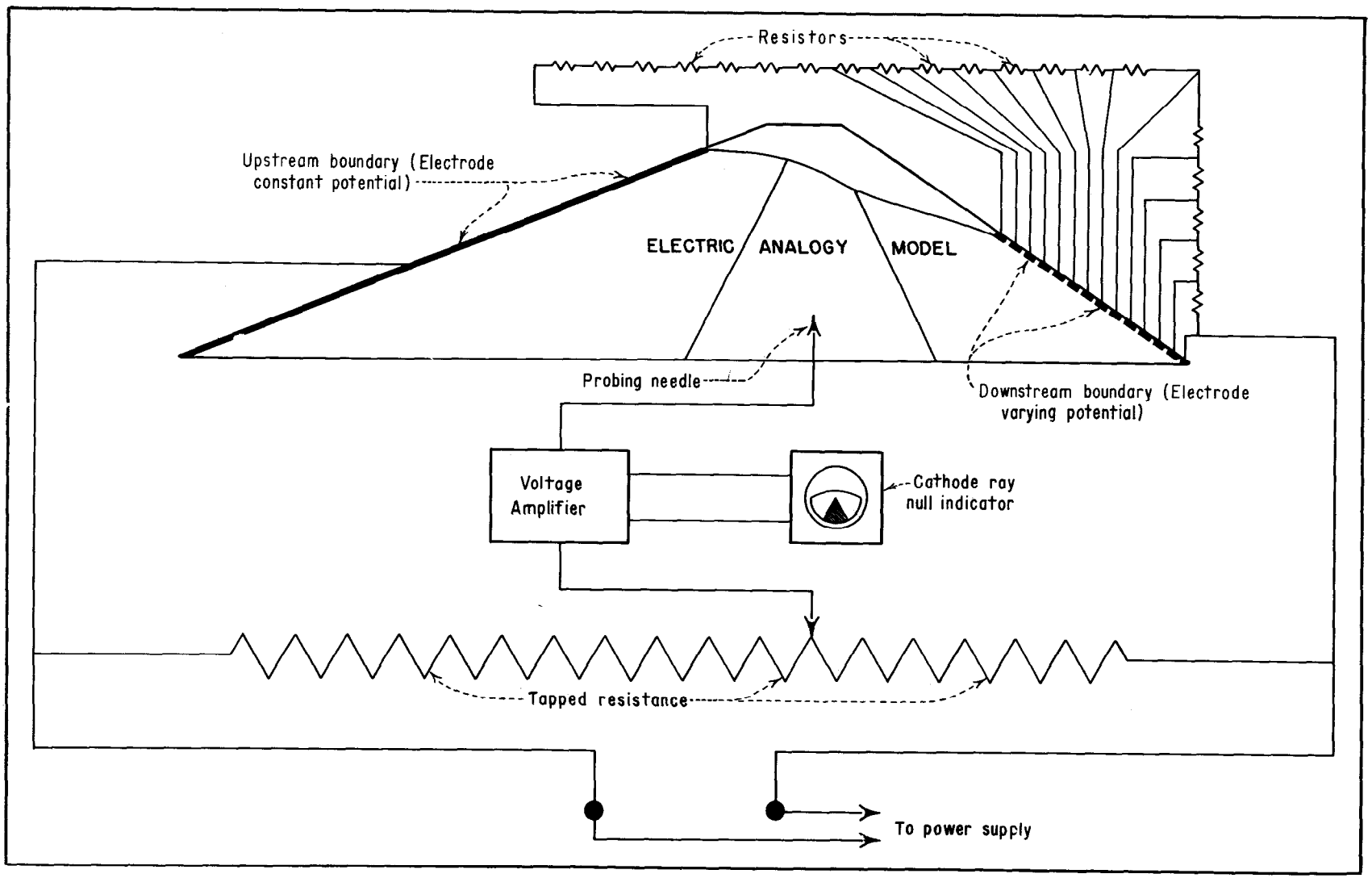

FIGURE 39 -- Electrical analogy tray diagrammatic layout--Wheatstone bridge circuit.

actual potential at a specific point is desired. The procedure to survey a potential line is as follows: The potential selector unit is first set for the required potential. The scanning device is then set at some coordinate, either x or y. The other coordinate of the point on the equipotential line is determined by moving the needle along the axis until the circuit is in balance. The circuit is in balance when the shadow in the indicator tube is at a minimum width. The coordinates are given to the recorder, who plots the point on the drawing of the model. The scanning device is then moved to a new coordinate, and the operation repeated. The spacing of the coordinates is so chosen that a smooth curve may be drawn through the plotted points. Where the curve is relatively flat, the points may be taken some distance apart; and, conversely, when the curvature is great, the points must be taken close together. This operation is repeated until the line is surveyed along its entire length. The recorder may, by inspection of the drawing and plotted points, have intermediate points taken where necessary to complete the curves. When a line is finished, the operator sets another potential value on the potential selector unit and surveys the new line in a similar manner. These operations are repeated until the entire equipotential net has been surveyed and plotted. If the potential value at a particular point is desired, the probe needle is placed at the point in question, and the switches on the potential selector unit adjusted until the indicator tube shows that the bridge is in balance. The potential value at the point can be read directly from the setting of the switches.

Smooth curves are then made to connect points of equal potential to form the equipotential net. It should be remembered that the equipotential lines must be normal to the stream lines. In Figure 38, the impervious foundation and the phreatic line are stream lines from the imposed conditions; therefore, the equipotential lines must be normal to them.

When the stream lines are superimposed on the equipotential lines, the resulting pattern is called the flow net. The stream lines are usually drawn in as a system of curvilinear squares, but under certain boundary conditions, they may be determined by use of the electrical analogy tray apparatus. In either procedure it should be remembered, as mentioned previously, that the two systems of lines are at right angles to each other at all points. It will be found convenient in simplifying the computations for quantity of seepage flow, if the flow net pattern is made to form a system of squares. If the stream lines are to be sketched in, the spacings between the equipotential lines should be measured, and the stream lines spaced that same distance apart. Proficiency will be acquired with practice.

If the stream lines are to be determined by use of the electrical analogy tray apparatus, the upstream and downstream faces of the dam are made nonconducting boundaries. The phreatic line is placed at zero potential, and the base or impervious foundation is placed at 100 percent potential. With this arrangement, the stream lines are surveyed. They form, actually, a new equipotential net. The spacings should, if possible, be such as to form squares with the original equipotential net. If this is not possible, then the lines should be used as guides to indicate the pattern that the flow is following, and the proper number of lines drawn in to provide the required system of squares.

The following requirements should be remembered in the construction of the flow net for the dam outlined in Figure 38 and for similar problems:

1. The phreatic line and the impervious foundation are stream lines.

2. Any surface exposed to standing water is an equipotential line.

3. The surface from the lower end of the phreatic line to tailwater is a free surface but not a stream line; therefore, the equipotential lines may intersect it at any angle.

4. Since the phreatic line and the impervious foundation are stream lines, the equipotential lines must intersect them at right angles.

The pressure net can also be determined from the equipotential net. Lines of equal pressure can be computed from the equation

$$P = \emptyset - y \quad \ldots\ldots\ldots\ldots \quad (23)$$

where the values of ϕ are selected at specific points on the equipotential net, and y is the percent of the total head, H, at the point at which ϕ is taken. The pressure, P, will also be in percent of the head, H. Figure 38 also shows the pressure net.

The seepage losses, if desired, are computed from the equipotential net. Darcy's Law may be written as

$$Q = KA \frac{\partial P}{\partial S} \quad \ldots\ldots\ldots\ldots (24)$$

where

Q represents rate of flow,

K, coefficient of permeability of soil,

A, cross-sectional area, and

$\frac{\partial P}{\partial S}$, pressure gradient.

Equation (24) may be modified by the substitution of finite increments as indicated on Figure 40. This gives

$$\frac{\partial P}{\partial S} \quad \frac{\Delta H}{\Delta L} \quad \ldots\ldots\ldots\ldots (25)$$

and equation (24) becomes

$$Q = KA \frac{\Delta H}{\Delta L} \quad \ldots\ldots\ldots\ldots (26)$$

If the distance between stream lines is ΔD, see Figure 40, and the thickness of the section is unity, the cross-sectional area of the flow tube is $(1)(\Delta D)$. Further, if ΔQ is the rate of flow for any flow tube, then equation (26) becomes

$$\Delta Q = K \frac{\Delta H}{\Delta L} \Delta D \quad \ldots\ldots\ldots\ldots (27)$$

but from the construction of the flow net $\Delta L = \Delta D$ so

$$\Delta Q = K \Delta H \quad \ldots\ldots\ldots\ldots (28)$$

If n_e = number of increments into which H is divided then

$$\Delta H = \frac{H}{n_e}$$

and

$$\Delta Q = K \frac{H}{n_e} \quad \ldots\ldots\ldots\ldots (29)$$

Since the quantity of water passing through each flow channel is equal, and, if the number of flow channels is n_f, the total quantity of water is

$$Q = n_f \Delta Q = KH \frac{n_f}{n_e} \quad \ldots\ldots (30)$$

Consistent units must be employed. The quantity of flow given by equation (30) will be for a section of unit thickness.

An alternate method of computing the quantity of flow consists of making electrical measurements of the current and voltage drop on the model and relating them to the prototype by the comparison between Ohm's Law and Darcy's Law given previously and repeated on page 62.

If $\frac{b}{L}$ and $\frac{b'}{L'}$ are considered as ratios, then, since the model and prototype are dimensionally similar, $\frac{b}{L} = \frac{b'}{L'}$.

From equation (34)

$$\frac{b'}{L'} = \frac{I}{K'Vd'} = \frac{b}{L} \quad \ldots\ldots\ldots (35)$$

Substituting $\frac{I}{K'Vd'} = \frac{b}{L}$ in equation (33)

$$Q = \frac{KHdI}{K'd'V} \quad \ldots\ldots\ldots\ldots (36)$$

Since the thickness of the section in the prototype has been taken as unity, equation (36) may be written

$$Q = KH \frac{I}{K'd'V} \quad \ldots\ldots\ldots (37)$$

Equation (34) can be written in the form

$$K' = \frac{IL'}{Vb'd'} \quad \ldots\ldots\ldots\ldots (38)$$

Equation (38) can be solved by calibration of the electrolyte in the model. To do this a small rectangular test tank is constructed

PROTOTYPE Darcy's Law	MODEL Ohm's Law
$Q = KA\frac{H}{L}$ . . . . . (31)	$I = K'A'\frac{V}{L'}$ . . . . . (32)
Q represents quantity of water,	I represents amount of current,
K, coefficient of permeability,	K', coefficient of conductivity,
A, cross-sectional area,	A', cross-sectional area,
H, head producing flow, and	V , voltage producing flow, and
L, length of flow path.	L', length of flow path.
Let A = bd where b is the height of the section and d the thickness; then	Let A' = b'd' where b' is the height of the section and d' the depth of solution; then
$Q = Kbd\frac{H}{L}$ . . . . . (33)	$I = K'b'd'\frac{V}{L'}$ . . . . . (34)

with electrodes on opposite ends. The same solution used in the experimental model is placed in the test tank, and the test tank is connected into the Wheatstone bridge circuit in place of the experimental model. The current and voltage drop are measured, and the dimensions L', b', and d' of the test tank are also measured. This gives all the required data to determine K' in equation (38).

With the experimental model back in the Wheatstone bridge circuit, the current and voltage drop between the 100 and 0 percent potentials can be measured. The depth, d', of the electrolyte can also be measured. With K and H of the prototype known, the quantity of flow can be determined by using equation (37).

The electrical analogy tray is most readily adapted to problems in which the coefficient of permeability is constant throughout the soil mass. However, certain variations in permeability can be introduced into the problem by proper construction of the model. A common type of variation of permeability is the condition shown by Figure 38 where a core of less permeable material than the outer zones exists in an earth dam. This is accomplished by a stepped construction and the use of the proper depth of electrolyte to give the ratios of permeability desired. It is advisable to fasten small metal strips or wires vertically on the boundaries of the stepped section of the model to insure the proper flow conditions, particularly if the ratio of the depths is large. Quite frequently, the permeability at any point is the same in all directions but diminishes with depth. This condition may be simulated by tilting the tray and allowing the depth of solution to be proportional to the permeability. Another condition of nonhomogeneity occurs when the permeability in a horizontal direction is greater than in a vertical direction. This is brought about by stratification of the foundation material. If the ratio C of horizontal permeability to vertical permeability is constant at all points, the condition may be represented by studying a model of the structure that has had its horizontal dimensions reduced by the ratio $1 \div \sqrt{C}$. The equipotential and stream lines are found for the compressed model and then expanded to the proper scale. The resultant flow net will not have flow lines orthogonal to the equipotential lines.

Another problem related to earth dam design that can be solved by the electrical analogy tray apparatus is that of rapid drawdown of the reservoir. In solving this problem the drawdown is considered to be instantaneous, and thus the head of water within the dam remains at the full reservoir water surface elevation. In other words, the point of intersection of the full reservoir water surface with the upstream face of the dam is the 100 percent potential. The surface from this point along the upstream face to

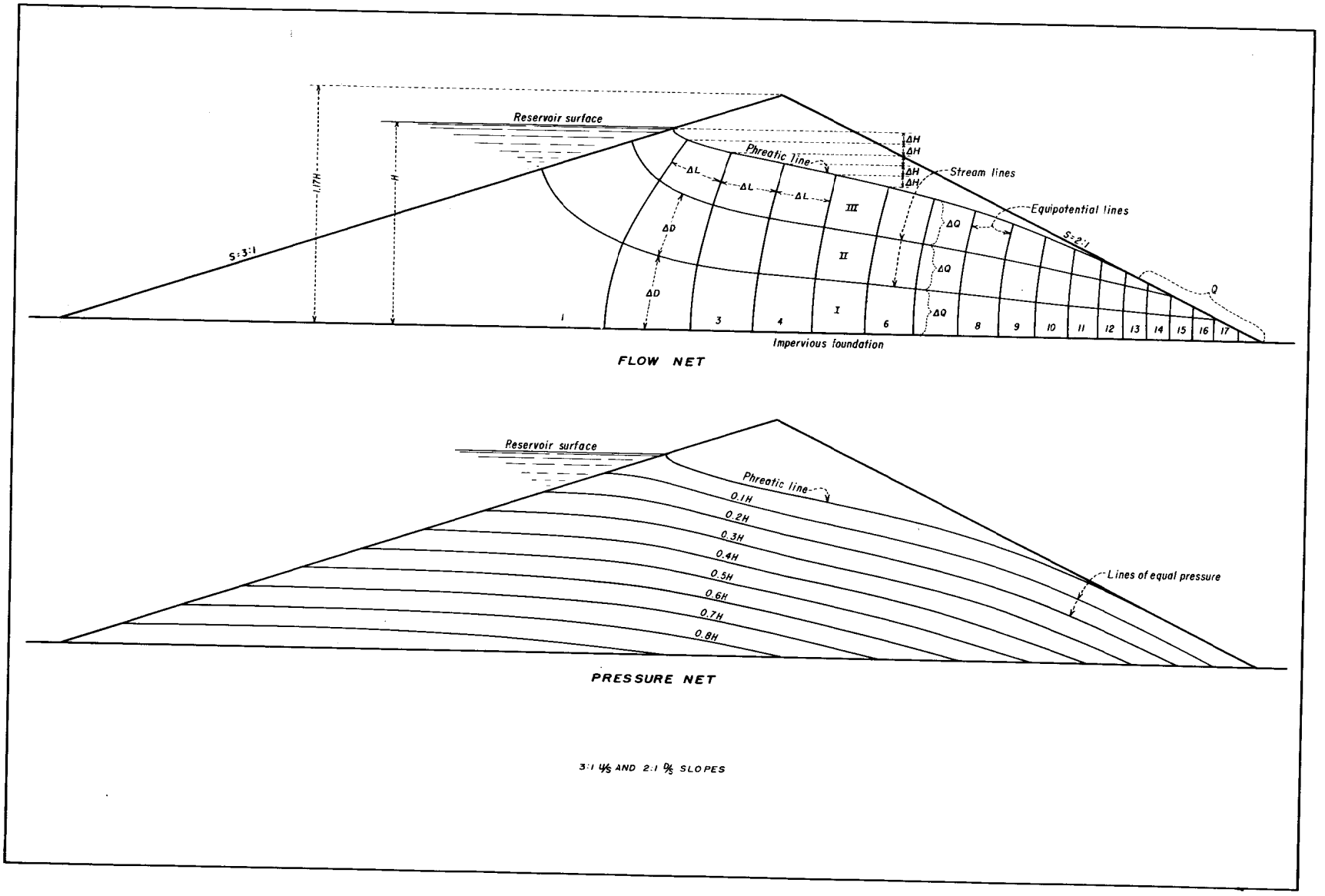

FIGURE 40 -- Electrical analogy tray study of earth dam. Homogeneus material, steady state of flow.

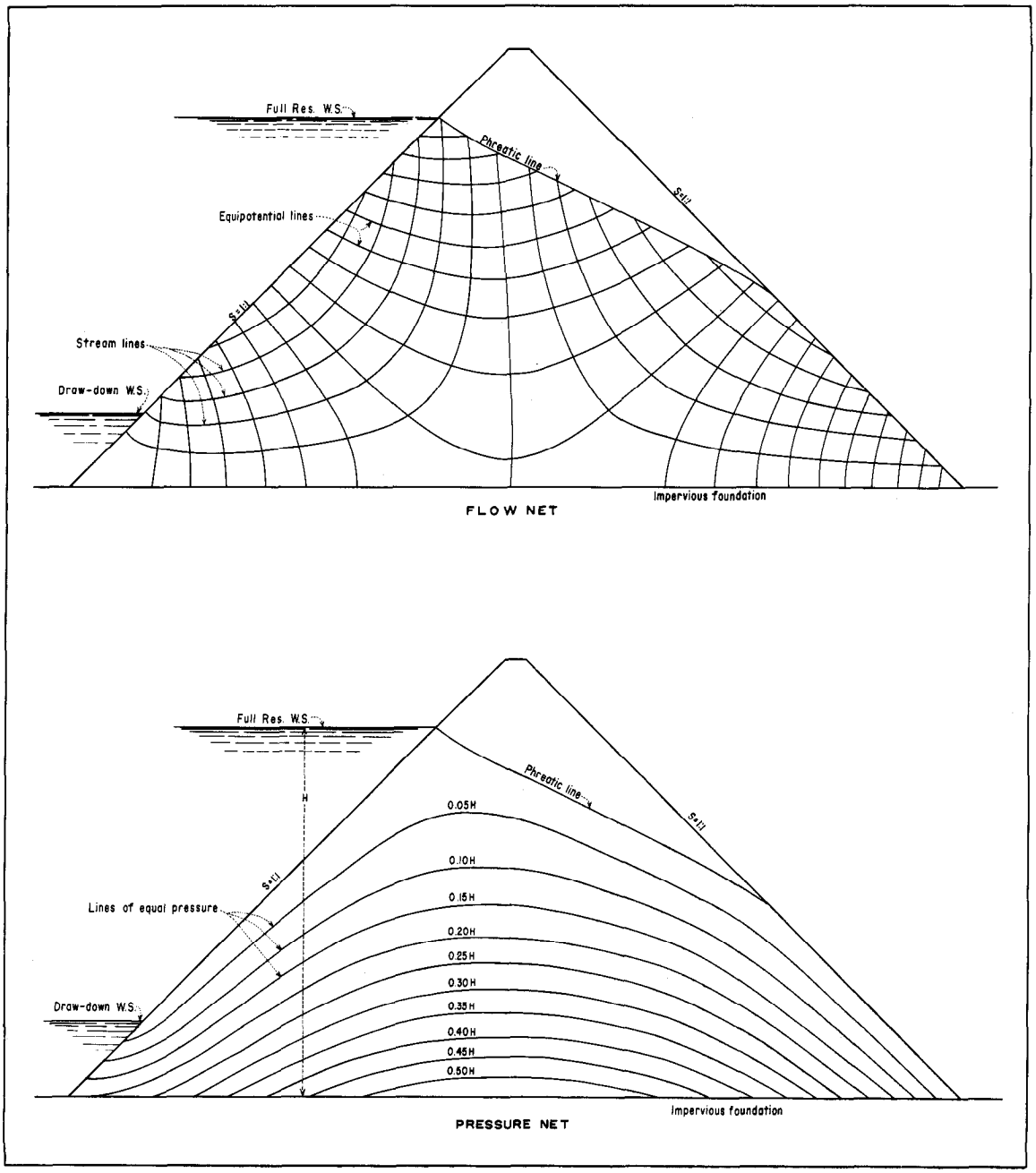

FIGURE 41 -- Rapid draw-down flow and pressure nets. Homogeneous and isotropic material.

the lowered water surface elevation is considered to be a free surface, and the portion below the lowered water surface is of a potential equal to the lowered elevation divided by the full reservoir elevation.

The phreatic line is first established for a full reservoir in the usual manner. The upstream, or 100 percent, electrode is then cut down to the elevation of the lowered water surface and then connected to the proper resistance. The remaining resistance is varied uniformly along the upstream face, reaching 100 percent of the entrance of the phreatic line and the original full reservoir water surface elevation. The equi-

potential lines are then surveyed in the usual manner.

With the equipotential lines thus established, the stream lines can be drawn to complete the flow net. From the equipotential net, the pressure net can be constructed by use of equation (23). An example of the flow net and the pressure net is given in Figure 41.

By proper consideration of model construction and boundary conditions, a great many types of problems can be solved by use of the electrical analogy tray apparatus. The example of an earth dam has been given in order to simplify the discussion of the technique, construction, and operation, and by no means represents the only type of solution obtainable from the apparatus.

An application of the electrical analogy tray to three-dimensional problems is the determination of flow conditions in an hydraulic structure such as a draft tube or needle valve. In problems of this type the velocity head is not negligible but must be evaluated from the spacing of the equipotential lines before the pressures can be determined. In problems such as a needle valve, where the flow lines do not cross planes containing the centerline of the structure, only a small sector of the structure need be simulated in the model. This is readily accomplished by use of a tilted type of model with the centerline of the structure at zero depth of electrolyte. The application of the analogy to problems of this type is based on the condition of laminar flow below the critical velocity.

Other applications of the electrical analogy tray include the effect of earthquake forces on dams[40], permeability determination studies[41,42], the effect of rapid drawdown of reservoirs, the effect of cut-off walls and clay blankets on seepage and pore pressures, the effect of drains of various sizes and spacings in reducing uplift, and many others similar problems. Although problems such as these are far removed from those of seepage flow and pore pressure in earth dams, they are mentioned here to illustrate the wide field of application of the electrical analogy tray apparatus.

THE MEMBRANE ANALOGY

General

The membrane analogy can be used to obtain experimental solutions to several types of problems, such as, (1) potential flow, (2) sum of the principal stresses throughout a structure, and (3) torsional stresses in various structural shapes. The electrical analogy tray can be used with greater ease for problems of the first type. There is no need to obtain the sum of the principal stresses in a model, since the photoelastic interferometer obtains each principal stress separately in direction and magnitude. As a result, the membrane analogy is now used by the Bureau of Reclamation only for obtaining torsional stresses in structural shapes.

Theory

From the mathematical theory of elasticity[43] it can be shown that Poisson's differential equation governs the displacements and stresses in prismatical bars subjected to torsion; that is

$$\frac{\partial^2 \phi}{\partial x^2} + \frac{\partial^2 \phi}{\partial y^2} = -2G\theta \quad \ldots\ldots\ldots \quad (39)$$

where

ϕ represents a stress function,

x and y, coordinates of a point in the cross-section of the bar

G, shear modulus of the material, and

θ, angle of twist per unit length.

It can also be shown[44,45,46] that the deflections of a thin membrane which is stretched across an opening of the same shape as a section being studied for torsion and

slightly distended vertically will satisfy the same differential equation that applies to a bar subjected to torsion. To do this the assumption must be made that the tension in the membrane is uniform in all directions and is independent of shape or location. Also, it must be assumed that the pressure acting under the membrane acts normal to the undistended surface rather than normal to the distended surface of the membrane. This assumption is very nearly true if the membrane is distended only slightly. From the above considerations it can be shown that the equation of the membrane surface is:

$$\frac{\partial^2 z}{\partial x^2} + \frac{\partial^2 z}{\partial y^2} = -\frac{p}{T} \quad \ldots\ldots\ldots\ldots \quad (40)$$

where

x, y, z represent rectangular coordinates,

p, unit uniform pressure applied to the membrane, and

T unit tension in the membrane

From an inspection of equations (39) and (40) the analogy is readily apparent. It is only necessary to represent $2G\theta$ with p/T.

The theory also indicates that the following conditions exist:

1. The torsional rigidity is proportional to the volume under the distended membrane.

2. The torsional shearing stress at any point on the cross-section is proportional to the maximum slope of the membrane at that point.

3. The contour lines on the membrane represent directions of maximum shearing stress.

From the above conditions it may be written:

$$\tau = \frac{M_T}{2V} \frac{\partial z}{\partial n} \frac{1}{s^3} \quad \ldots\ldots\ldots\ldots \quad (41)$$

where

τ represents torsional shear in the direction of the contour,

M_T, torsional moment,

V, the volume under the membrane below the contour line where τ is being determined,

$\frac{\partial z}{\partial n}$, the maximum slope at the point in question, and

s, a linear scale factor between model and prototype.

Procedure

The procedure used here is to cut an opening, similar in shape to the cross-section of the structural shape being studied, in a thin metal or wood plate. A thin, uniformly stretched, rubber membrane is then placed between this plate and a base plate. In order to obtain a constant tension, T, throughout, the membrane is ruled with equally spaced lines in two perpendicular directions, and is then stretched over a frame until the ruled network is about doubled in size but still forms equal squares throughout.

Through an opening in the base plate, the membrane is subjected to a low air pressure. This causes the membrane to assume a deformed shape which can be surveyed by means of a scanning device and depth gage such as that shown in Figure 42. Lines of constant elevation (contours) are surveyed on the deformed membrane and plotted. The derivation of the differential equation for the stretched membrane includes the assumption that the slope of the membrane at all points is sufficiently small, so that the cosine of the slope angle may be taken as equal to unity. The smaller the distortions are made, the greater will be the conformity of the analogy. However, if the distortions are too small, there will be considerable error in surveying the contours of the deformed sheet. It, therefore, becomes important that the scanning device be capable of measuring very small changes and that some means be provided for accurately determining when the scanning needle contacts the distorted sheet. The first condition is fulfilled by

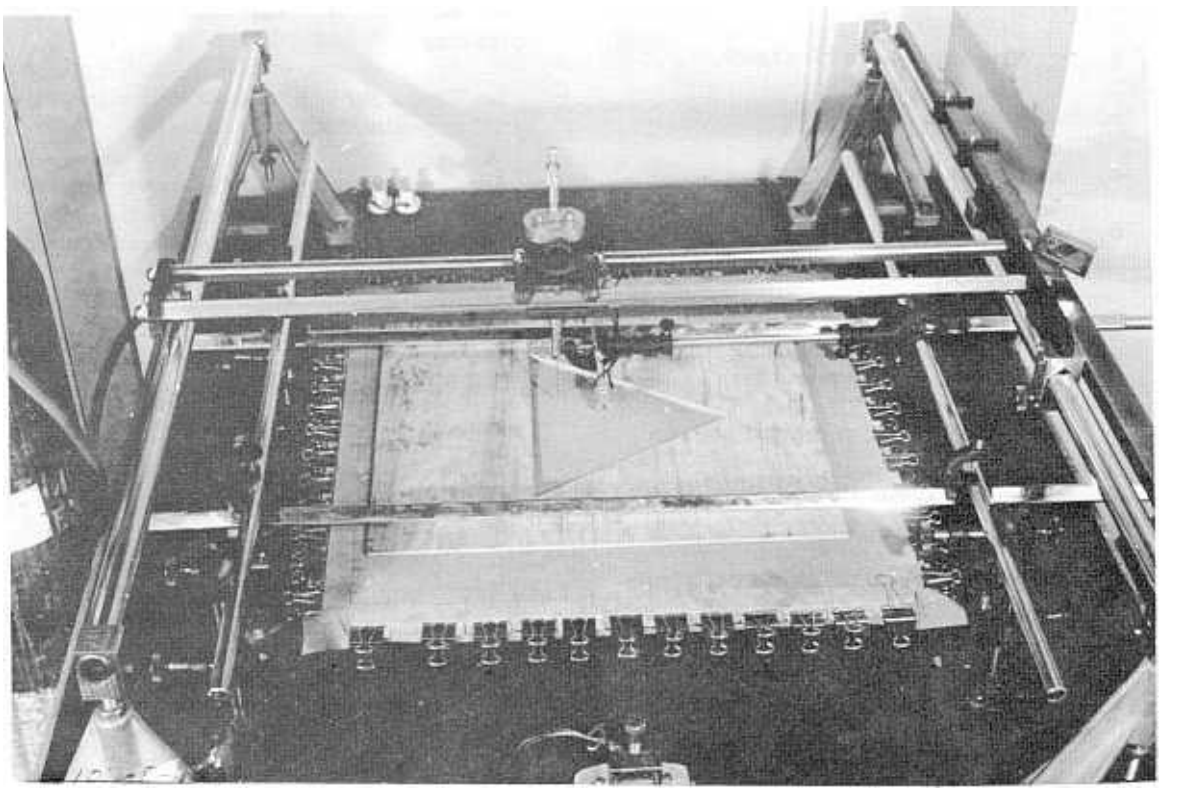

FIGURE 42 -- The membrane analogy apparatus.

constructing the scanning needle from a micrometer depth gage having a range of one inch and graduated to read in thousandths of an inch. By having several interchangeable needles differing in length by even inches, the depth gage can be extended to cover the necessary range. The second condition is fulfilled by having the needle close an electrical circuit and illuminate a small neon glow lamp when it contacts the membrane. The membrane is made electrically conducting by varnishing and brushing on a thin layer of flake graphite.

The slope of the membrane and the volume under it are easily determined from the contour plot. Increments of volume are found by using a planimeter to measure the area enclosed by any contour and then multiplying by the contour interval. Summing these increments of volume gives the total volume.

Torsional shearing stresses can then be found at any point in the cross section by use of the proper values in equation (41).

PHOTOELASTIC MATERIALS AND MODEL PREPARATION

Materials

General--A great many materials currently available possess photoelastic properties to some degree. Glass was perhaps the original material used in photoelastic studies. With the development of synthetic resins in the past few years, the number of materials available for use in photoelastic stress analysis studies has increased greatly.

In the following paragraphs the requirements of an ideal photoelastic material are discussed, some of the more common materials are listed, and the physical and optical properties of these are given.

Requirements--An ideal photoelastic material should possess the following properties:

1. Transparency

2. Birefringent when stressed

3. High optical sensitivity

4. Optical and physical homogeneity

5. Linearity of stress-strain and stress-fringe relations within the working stage

6. High proportional limit

7. High modulus of elasticity

8. Low mechanical or optical creep

9. Freedom from initial stress, or easily annealed

10. Freedom from development of time-edge stresses

11. Constancy of physical and optical properties for moderate temperature variation

12. Machinability

13. Adequate hardness

14. Sufficient rigidity

15. No permanent deformation or residual stress upon removal of load

16. Cementable for built-up models

17. Available in large sheets with flat polished surfaces

18. Economical cost.

The above requirements apply in general to plastics for both two- and three-dimensional studies. The following are additional requirements for a three-dimensional model material:

1. Chemical stability at the softening temperature

2. Constant stress-optical coefficient at the softening temperature

3. Absence of rind effect

4. Absence of creep after freezing and unloading

5. Available in blocks of sufficient size for three-dimensional models.

As stated previously, the above requirements are for an ideal photoelastic model material. No one material possesses them all.

Various Materials--Following is a list of some of the various materials which have been used in photoelastic stress studies:

1. Glass

2. Pyralin (Celluloid)

3. Catalin 61-893 (Formerly Bakelite BT61-893)

4. Columbia Resin, CR-39

5. Kriston (No longer available)

6. Fosterite

7. Gelatin

8. Plexiglas

9. Marblette.

All of the materials listed above have been used with varying degrees of success by the Bureau of Reclamation.

At the present time Columbia Resin, CR-39, is used in most two-dimensional stress studies. Fosterite is used for three-dimensional problems where the stresses are frozen into the model.

Properties--Physical and optical properties of the common kinds of photoelastic materials are listed on Figure 43 and Fig-44. Figure 43 lists the properties of the materials at room temperature (approximately 25° C). Figure 44 lists the properties of the materials used in the stress freezing method of three-dimensional stress analysis and gives the values at the critical temperature for each material.

It has not been possible to conduct comprehensive, independent studies to determine

Material Trade Name	Chemical Classification	E (lb./in.²)	μ	Ultimate Tensile Strength (lb./in²)	Ultimate Comp. Strength (lb./in²)	Proportional Limit (lb./in²)	Hardness (Rockwell M)	Specific Gravity	Fringe Value*	Index of Refraction	Source of Data**	Time-edge Effect	Plastic Flow or Creep	Machinability	Remarks
Plate Glass		9.0×10^6	0.40	10,000					1150		47	Very Low	Very Low	Difficult	
		10 to 11×10^6		6,500				2.5		1.52	48				
		9.0×10^6	0.2 to 0.27	4,000 to 12,000					800	1.4 to 2.0	49				
Pyralin	Cellulose Nitrate	3.18×10^5	0.30	5,000 to 10,000					226		47	Low	Great	Good	
		3×10^5	0.35	5,000 to 8,000					300	1.46 to 1.50	49				
Catalin 61-893 (Formerly Bakelite BT 61-893)	Glycerin Phthallic Anhydride	6.30×10^5	0.36	14,500		5,500			87	1.576	47	Medium	Low	Good	
		6.15×10^5		8,500		6,940					50				
		6.15×10^5			17,000	7,000					51				
Columbia Resin CR-39	Allyl Diglycol Carbonate	2.5 to 3.3×10^5		5,000 to 6,000	22,800	2,500	95 to 100	1.31	87	1.504	48	High	Medium	Fair	
		2.8 to 3.6×10^5	0.2 to 0.3						85 to 100		52				
Kriston	Allyl Ester	4.5×10^5			19,600		116	1.34 to 1.40	80	1.575	53	Very Low	Low	Good	Cast as required
		5.4×10^6		8,200		2,700+			80		54				
Gelatin	Water 65% Glycerin 14%	15	0.50						0.19		47				Properties vary w/ H_2O content
Plexiglas	Cast Methyl Methacrylate	2.8 to 3.6×10^5	0.33	7,000 to 8,500	13,500		70	1.19		1.49	55		High	Excellent	
Marblette	Phenol Formaldehyde	2.74×10^5	0.29	4,500		2,750			51	1.5 to 1.7	47		Medium	Good	
		4.0×10^5		8,000 to 12,000	15,000 to 30,000			1.30 to 1.32			56				

Notes:

* Units of Fringe Value are lb./in.²/fringe/inch thickness.

** Source numbers refer to similar numbers in Bibliography.

PHYSICAL AND OPTICAL PROPERTIES OF VARIOUS PHOTOELASTIC MATERIALS

ROOM TEMPERATURE (APPROX. 25° C.)

O-PEL-117

FIGURE 43 -- Properties of photoelastic materials at room temperature.

Material / Property	Catalin 61-893	Fosterite	Kriston[4]
Temperature for freezing	110° C.	70° C.	134° C.
E	1100 psi	2320 psi	13,800 psi
Ultimate Strength	400 psi	975 psi[1]	680 psi
Proportional Limit		190 psi[2]	Near 680 psi
μ	0.5	0.48[2]	
Index of Refraction	1.58[3]	1.61	1.57[3]
Fringe Value	3.3	3.85	6.25
Time-edge Effect	High	Low	Nil
Machinability	Fair	Good	Fair
Remarks	[3]USBR Tests	[1]24-hr loading [2]At 87° C.	[3]USBR Tests [4]Model must be cast first. See Tech Bul PM 5, 'Kriston Thermosetting Resin', B.F. Goodrich Chemical Co. for data and technique on casting.
Source of Data	M. Hetenyi, Journal of App Mech, Dec 1938, pp A-149 to A-155	Proc SESA, Vol. VI, No. 2, pp 106 to 110	Proc SESA, Vol. VII, No. 2, pp 155 to 172

FIGURE 44 -- Properties of photoelastic materials at elevated temperatures.

the values of the physical and optical properties listed in Figures 43 and 44. Therefore a survey of current literature was made and the values given are those found by various manufacturers and experimenters. Sources of this information are given in the Bibliography.

At best the values given are average values. Variations between batches of the same material and variations betweer experimenters are to be expected. Most physical properties are reasonably constant at room temperature and for a few degrees variation above and below the approximate value of 25° C selected as room temperature. However, some slight difference may exist due to this temperature condition.

It has been found to be sound practice to make frequent checks on the fringe value and interferometer calibration constants of

the material being used.

All of the materials listed in Figure 43 have clear, polished surfaces as received, with the exception of Catalin 61-893, Kriston, and gelatin. Kriston and gelatin are both cast between glass plates and therefore, when used, have clear surfaces that are suitable for the transmission of light and observation of the photoelastic fringes. Catalin 61-893, as received, is in sheets of various thicknesses with the surfaces unpolished. The polishing will be treated in a later section.

One-quarter or one-half inch thick material is usually used for two-dimensional stress studies. The thickness of material used is governed by the size of model, the method of loading, and the rigidity required.

Immersion Fluids--In certain types of models, especially three-dimensional ones which are sliced, the surfaces will not be sufficiently transparent to give a clear fringe pattern. If polishing is not feasible due to time or other factors, the model may be made transparent by immersing it in a fluid.

Two essential requirements of an immersion fluid are:

1. No physical or chemical reaction with the model material or the immersion tank, and

2. An index of refraction approximately equal to that of the model material

Values of the index of refraction of the various model materials are tabulated with their other properties on Figures 43 and 44.

Values of the index of refraction of various immersion fluids used are listed in table 2.

Since it is not always possible to secure commercially an immersion fluid which has an index of refraction equal to that of the model material, it may be necessary to blend two of the fluids together to produce one with the required index of refraction. Proportioning the fluids by weight in relation to the required index of refraction will give a satisfactory blend.

For models or slices of models which have parallel faces normal to the light path of the photoelastic polariscope, it may be satisfactory to coat the surfaces with the immersion fluid. Greater clarity, however, will usually be achieved if the model is actually immersed. For models with nonparallel sides it will be necessary to immerse the model completely in the immersion fluid.

It is necessary to have an immersion tank of sufficient size to hold the model or slice of model. This tank must have at least one pair of opposite faces which are transparent, parallel, and free from stress for viewing models using the frozen-stress technique.

For the scattered light method of three-

TABLE 2

Index of Refraction of Various Immersion Fluids

Immersion Fluid	Index of Refraction	Temperature Correction*
Halowax No. 11-1 at 25° C	1.5730	± 0.0003/1° C
Halowax No. 1007 at 25° C	1.6348	± 0.0002/1° C
White Rose Oil at 25° C	1.4828	± 0.0004/1° C
Mineral Oil at 25° C	1.4675	

*For temperatures lower than 25° C, add.
For temperatures higher than 25° C, subtract.

dimensional stress analysis, the immersion tank must be of sufficient size to hold both the model and the loading mechanism. In addition, all sides and the bottom must be transparent and free from stress.

Preparation

General--As stated previously, Columbia Resin, CR-39 is used in most two-dimensional stress studies. As received from the manufacturer it has highly polished surfaces and is almost entirely stress-free. Therefore, it can be used directly for models. Any slight residual stress is usually confined to the outside edges of the plate and will rarely extend more than 1/4-inch into the plate. The relative economy of CR-39 makes any loss due to the wastage of the outer edges of the plates very slight.

Catalin 61-893 has certain properties which makes its use desirable for some problems. However, as received the plates are unpolished and usually highly stressed making it necessary to anneal and polish the material before it can be used for models. The section on annealing and polishing, which follows, will apply primarily to the annealing and polishing of Catalin 61-893, but will also, in general, apply when it may be necessary to anneal or polish other plastics.

Subsequent sections will apply to all photoelastic materials relative to fabrication, built-up models, and loading methods.

Annealing and Polishing--Catalin 61-893 as received from the manufacturer is usually in the rough state. The faces may be unparallel and the plates may be warped. Stress of some magnitude will almost always be present. By coating the plates with a thin film of halowax or mineral oil, the stress in the plate may be located and evaluated approximately by observing it in the polariscope.

The greatest initial stress usually occurs along the edges of the plate. Sawing off a strip about 1/4-inch wide all around the plate will aid the annealing process by allowing the inner stresses to escape.

The annealing is best done in an oil bath, the surface of the oil being at least one inch above the top of the plastic. The oil gives a uniform distribution of heat around the plate during heating and cooling. An oil with a high flash point such as castor or mineral oil should be used.

The plastic plate is placed in the oil bath on a rigidly supported glass plate. No weight should be placed on the top of the plastic except in cases of extreme warping, and then care should be taken that the load is uniformly placed. For cases of extreme warping, one or two pieces of the plate glass, such as those used for supporting the plastic, will be satisfactory for loading the warped plate. The plastic should be centered on the supporting glass plate, since unequal distribution of weight will cause initial stress. If it is desired to anneal more than one sheet at a time, wooden separators may be used between the glass plates. These separators should be placed on each side of the plastic plate and should be thick enough to hold the top glass at least one inch clear above the plastic plate.

The plastic plates, in the oil bath, are placed in the electric oven and the temperature raised to approximately 120° C in a period of about two hours. The temperature should be maintained at the constant value of 120° C for one hour and then gradually reduced to room temperatures at a rate not exceeding 3° C per hour.

For plates which are not too highly stressed, the stress condition may be relieved in one cycle of annealing. For other plates it may be necessary to repeat the cycle several times. One procedure which has been found to be very effective for annealing highly stressed plates is, after raising the temperature to 120° C and holding it for one hour, to lower the temperature at the rate of 3° C per hour to only 60° C. Repeating this cycle four or five times will usually produce stress-free plates from even the most highly stressed ones and is much speedier than lowering the temperature to room conditions for each cycle.

Although the specific values given above apply to Catalin 61-893, the same procedure may also apply to other plastics which require annealing. Reference to the appropriate technical bulletins will give the proper values of temperatures and time requirements to be used.

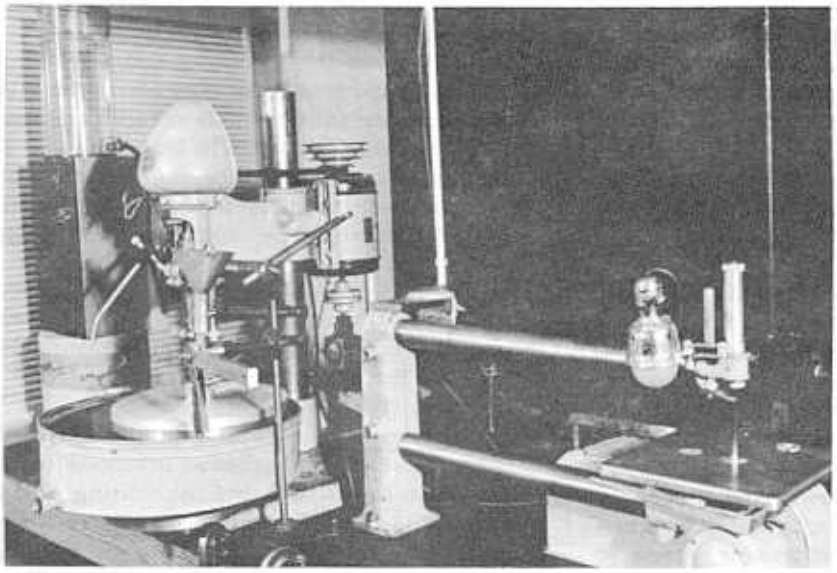

FIGURE 45 -- Arrangement of equipment for polishing.

The following procedure covers grinding and polishing a plate of Catalin 61-893 from the rough state to the final polish. The grinding and polishing compounds used are alundum, grades 120 and F, and plastic pac. The plastic pac is a diatomaceous earth which has been levigated three times, each time retaining only that part which remains in suspension. The equipment used consists of a drill press, less motor, a motor driven flexible shaft; a rotatable base plate to which is fastened the plate of plastic; and cast iron and aluminum polishing disks. Also required is a water tank to furnish a water supply, a dispenser to supply the grinding compound, and sheets of canvas and billiard-table cloth for use on the grinding and polishing disks. The arrangement of the components is shown in Figure 45. The motor on the drill press is used only for convenience in connecting the flexible shaft to the spindle. Figure 46 shows the belt arrangement on the flexible shaft assembly.

After the plates have been annealed and checked to see that they are stress-free, they should be checked for warping and parallel faces. If the plates are warped badly, it may be necessary to reanneal them with glass plates placed on top of the warped plates to straighten them. For plates where the warping is slight or the faces are not parallel by an amount greater than 1/32-inch, it is usually necessary that the entire plate be either turned in a lathe or surfaced with a shaper until the faces of the plate are approximately parallel. Sharp corners and edges should be rounded with a file to avoid possible tearing of the polishing cloth.

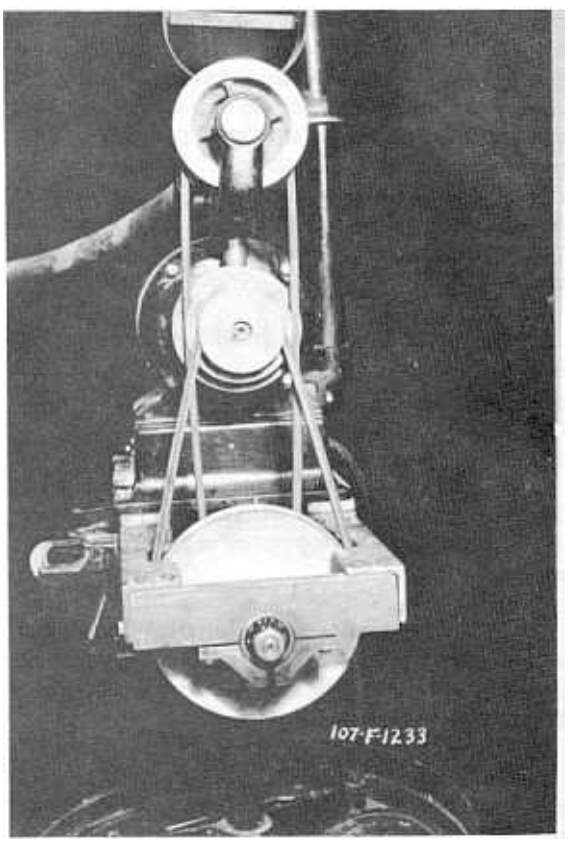

FIGURE 46 -- Arrangement of belts on flexible shaft.

The plastic plate should now be placed on the rotatable base plate and fastened in position by means of small blocks of pyralin pressed against the four edges of the plate and held in position by moistening with acetone.

There are five steps in the grinding and polishing procedure:

Step one is primarily a grinding process. The plastic plate is usually quite rough, and it is necessary to remove the ridges and pockets and obtain a flat surface. This is done by the use of the perforated iron grinding disk and alundum, grade 120. The alundum is applied directly to the plastic. A very generous use of water is necessary in this and all succeeding steps in order to eliminate the introduction of temperature stresses due to the polishing. The lap is rotated at a slow speed while kept in contact with the plastic plate by means of a slight pressure on the vertical feed mechanism of the drill press. The rate of feed of the water and grinding compound should be adjusted to give an adequate supply of each. It may be necessary to apply some braking action to the rotatable base to prevent its moving at too great a speed. However, some rotation should be allowed as this will prevent grinding in an unchanging pattern. The grinding is continued until the surface of the plastic plate is smooth and flat. The other side of the plastic plate is treated in a similar manner.

Step two is also a grinding process. It makes use of the solid cast-iron disk and alundum, grade F. The procedure is the same as for step one.

Step three makes use of an aluminum disk which is covered with canvas, and alundum grade F. The procedure remains the same.

In step four the same grinding compound, alundum, grade F, is used but the canvas cover on the disk is replaced by one of billiard-table cloth.

In step five, billiard-table cloth is still used on the disk but plastic pac is used as the polishing agent.

Each step will produce a finer surface. Step three is the first to produce a transparent surface. The operator must be very careful to keep the grinding and polishing disks clean and free from coarser materials, as any coarser particle will scratch and may destroy the work done up to that time. It is necessary that all the equipment be thoroughly washed between successive steps. The canvas and the billiard-table cloth wear out quite rapidly, and should be replaced before they tear and allow the metal disks to scratch the plate. A rather slow speed must be used during the first two steps, but this may be increased for the other steps.

Fabrication--The procedure outlined herein presents the general methods to be followed in the layout and machining of the photoelastic models for two- and three-dimensional studies in both the photoelastic polariscope and photoelastic interferometer. It should be remembered that these instructions are of a general nature and that each individual study may require modification of the procedure.

A sheet of plastic of the required thickness and size should be selected and checked in the photoelastic polariscope for stress. If the preceding steps of annealing and polishing have been carried out properly, only slight stress around the boundaries should exist. The extent and location of these boundary stresses should be noted and avoided if possible when laying out the model.

It has been found that, for the equipment and tools currently available, the most rapid and convenient method is to lay out the model directly on the plastic plate. By using a sharply-pointed scratch awl or stylus a very fine yet plainly visible line can be made. Care should be taken to avoid making scratch marks within the area of the model. All boundary lines should be scaled as accurately as possible, since small errors in dimensioning the model will be magnified, proportional to the scale ratio, on the prototype.

After the model has been laid out, the next step is to saw it to its approximate size. This is done on the scroll saw usually using a blade which is 0.020 inch thick, 0.110 inch wide, and has 20 teeth per inch. It is recommended that a new blade be used when beginning to cut a model, since the blades

are dulled very rapidly by cutting plastic. The saw should be run at a medium speed of about 1200 cutting strokes per minute and the model fed into the saw at a slow rate. With a sharp saw blade and a slow rate of feed, it has been found possible to cut within 3/32 inch of the dimension line without inducing undue stress or causing chipping to extend inside the dimension line. The underside of the model should be protected against scratches by either masking with tape or using wrapping or similar paper between the model and the saw table. No coolant is required if the saw blade is sharp and the material is not fed too fast.

The next step is to cut the model to its final size. For straight boundaries this is done on the milling machine. Different sizes of cutters may be used for special conditions, but, generally speaking, for nearly all straight outside boundaries, best results are obtained by using a 1/2- or 5/8-inch spiral fluted end mill with 7 or more flutes. The cutting is done with the sides of the cutter rather than with the end. The milling machine is operated at maximum speed, and the model is fed at as uniform a rate of speed as is possible. As with the sawing operation, no coolant is required provided the cutters are sharp and the speed of cutting is not excessive. Depth of cut should not exceed about 0.02 inch, reducing this to 0.01 or even 0.005 inch as the final boundary line is approached. The model should be firmly clamped in the vise of the milling machine, care being taken to protect the polished faces of the model. If necessary, C-clamps can be used at the top edges of the large jaw-plates to provide additional rigidity to the clamping.

Some curved boundaries can be shaped with a regular cutter on the milling machine. However, most curved boundaries will require shaping by hand. A very satisfactory method has been the use of small diameter end mills (1/4 inch or smaller) in the drill press. The drill press is operated at a high speed, and the model is hand-fed into the cutter until the dimension line is reached.

It is necessary to use a file to form sharp re-entrant corners. The filing is done using the scroll saw with a file in the lower chuck. If a milling cutter 1/4 inch or smaller in diameter has been used up to the corner, a minimum of filing will be required. Corners can be best filed by use of a knife-shaped file with a 1/8 inch shank. After the file is clamped in the chuck a check should be made to insure that the file is normal to the table in all directions. Filing is the least desirable method of machining, since it is the most likely to produce stresses in the model. However, by taking small cuts and using very little pressure against the file, it is possible to obtain stress-free boundaries. As in previous operations, no coolant is used while filing, but only sharp files should be used and small cuts taken.

Circular openings may be drilled if the opening required is a standard drill size. Due to the confined nature of the opening it is necessary to use a coolant, such as a water-soluble cutting oil, in this operation. It is also necessary that the model material be supported on the leaving side by another piece of plastic to prevent chipping. The drill press can be operated at a speed somewhat greater than that used in drilling holes of similar size in brass. The rate of feed should be slow and the hole should be cleared of chips frequently. As with other methods of machining, only sharp tools should be used. The work should be clamped securely to the table of the drill press for the sake of safety and to prevent vibration and possible chipping or cracking of the model.

It is impossible, even with the best milling cutters, to produce a boundary with a very smooth surface. Regardless of the care taken in milling or the sharpenss of the cutter, the final milled surface will be somewhat uneven. This will result in minor stress concentrations in the immediate vicinity of a loaded boundary. This type of surface is entirely satisfactory if it is not necessary to use the fringe pattern or take interferometer readings close to the boundary.

It becomes necessary, occasionally, to obtain the stresses along a loaded boundary. A very satisfactory contact can be obtained by lapping the two surfaces together using a grade F alundum grinding compound and sufficient water to keep the surfaces very wet. Care must be taken to avoid rounding the contact surfaces in either direction.

In applying a uniform load to a model, such as occurs in studying stresses around

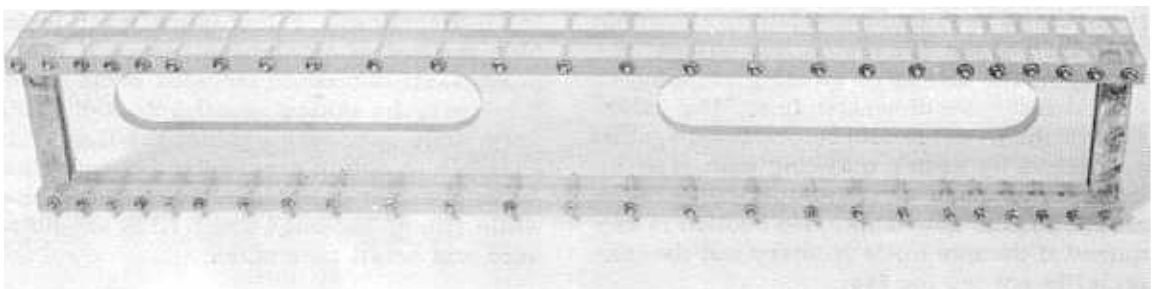

FIGURE 47 -- Built-up model of beam--flange same material as web of beam.

openings in a large plate, it is imperative that the two sides which are loaded be parallel. Otherwise, it is almost impossible to obtain a symmetrical pattern in the model.

As has been mentioned previously, time-edge effects develop rapidly, particularly in Columbia Resin, CR-39. For this reason, the work of preparing the loading mechanism and fabricating the model should be scheduled so that a minimum of time elapses between the first cut on the model and the photographing of the isochromatics. Development of time-edge stress is so rapid in Columbia Resin, CR-39, that a distorted fringe pattern will develop on a finished edge in a few hours. Catalin 61-893, while somewhat better in this regard, than Columbia Resin, CR-39, will develop enough time-edge stress in one day to cause a distorted fringe pattern. Fortunately, the time-edge stresses do not affect the readings in the photoelastic interferometer, except at the very boundaries of the model in regions of low stress. In most cases these boundary stresses are obtainable from the photoelastic polariscope fringe pattern, so that speed, in the use of the model, is not an essential requirement for the photoelastic interferometer.

Built-up Models--Some three-dimensional structures can be analyzed using the two-dimensional approach when the region in which the stresses are desired can be, in itself, considered as two-dimensional. An example of such a structure is a flanged beam, when the stresses are desired in only the web of the beam. Figures 47 and 48 show such beams. In these examples the size and shape of the openings in the web of the beam required a knowledge of the stress distribution in the web. The effective flange of the beam is represented by strips which have been proportioned so that the ratios of the EI values of the flange to the web of the model and actual structure are equal. These strips are bolted to the web piece with a sufficient number of bolts to insure continuous action between the parts. In Figure 47 the flanges are of the same material as the web, Catalin 61-893. In Figure 48, however, the flanges are of brass.

Figure 49 is a photograph of a model of a rib-reinforced power plant roof deck. In this case the ribs have been made of the same materials as the model itself which is Columbia Resin, CR-39. The ribs were cemented to the slab by use of Kriston. More recently a new resin, Scotchcast, has been used which gives joints nearly as strong as the model material itself.

Loading Methods--As important as the fabrication of a stress-free, accurate scale model is the application of the proper loads

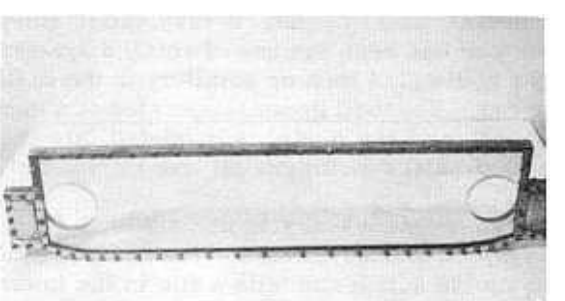

FIGURE 48 -- Built-up model of beam--flange of brass with web of Catalin 68-893.

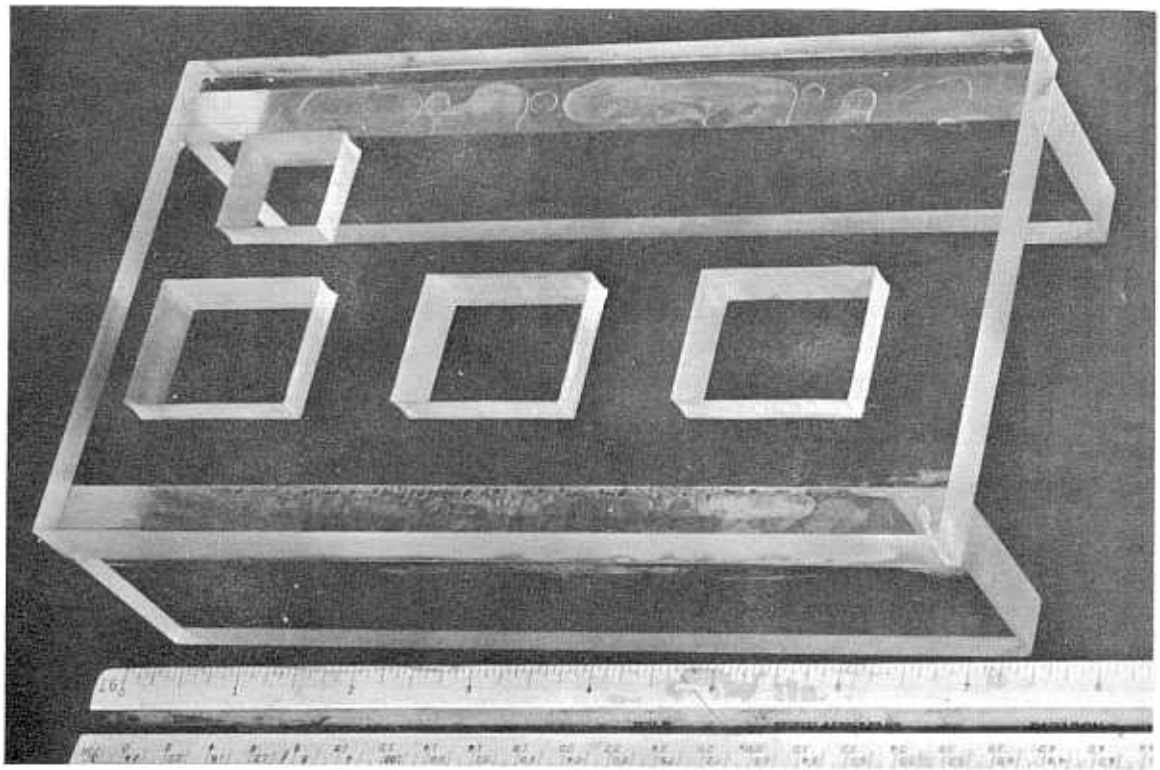

FIGURE 49 -- Built-up model of powerplant roof deck.

so that actual conditions existing in the structure are represented in the model.

Judicious application of Saint Venant's principle* will simplify loadings in many cases. In other problems it may be found that the loading can be broken down into two or more parts and the separate effects combined by the method of superposition of stresses.

It is impossible to predict what the loading requirements may be in advance of a knowledge of the actual problem. For that reason this discussion will cover only a few of the more interesting loading problems that have been encountered. It is hoped that they will serve as an indication of what can be done.

*This principle states that, whatever the distribution of forces over a small area may be. the stress distribution actually produced in a body, at some distance away, is the same as that which would be produced by the resultant of these forces.

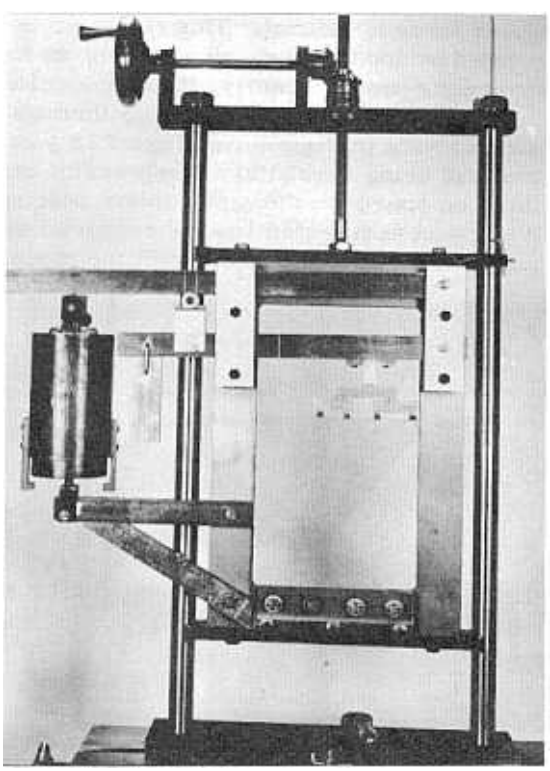

FIGURE 50 -- Loading methods--unequal uniform loads applied over small areas.

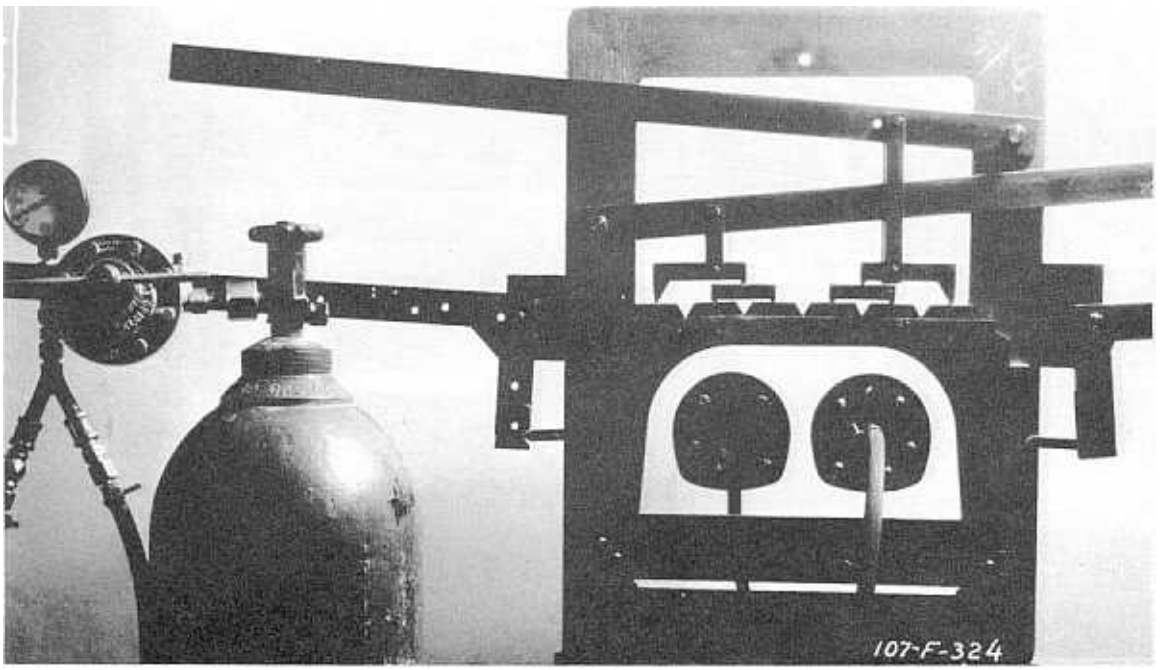

FIGURE 51 -- Loading methods--external and internal loads applied to a double-barrel conduit.

Care must be taken in applying a load normal to the boundary of a model that no shear force is induced. This can be accomplished by loading through pins, or, as has been done more recently, through a roller bearing. An example of loading through a pin is shown in Figure 58. Figure 18 shows the load being applied to a compression calibration specimen through a roller bearing. When a concentrated load is required the roller is placed in contact with the model.

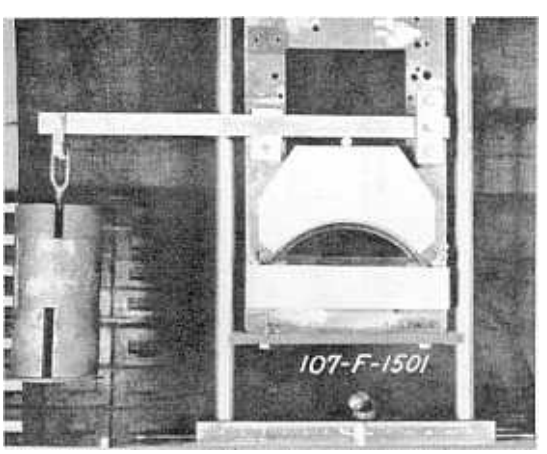

FIGURE 52 -- Loading methods--uniform normal load applied to an arch.

For distributed loading the roller is placed between the lever arm and the loading shoe on the model.

Other examples of special loading devices are shown in Figure 50 through Figure 57.

Figure 50 shows a method of applying four loads of different magnitudes over small areas. The magnitudes of the various loads are governed by the spacings of the bearing pins.

Figure 51 is a model of a twin-barrel conduit. Loads on the actual structure consisted of vertical and lateral soil pressures on the external boundaries of the conduit and water pressure in neither, either, or both of the barrels. In the model the external soil pressures were simulated by applying forces to articulated shoes which acted on a sheet of rubber one-half inch thick. A central hole was cut in the rubber so that it fit snugly around the model. Lateral loads were applied in the desired proportion to the vertical loads. Internal water loads were applied by means of air pressure in confined rubber tubing in the barrels.

Figure 52 is a model of an arch section

FIGURE 53 -- Loading methods--flat-plate clevis loaded through a pin.

which was subjected to a uniform load normal to its surface. This was accomplished by loading through a sealed rubber tube filled with water. A wooden block was shaped to the curvature of the arch and a recess cut in the curved face to confine the tube.

Figure 53 shows a method of loading a flat plate clevis so that a minimum area of the plate is covered. The load is applied through straps made of sheet metal. In the example shown, the plate and the pin are of the same material with a shoulder turned on the pin so that the sheet metal straps do not cover the contact surface between the pin and plate.

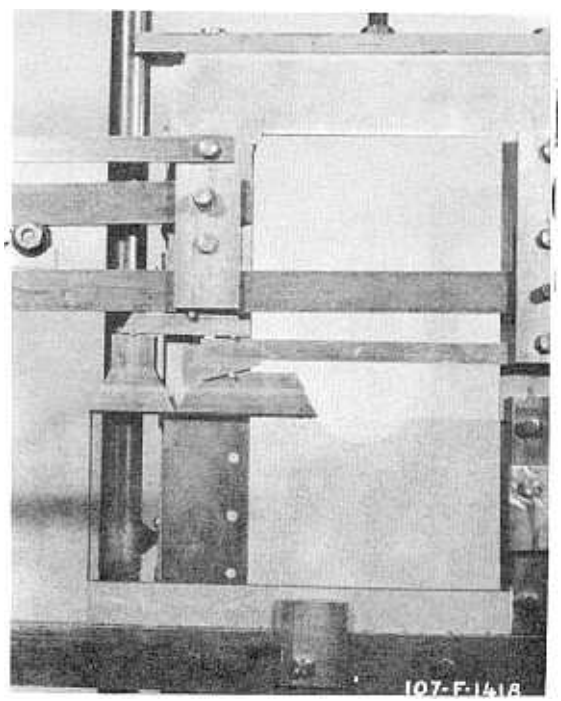

FIGURE 54 -- Loading methods--stresses around a spillway bucket.

Figure 54 presents a loading around a spillway bucket. The effect of the dead weight of and water load on the dam is produced by the shoe on the right, with the load being applied along the line of action of the resultant of the dead weight and water load.

FIGURE 55 -- Loading methods--uniformly varying load applied to boundaries of a wall.

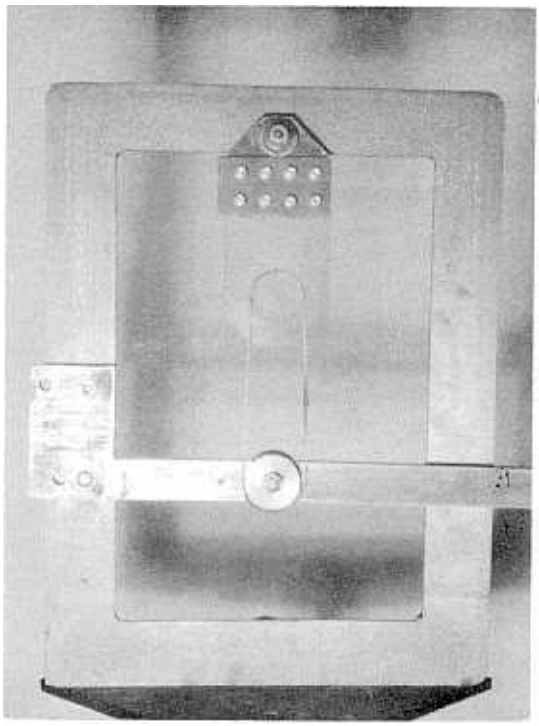

The shoe on the left represents the effect of the reservoir water load on the foundation upstream from the dam.

Figure 55 is a model of a wall in which several large openings occur. One condition of loading assumed to exist was a load

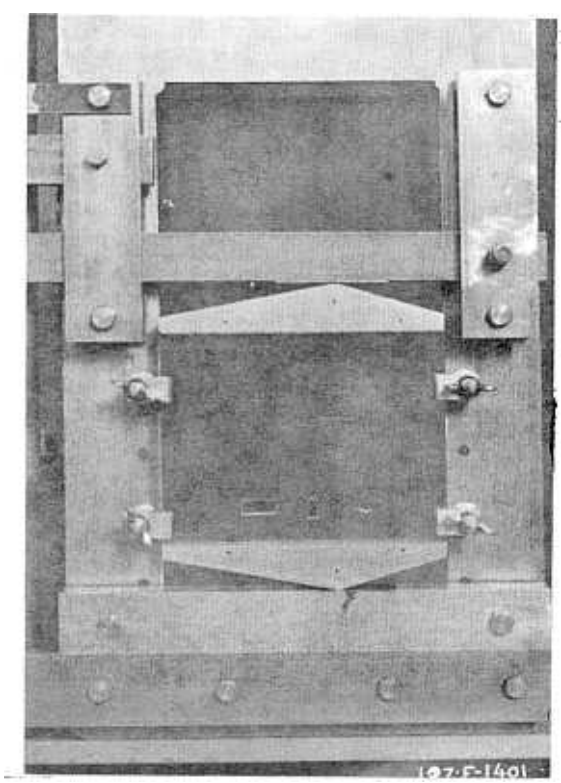

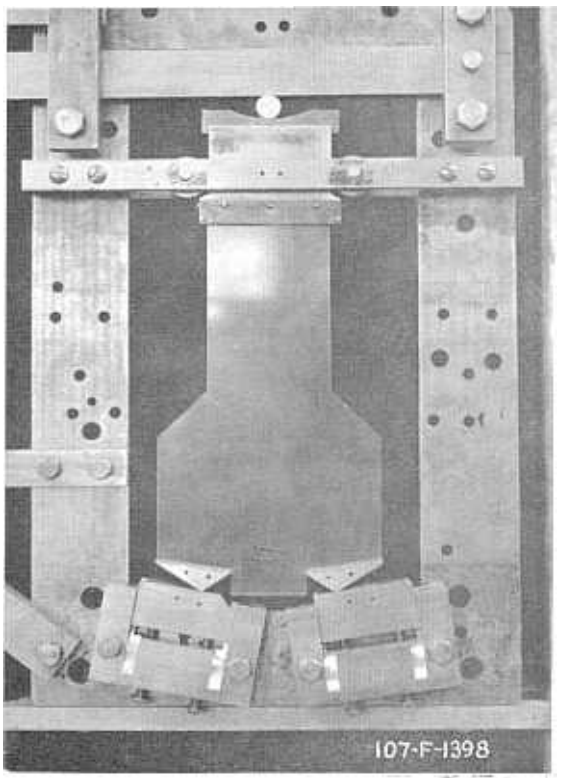

FIGURE 56 -- Loading methods--loads applied to a corbel buttress.

varying uniformly from a maximum at the top to zero at the bottom. In the figure the model is turned on its side from the actual position. The loading shoes, top and bottom, were made to give a uniformly varying load. This was done by trial, by taking readings in the model immediately adjacent to the shoe using the photoelastic interferometer and adjusting the shape of the shoe to give the required distribution. The clamps shown on the side are for stability only and have no effect on the load.

Figure 56 is a model of a corbel buttress of a dam. The load being applied represents a triangular distribution on the corbel face varying from a maximum toward the center to zero at the edge. Adjustments are provided in the mechanism to permit use of different shapes of shoes for various loading conditions and also for providing stability.

Figure 57 shows a method of loading a circular conduit which is supported over less than half of its circumference. The top shoe in this case is of metal with a piece of 1/4-inch thick gasket rubber between it and the model. The conduit and its foundation are separated by a thin piece of rubber.

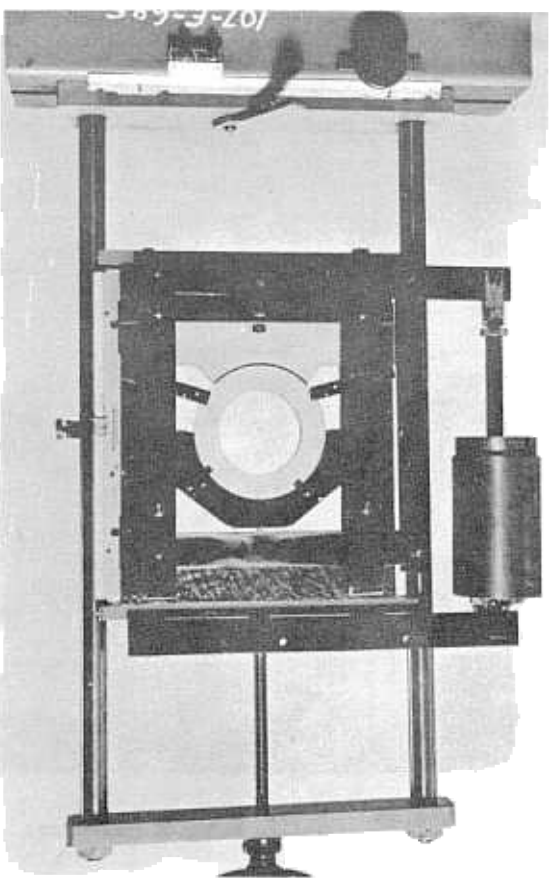

FIGURE 57 -- Loading methods--loads applied to a circular conduit.

PHOTOELASTIC MODEL LOADING FRAME ASSEMBLY

General

It is convenient to have a standard loading frame assembly for use in loading the photoelastic models. Therefore, the assembly described in this chapter was designed and built for that purpose. It is suitable for use in both the photoelastic polariscope

and the photoelastic interferometer and is adaptable to all model and loading conditions normally encountered. Figure 58 is a photograph of the loading frame assembly. The model shown in the drame is a standard inspection gallery.

Description

The loading frame assembly consists of several component parts which are interchangeable between assemblies. Figures 59 through 72 show details of the construction and assembly of these parts.

The figures are almost self-explanatory, but a few general remarks may help to explain the use of the loading frame assembly.

Stress analysis using the photoelastic interferometer involves a point by point survey of the model. This requires a means of establishing an accurate coordinate system for securing the required readings at each point of interest. As can be seen from the figures, screw feeds for both vertical and horizontal movements are provided. These screws are cut ten threads per inch. In addition, indicator rings which are divided into twenty divisions are mounted on each motion. Therefore, it is possible to set the model to the desired position with an accuracy of 0.005 inch both vertically and horizontally. These movements also permit the centering of the model in the field of the photoelastic polariscope or otherwise adjusting it to the region of interest.

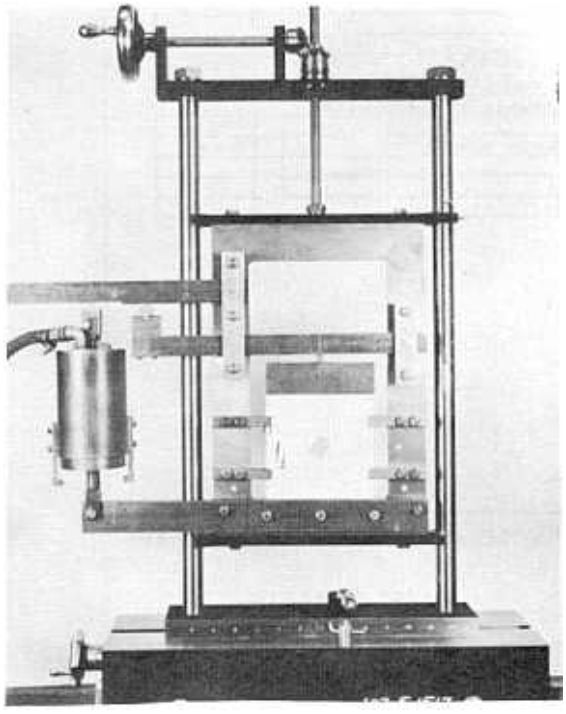

FIGURE 58 -- Photoelastic model loading frame assembly.

Since no two models will normally be alike in size or method of loading, it has been found convenient to provide a loading frame, that is adaptable to any required condition and yet replaceable and inexpensive (see Figure 69).

Standard lever arms are used for applying the loads to the model. These have been fabricated of both steel and aluminum. Steel lever arms of three lengths; 12, 15, and 18 inches, are used. Aluminum lever arms, 12 and 15 inches long, are used for models requiring very light loads. All lever arms have ball bearings inserted at the pivot point to reduce friction. Details are shown in Figure 72.

The procedure in making a stress analysis with the photoelastic interferometer involves reading fringe movements between two increments of load. Therefore, a method of rapidly loading and unloading the model is necessary. The load is applied using cast iron weights of 1, 5, 10, and 20 pound sizes. These weights are also used for loading the models in the photoelastic polariscope. Figure 73 shows a model with the load being applied by means of these weights. A pneumatic piston is used to unload the photoelastic interferometer. Compressed air is introduced into the pneumatic piston through a pressure reducer which is adjusted to provide just enough air pressure to completely lift the dead weight from the model. A system of valves, mounted near the operator, permits introduction and exhaustion of the air supply for the piston. The relation of the pneumatic piston to the model and loading frame can be seen on Figures 58 and 73. Details of construction are shown on Figures 70 and 71.

The loading frame assembly is mounted on ball bearings to facilitate movement between the photoelastic interferometer and the photoelastic polariscope. Guide rails, with locking screws to position and to securely hold the loading frame assembly, are mounted on the photoelastic interferometer table. The loading frame assembly can be

LIST OF PARTS

PART NO.	DESCRIPTION	MATERIAL	NO. REQ'D	NOTES	DRAWING NUMBER
1	Guide rail	Brass	2		O-PEL-99
2	Rail lock	As shown	4		"
▼3	Base assembly	As shown	1		O-PEL-100
4	Lead screw	Steel	1		O-PEL-101
5	Bearing, horizontal movement	Oilite	2		"
6	Indicator ring, horiz. movement	Steel	1		"
7	Index collar	Steel	1		"
8	Thrust washer	Steel	2		"
9	Wheel assembly	As shown	2	For specifications of bearing see Dwg. O-PEL-102	O-PEL-102
▼10	Lock handle (Lock assembly)	Steel	1	Standard alloy cast handle, H-1	"
▼11	Hand knob, horiz. movement	As shown	1	Standard cast iron hand knob, M-2	"
▼12	Sliding base	Steel	1		O-PEL-103
13	Drive nut	Oilite	1		"
14	Pointer assembly	As shown	1		O-PEL-104
▼15	Frame guide	As shown	2		"
16	Guide posts	Steel	2		O-PEL-105
17	Guide post nuts	Steel	2	Standard hexagon nut, semi-finished, $\frac{3}{4}$" x 10	No detail
18	Jam nuts	Steel	2	Standard hexagon nut, semi-finished, $\frac{1}{2}$" x 13	"
19	Lifting screw	Steel	1		O-PEL-105
20	Thrust bearing	Steel	1	For specifications of bearing see Dwg. O-PEL-105	"
21	Shaft	Steel	1		"
22	Bearing, vertical movement	Oilite	2		"
▼23	Cross bar assembly	Steel	1		O-PEL-106
24	Miter gears	As shown	2	Bond gear No. S12M	"
25	Spacer	Bearing bronze	1		"
26A	Indicator ring, vert. movement	Brass	1		"
26B	Index	Plastic	1		O-PEL-105
▼27	Hand wheel, vert. movement	Cast iron	1	Standard offset hand wheel OW-4, 4" Dia.	No detail
28	Model mounting frame	Steel	2		O-PEL-107
29	Cylinder	Brass	1		O-PEL-108
30	Piston	Brass	1		"
31	Cylinder head	Brass	1		O-PEL-109
32	Pressure plate	Brass	1		"
33	Expansion stop	Brass	2		"
34	Clevis	As shown	1		"
35	Sleeve	Steel	4		"
36	Adjusting nut	Brass	1		"
37	Toggle screw	Steel	1		"
38	Toggle	Brass	1		"
39	Guide pin	As shown	1		"
40	Street elbow	Iron	1	Standard $\frac{1}{8}$" N.P. fitting	No detail
41	Coupling	Brass	1	DeVilbiss coupling, type H-1498	"
42	Bellows	Brass	1	Fulton Sylphon Co. Reference line No. 1098	"
43	Lever arm	Steel	As req'd.		O-PEL-110
44	Bearing, lever arm	Steel	As req'd.	New Departure bearing No. 77R6	No detail

NOTES

All machine screws required are standard flat or round head machine screws as indicated on drawing unless detailed or specified.
Details of parts and assemblies are shown by drawings indicated.
Finish parts marked ▼ with black ripple enamel.
Exceptions are noted on detail drawings.

PHOTOELASTIC MODEL LOADING FRAME

LIST OF PARTS

O-PEL-97

FIGURE 59 -- Loading frame assembly--list of parts.

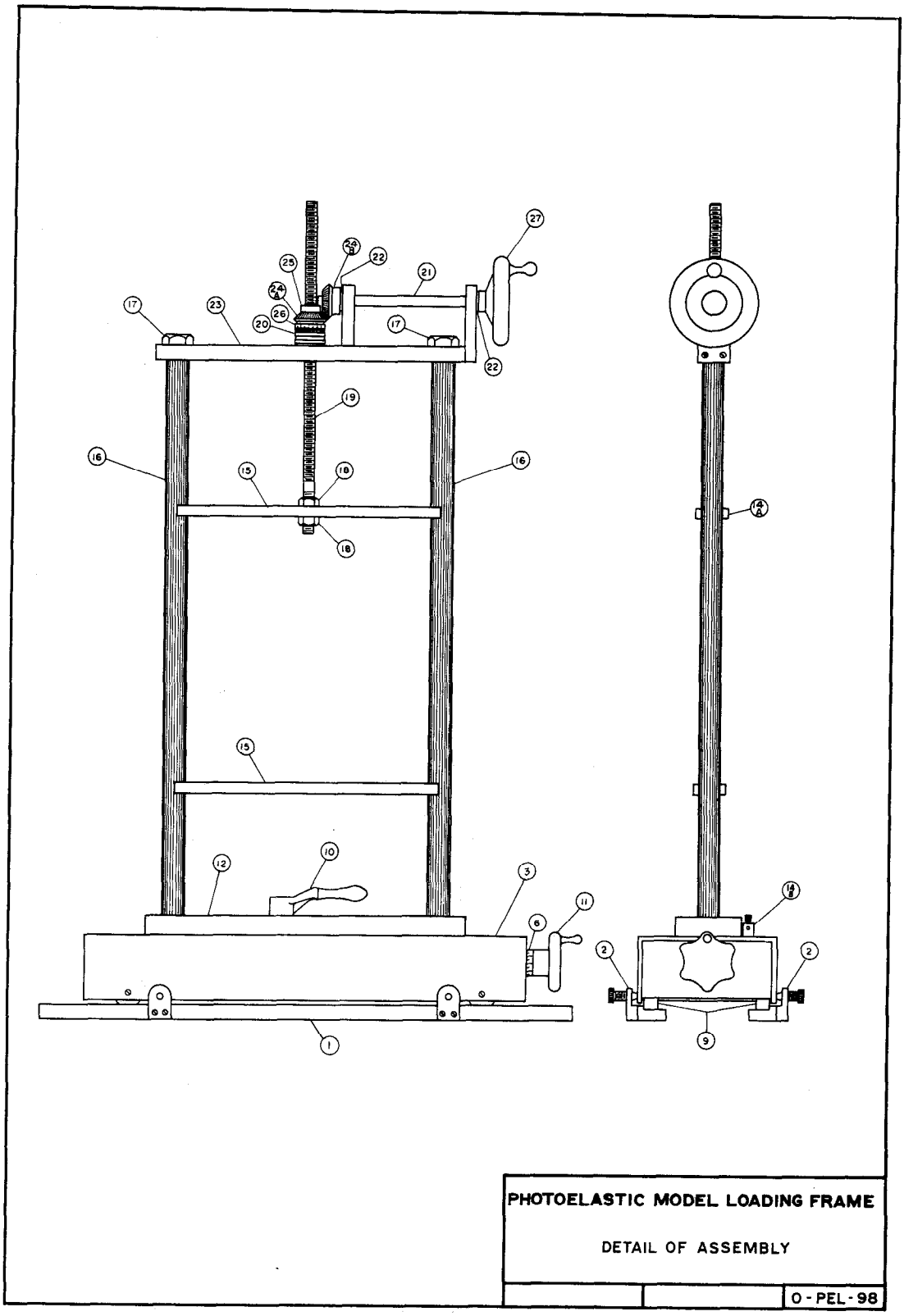

FIGURE 60 -- Complete loading frame assembly.

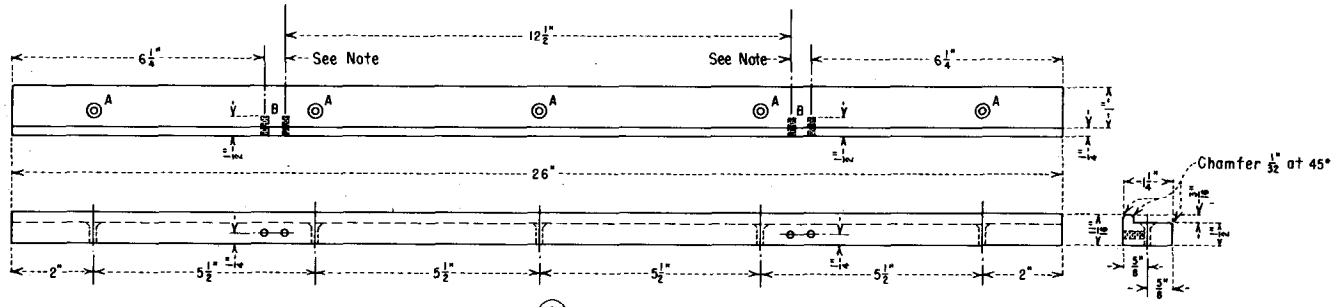

① **GUIDE RAIL**

BRASS - TWO REQ'D.

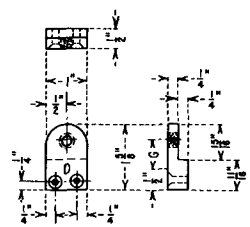

LOCKING SCREW SUPPORT

BRASS - FOUR REQ'D.

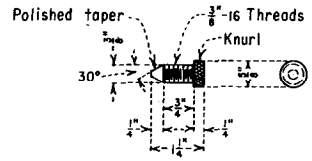

LOCKING SCREW

TOOL STEEL - FOUR REQ'D.

NOTE: Drill and tap hole marked C to fit locking screw, 3/16"-16 thread.
Drill and countersink holes marked D for 10-24 machine screws (FH., 7/8" long)

② **RAIL LOCK**

MATERIAL AS SHOWN - FOUR REQ'D.

NOTES

Drill and countersink holes marked A for No. 8 wood screws.

Drill and tap holes marked B for 10-24 machine screws. Space to fit holes marked D on locking screw support.

The location of the tapered rail locking screws and corresponding holes J in the base assembly must be such as to provide interchangeability between other similar frames and rails. This may require the use of a drill jig.

PHOTOELASTIC MODEL LOADING FRAME

GUIDE RAIL AND RAIL LOCK

O-PEL-99

FIGURE 61 -- Loading frame assembly--guide rail and rail lock.

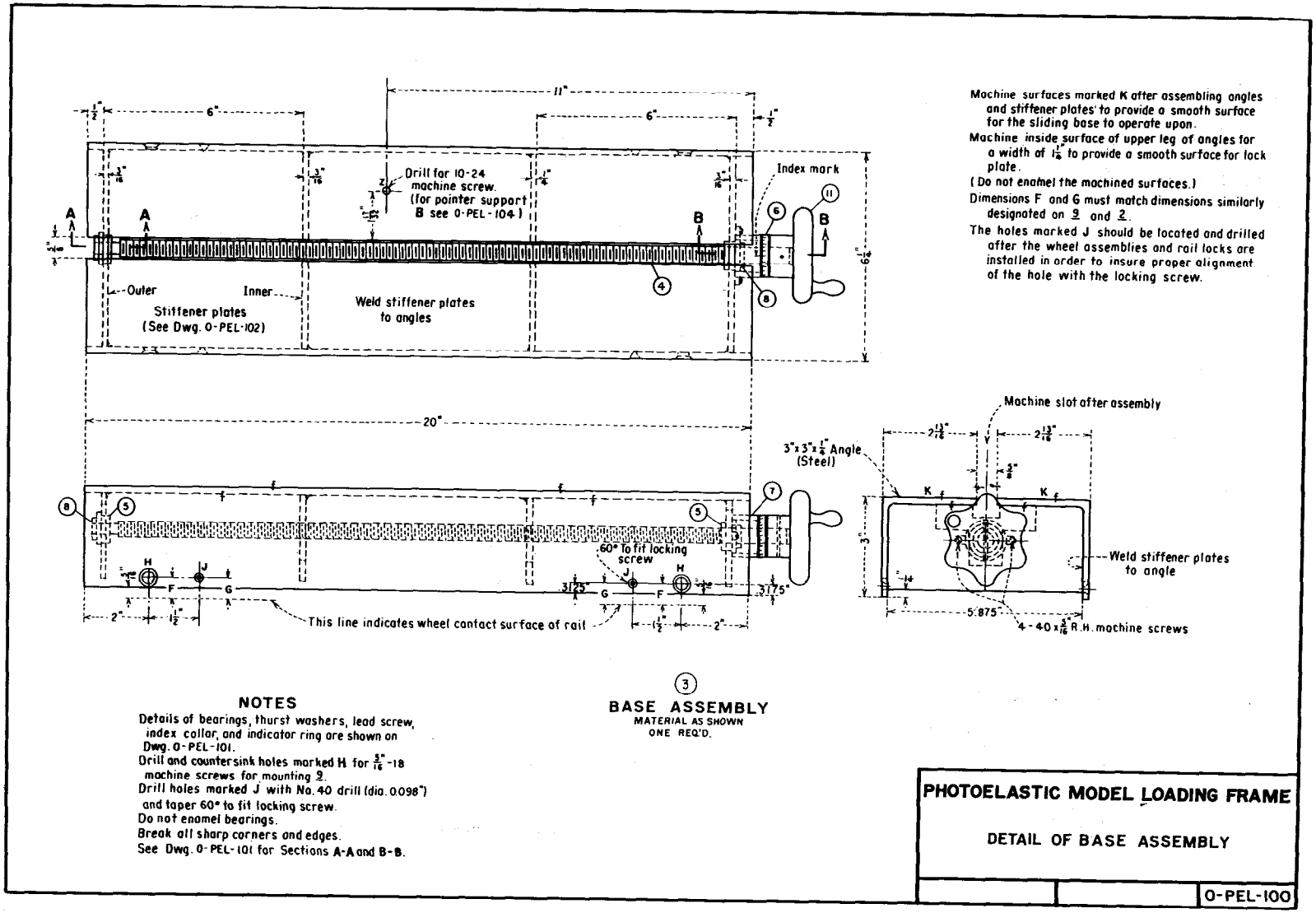

FIGURE 62 -- Loading frame assembly--detail of base.

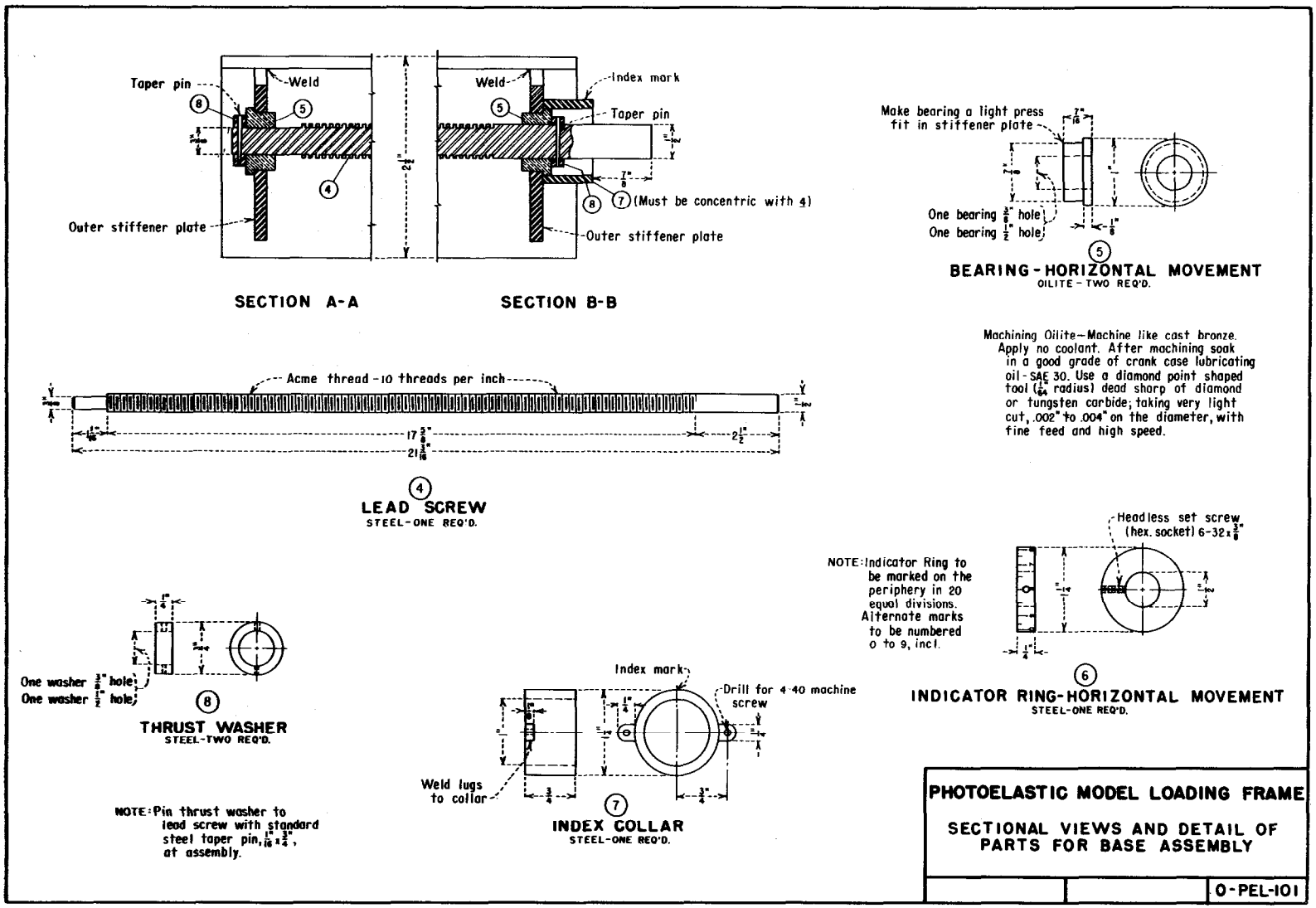

FIGURE 63 -- Loading frame assembly--component parts of base.

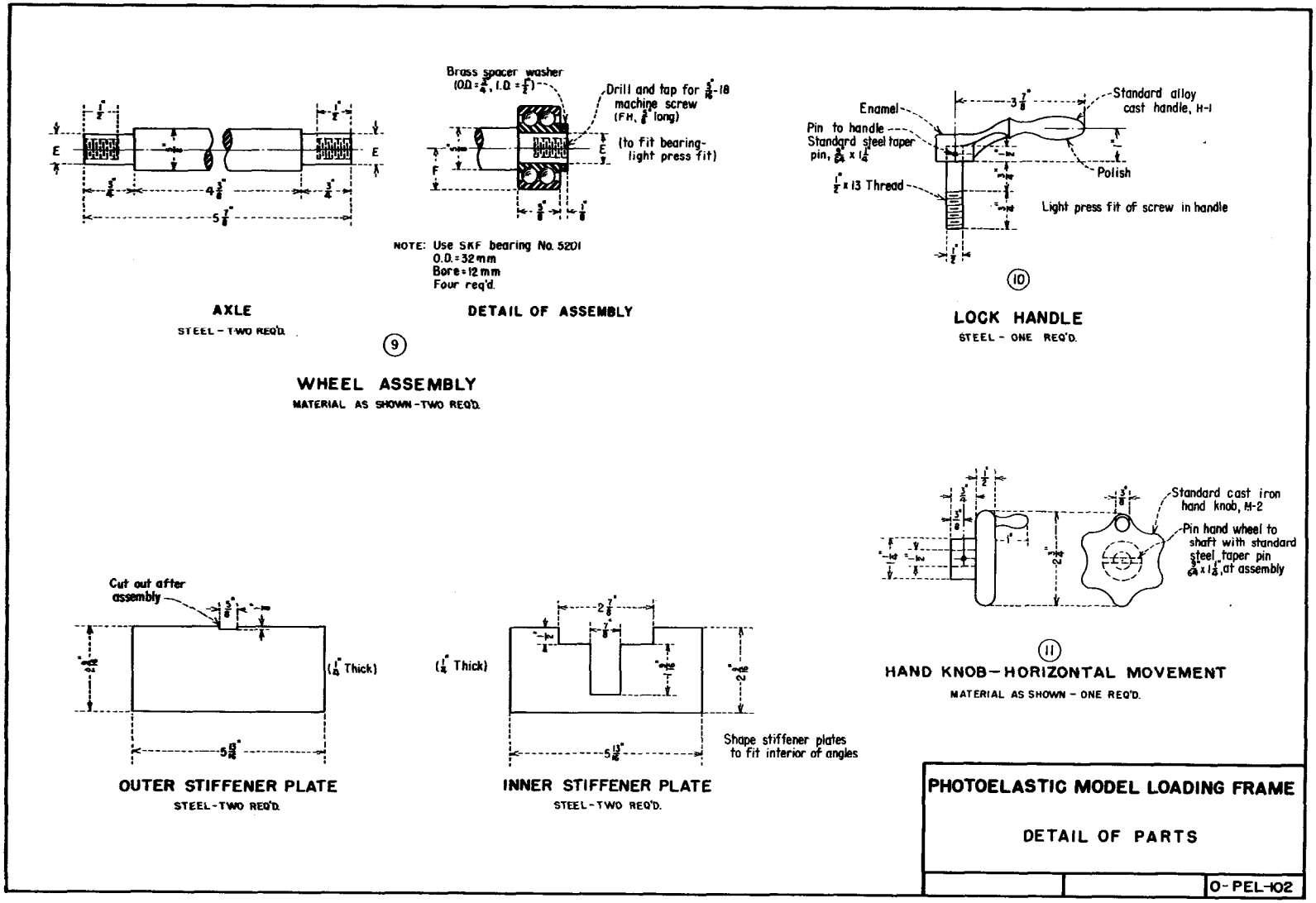

FIGURE 64 — Loading frame assembly--component parts of base (continued).

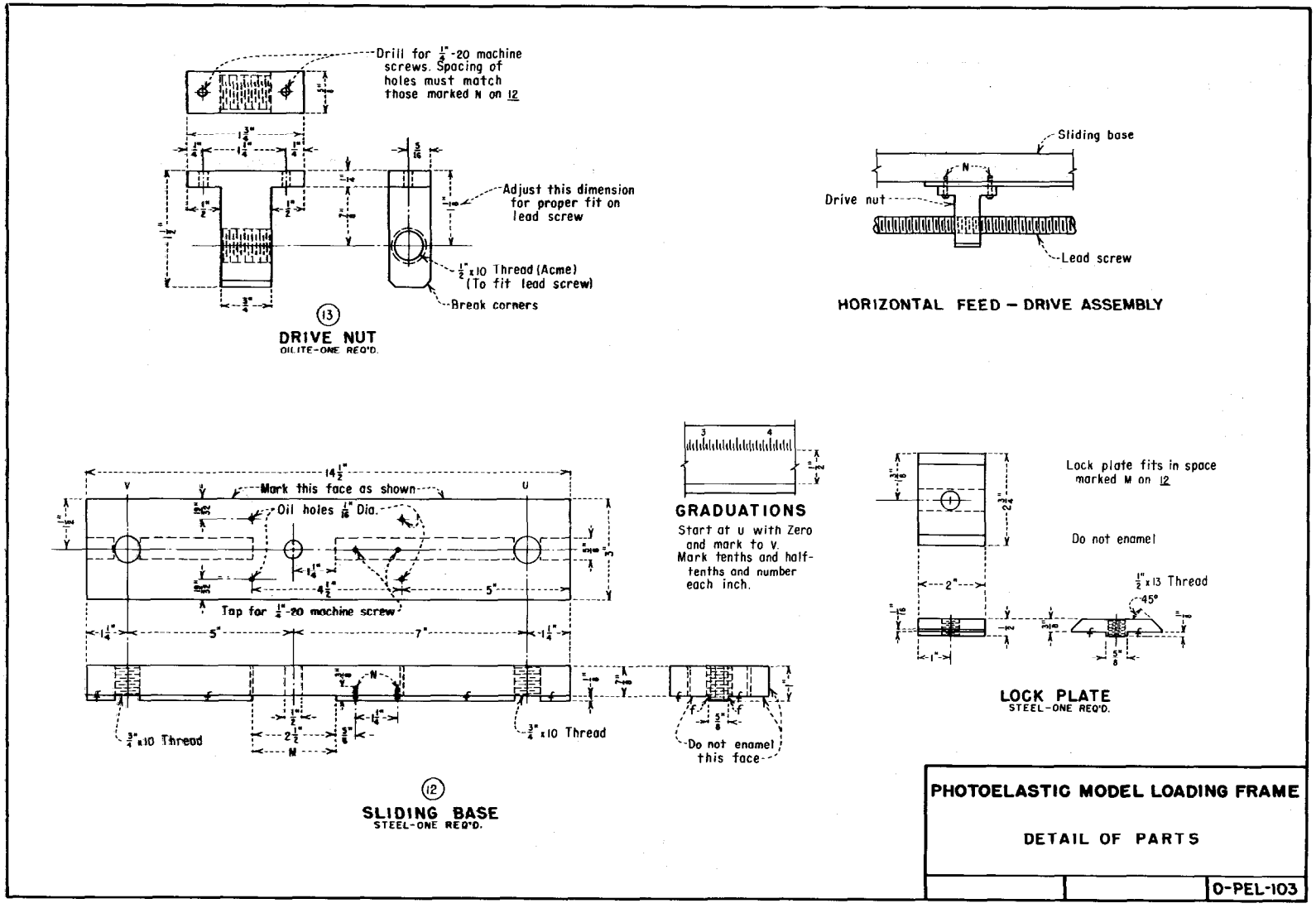

FIGURE 65 -- Loading frame assembly--component parts of base (continued).

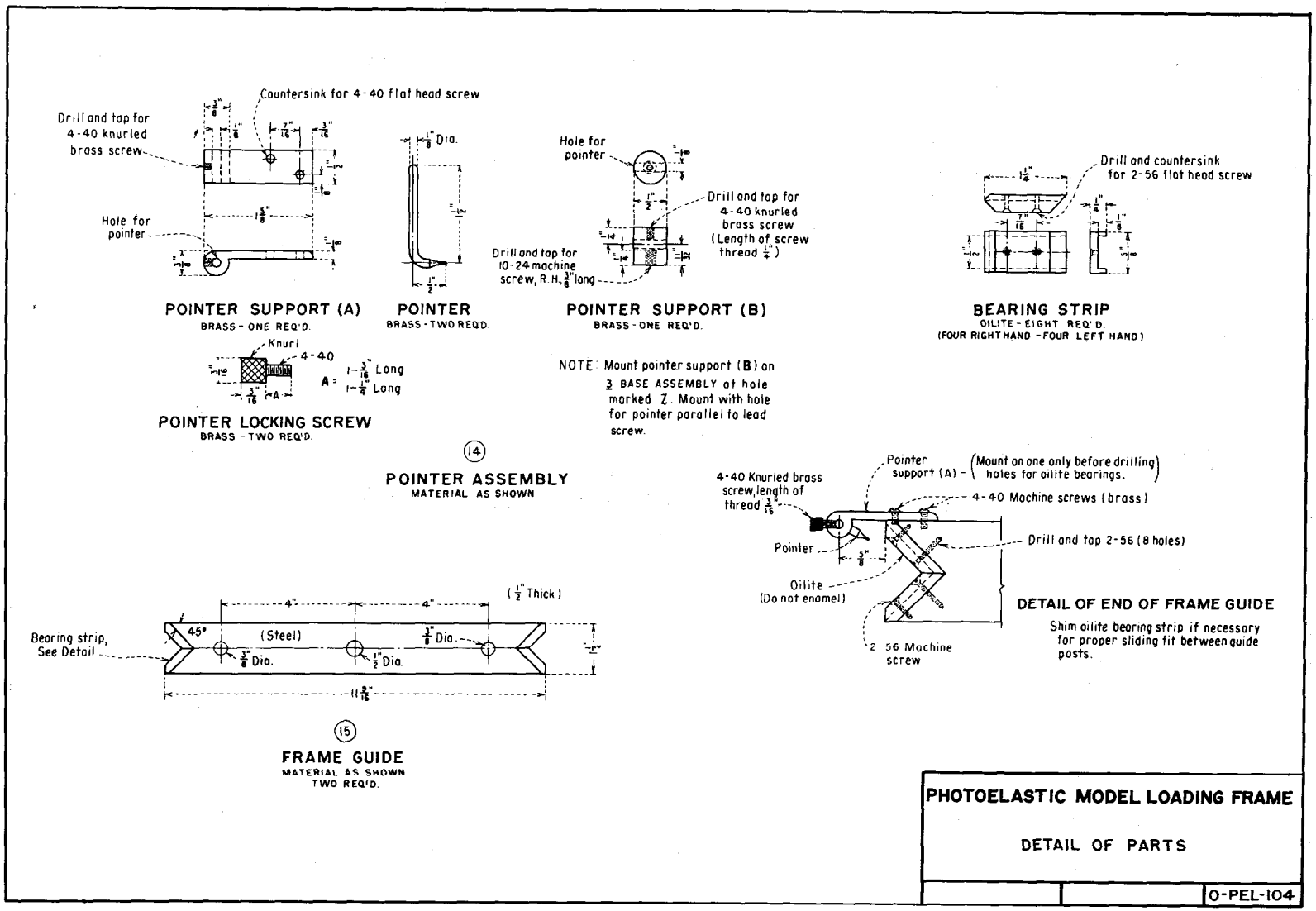

FIGURE 66 -- Loading frame assembly--details of mounting frame guides and pointers.

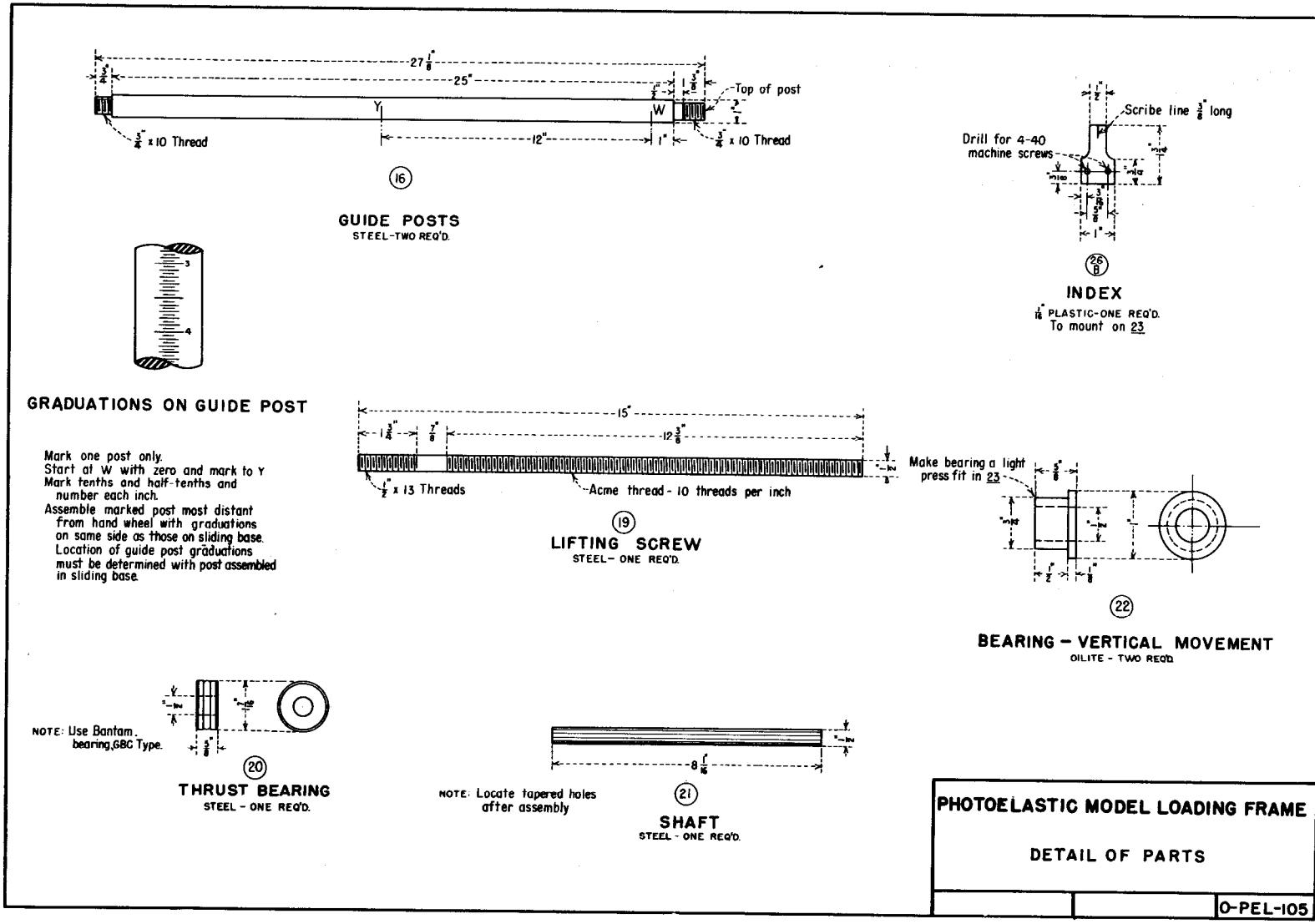

FIGURE 67 -- Loading frame assembly--details of guide posts and lifting screw.

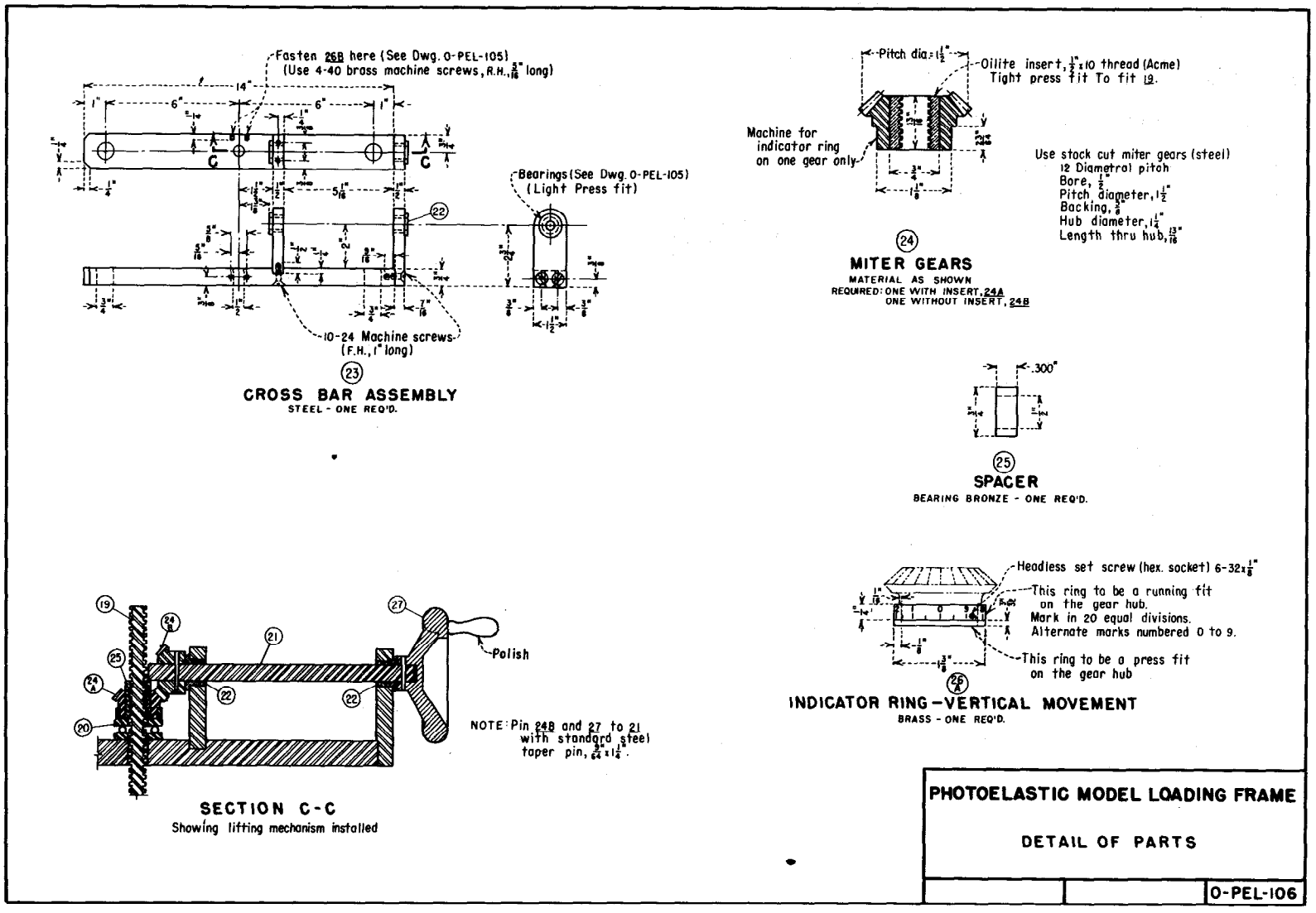

FIGURE 68 -- Loading frame assembly--component parts for vertical movement mechanism.

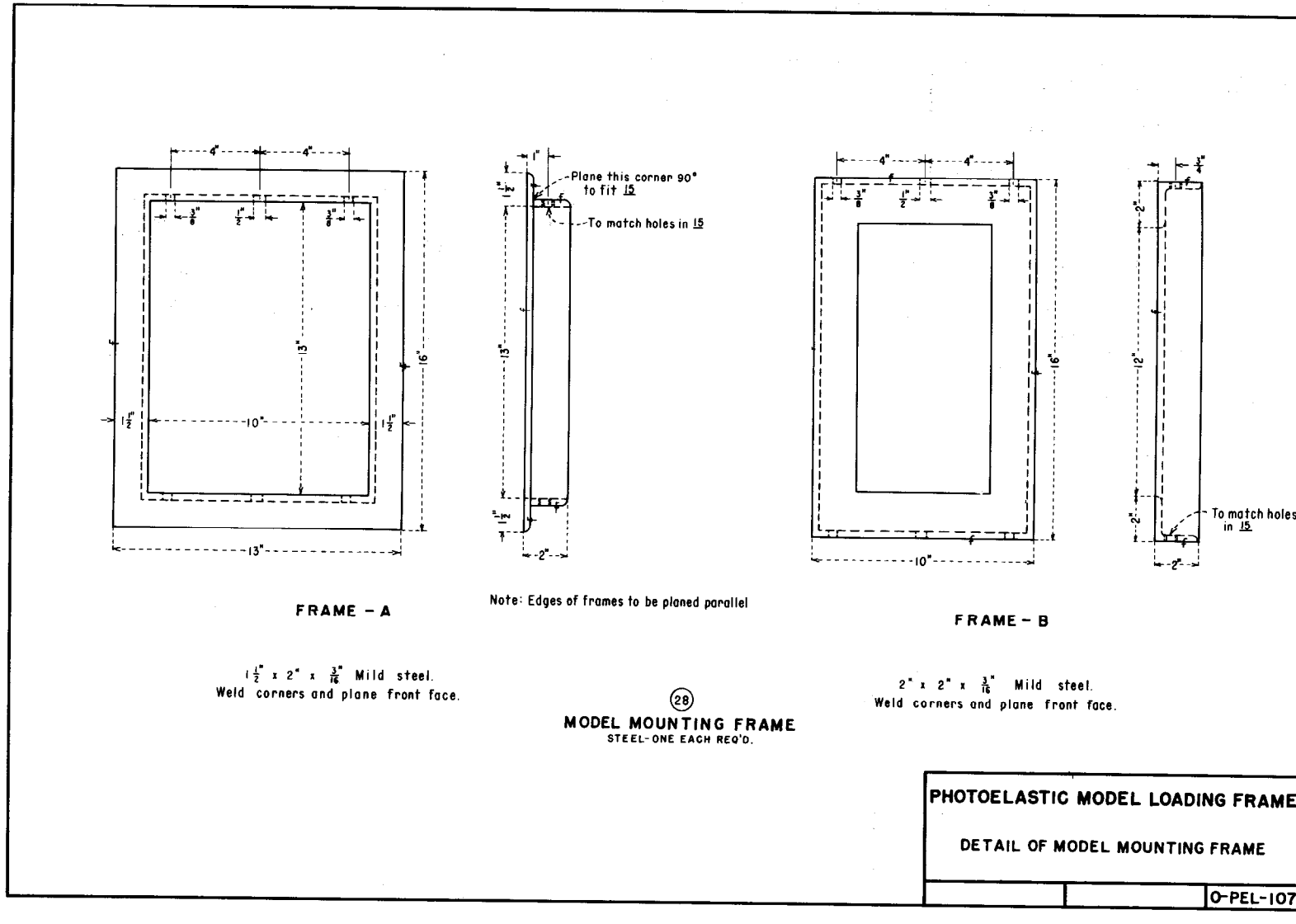

FIGURE 69 -- Loading frame assembly--model mounting frame.

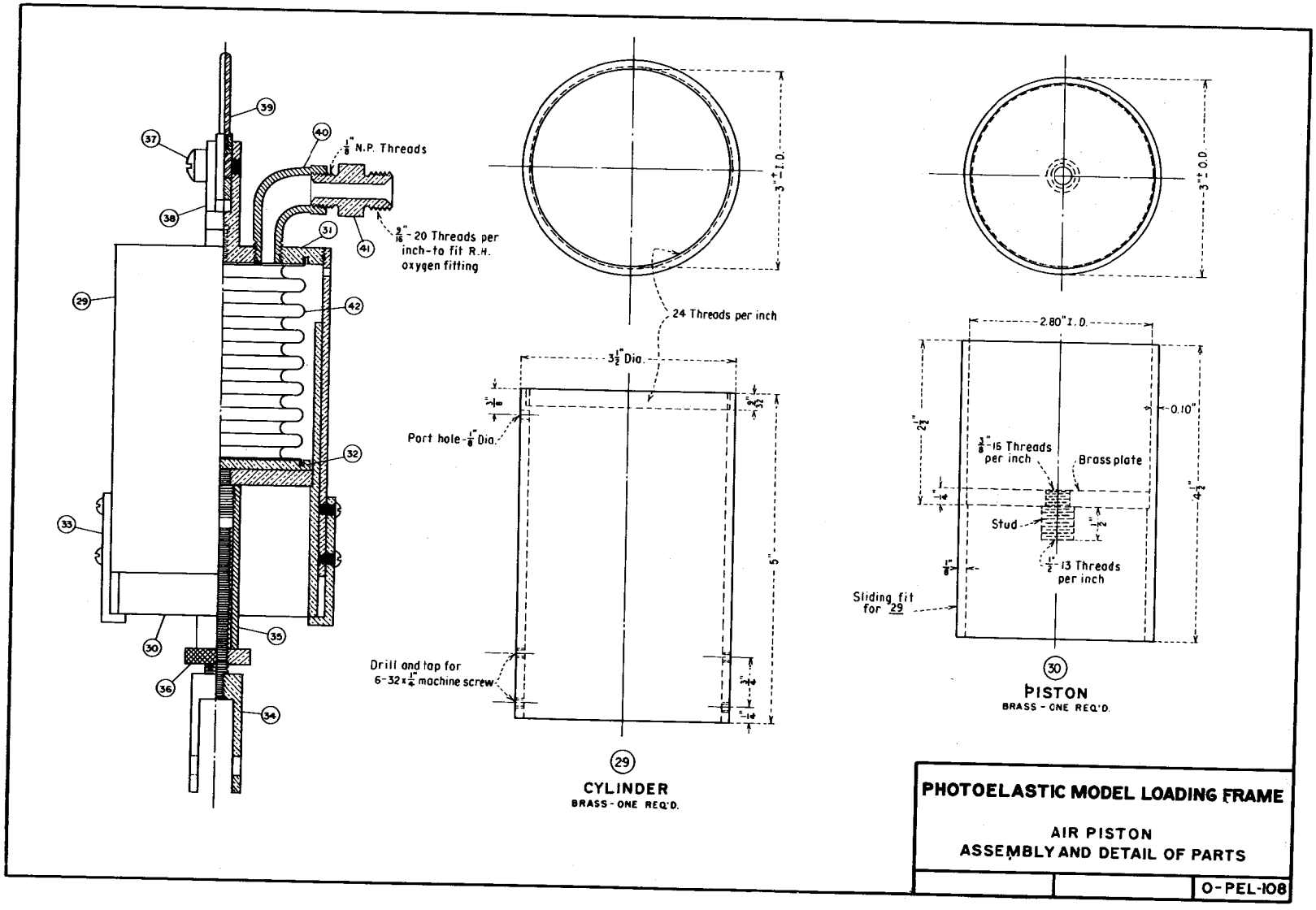

FIGURE 70 -- Loading frame assembly--air piston assembly.

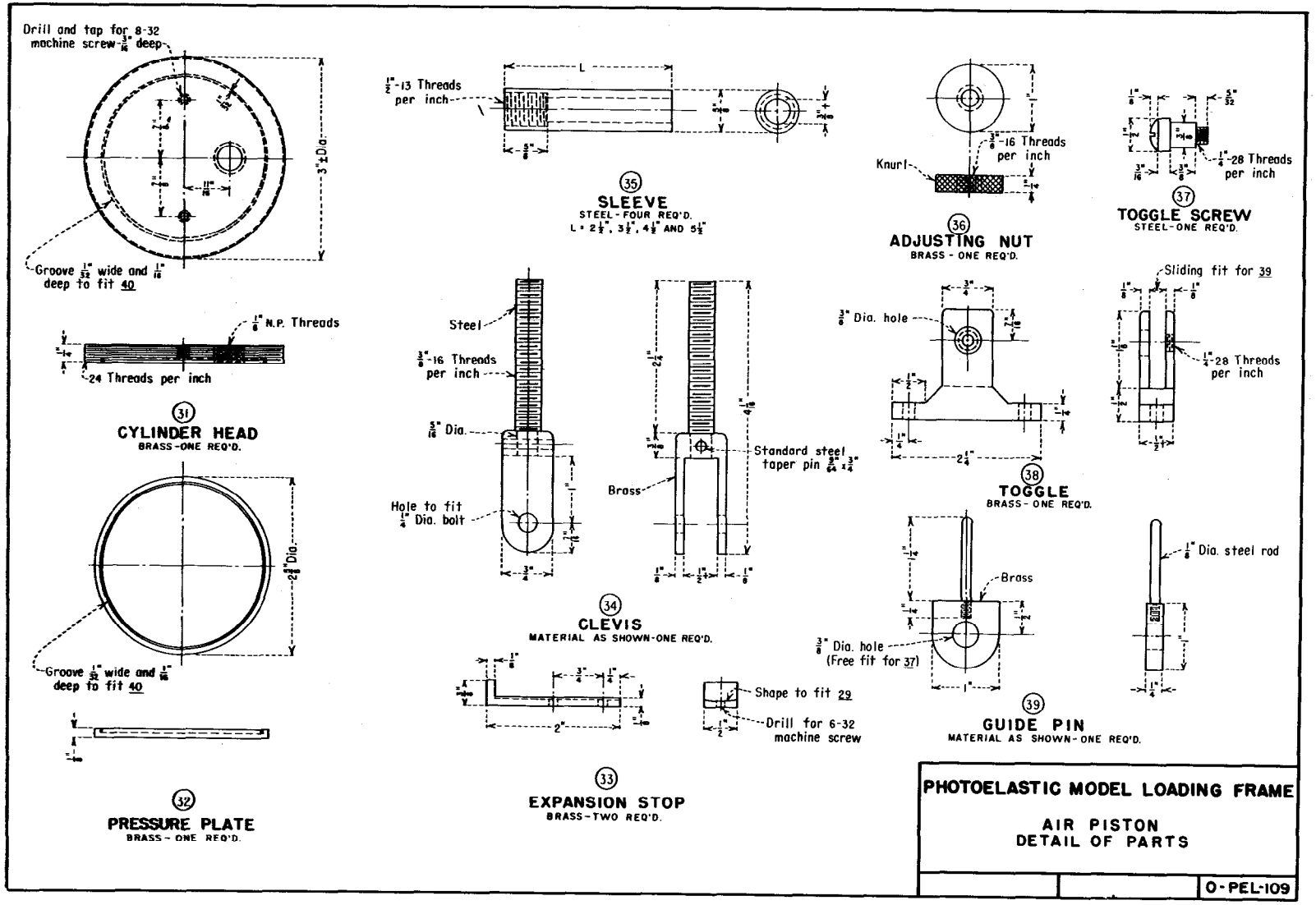

FIGURE 71 -- Loading frame assembly--air piston parts.

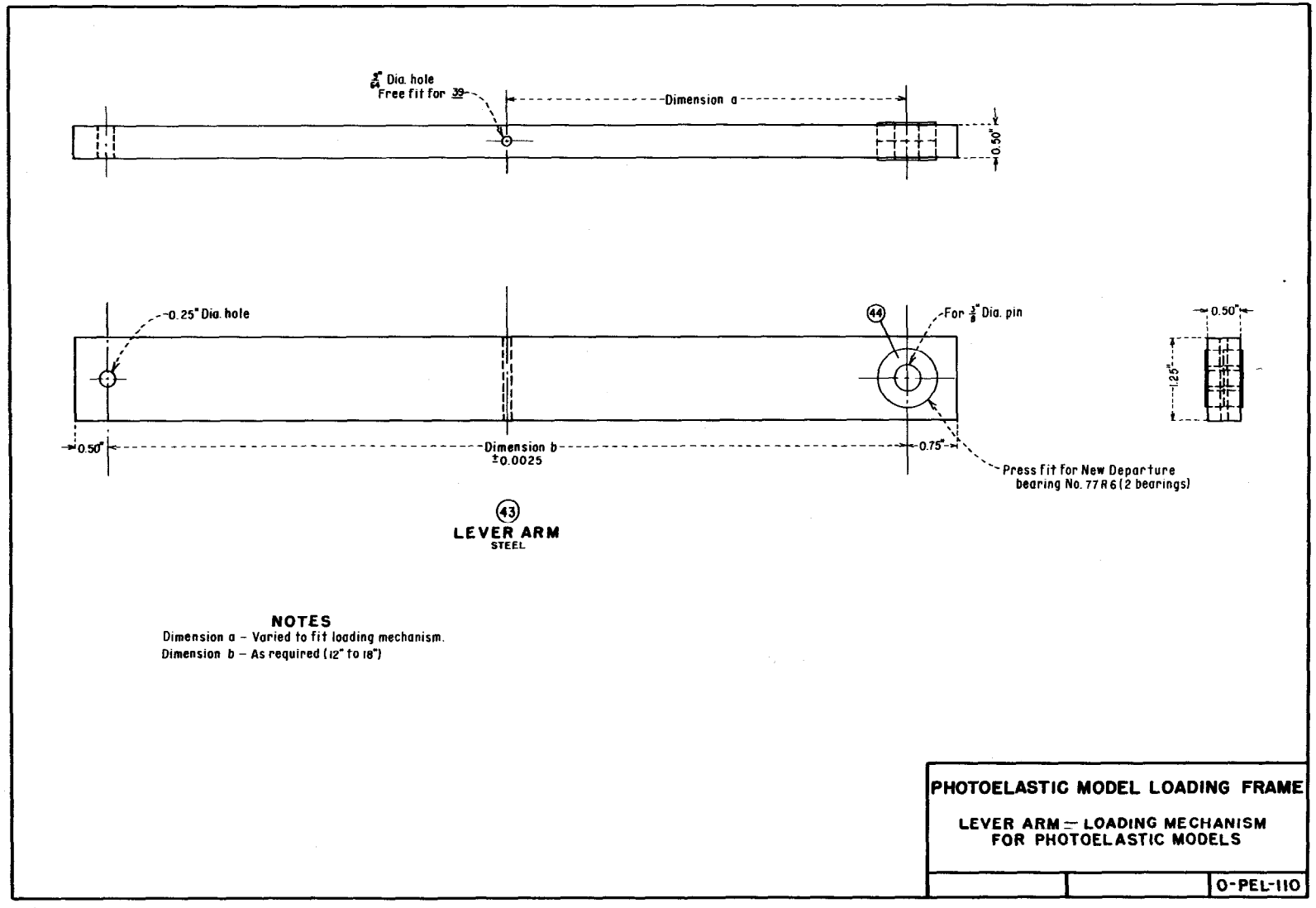

FIGURE 72 — Loading frame assembly--lever arm.

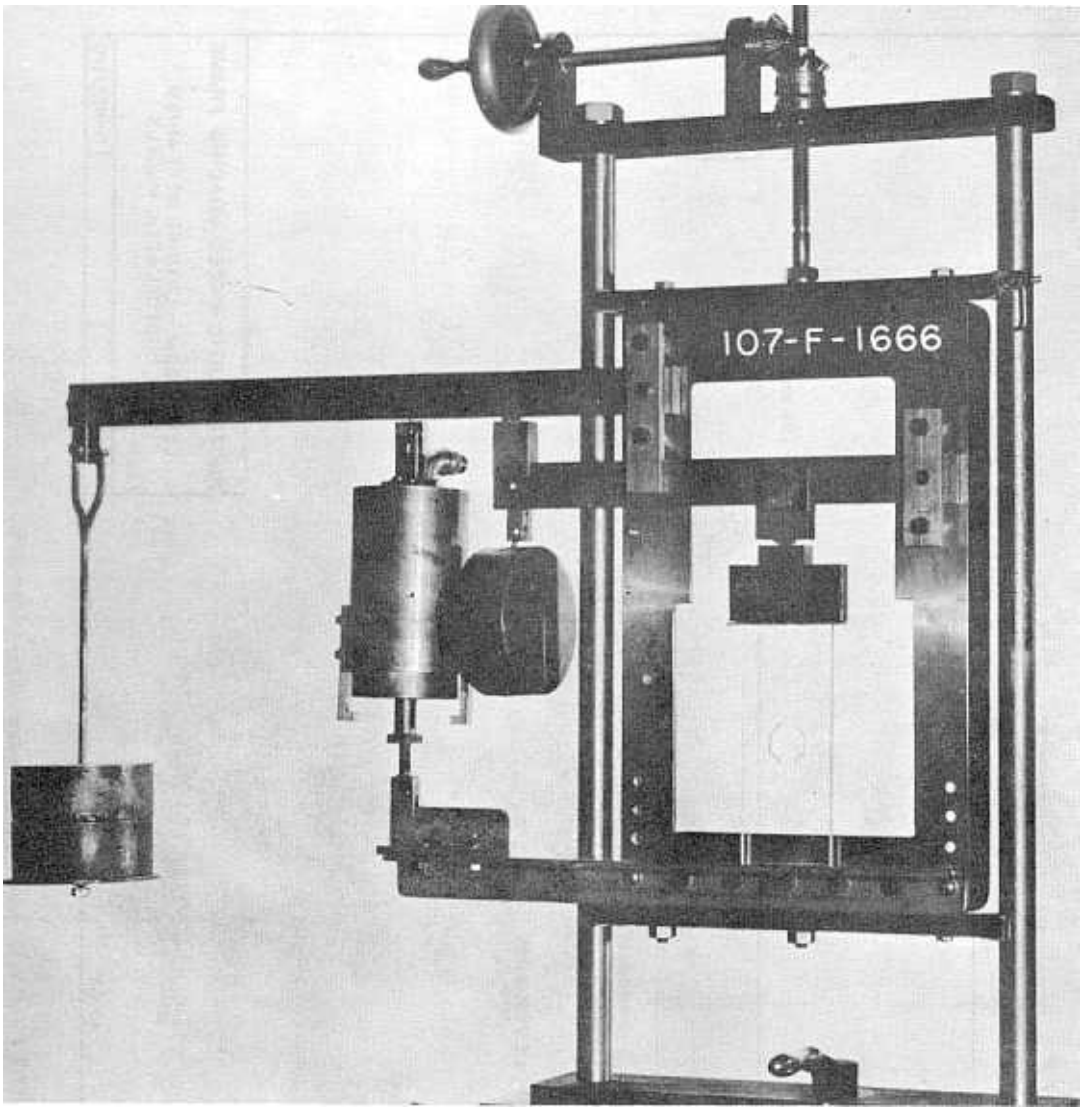

FIGURE 73 -- Loading frame assembly showing air piston and weights.

rolled easily from the special table used in the photoelastic polariscope into position on the photoelastic interferometer table. The special table used in the photoelastic polariscope is also provided with guide rails and locking screws. This table is mounted on large rubber casters to provide a shock-free movement when transferring the loading frame assembly, with its model, between instruments.

MISCELLANEOUS EQUIPMENT AND TOOLS

Description

It has been found desirable to have certain power tools available for use in building loading devices and in fabricating models. This is necessary, since the machining of plastic requires an entirely different technique to produce stress-free models than is ordinarily used in machining either metal or wood. Careful planning and coordination is required to insure completion of the model and loading mechanism in sufficient time to

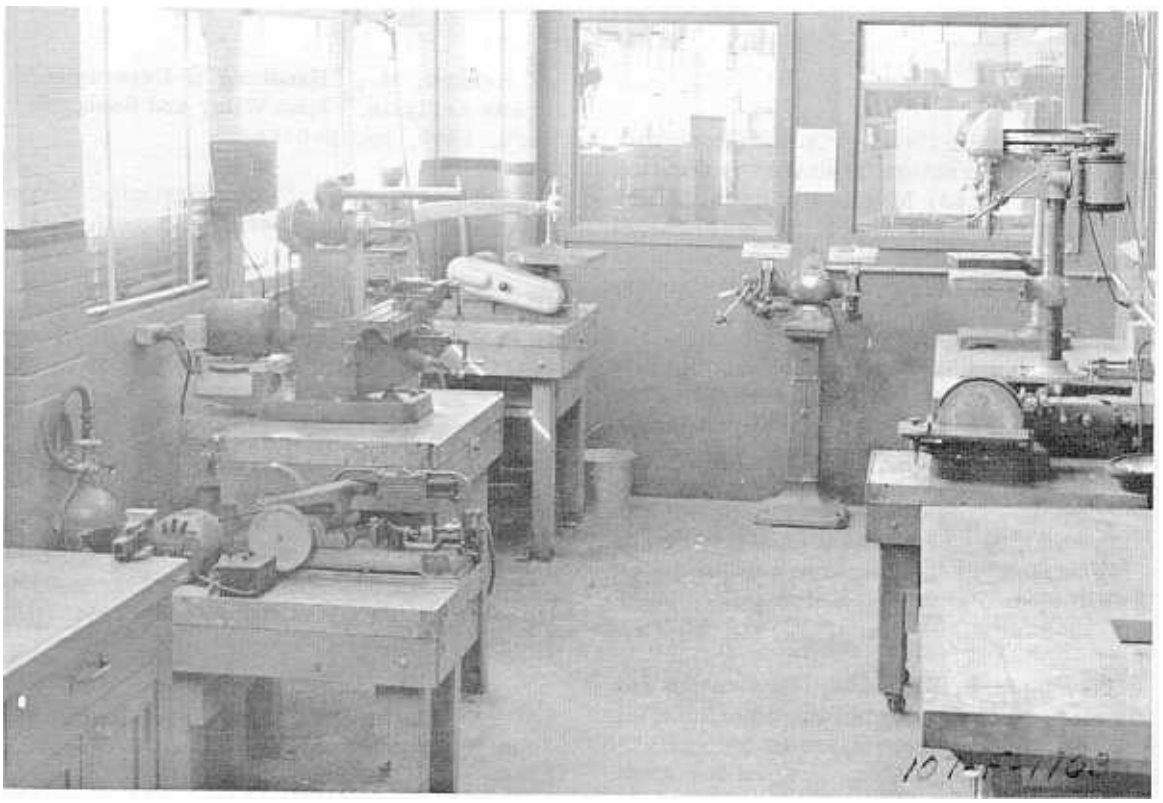

FIGURE 74 -- General view of laboratory shop.

permit loading and photographing before time-edge stresses develop in the model.

Power equipment available includes a drill press, scroll saw, sander, milling machine, hack saw, and grinder. In addition a small air compressor furnishes an air supply for use in loading and unloading models during actual testing, and to supply air for use in the shop for cleaning and other purposes. A view of a portion of the shop is shown by Figure 74. An adequate collection of miscellaneous hand tools is also available. These include precision scales, squares, and micrometers to aid in accurately laying out and checking model dimensions.

Another item of equipment, previously mentioned, is a large electric oven used for annealing plastics, for three-dimensional stress-freezing studies, and for other purposes. The oven has an automatic temperature control. Cams can be cut to provide for any desired cycle of temperature variation. Complete instructions for its operation were furnished with the oven. Figure 75 is a photograph of the oven showing its interior and the automatic control panel.

FIGURE 75 -- Electric oven.

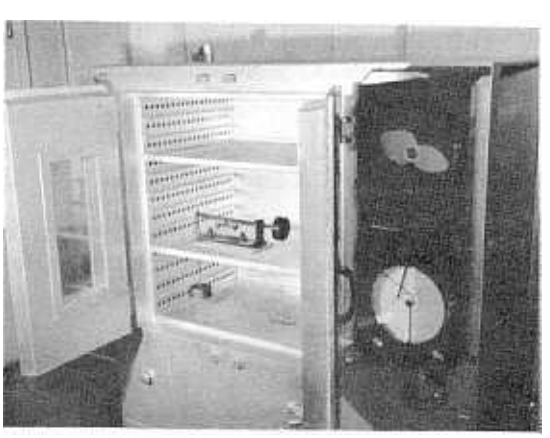

BIBLIOGRAPHY

Introduction

[1] Brewster, Sir David, "On the Communication of the structure of doubly refracting Crystals to Glass, Muriate of Soda, Fluor Spar and other Substances, by mechanical Compression and Dilatation," Philosophical Transactions of the Royal Society of London, 1816, pp. 156-178.

[2] Biot, M., "Sur une nouvelle propriété physique qu'acquièrent les lames de verre quand elles exécutent des vibrations longitudinales," Annales de Chimie et de Physique, Volume XIII, 1820, pp. 151-155.

[3] Fresnel, A., "Résumé d'un Mémoire sur la réflexion da la lumière," Annales de Chimie et de Physique, Volume XV, 1820, pp. 379-386.

[4] Neumann, F. E., "Über die Gesetze der Doppelbrechung des Lichts in comprimierten oder ungleichförmig erwarmten unkrystallinischen Körpern," Abhandlungen der koniglich preussischen Akademie der Wissenschaften Zu Berlin, 1841, Part II, pp. 1-254.

[5] Wertheim, G., "Mémoire sur la double réfraction temporairement produite dans les corps isotropes, et sur la relation entre l'élasticité mécanique et l'élasticité optique," Annales de Chimie et de Physique, Series III, Volume 40, 1854, pp. 156-221.

[6] Maxwell, J. C., "On the Equilibrium of Elastic Solids," Transactions of the Royal Society of Edinburgh, Volume 20, 1853, pp. 87-120.

[7] Coker, E. G. and Filon, L. N. G., "A Treatise on Photoelasticity," Cambridge University Press, London, 1931.

The Photoelastic Polariscope

[8] Maxwell, J. C., "On the Equilibrium of Elastic Solids," Transactions of the Royal Society of Edinburgh, Volume 20, 1853.

[9] Coker, E. G. and Filon, L. N. G., "A Treatise on Photo-elasticity," Cambridge University Press, London, 1931, pp. 197-198.

[10] Hetényi, M., "Handbook of Experimental Stress Analysis," John Wiley and Sons, New York, 1950, pp. 850-854.

[11] Frocht, Max M., "Photoelasticity," John Wiley and Sons, New York, Volume I, 1941, pp. 177-209.

[12] Jessop, H. T. and Harris, F. C., "Photoelasticity, Principles and Methods," Dover Publications, New York, 1950, pp. 73 to 88.

Three-Dimensional Photoelasticity

[13] Jessop, H. T. and Harris, F. C., "Photoelasticity, Principles and Methods," Dover Publications, New York, 1950, pp. 89-99.

[14] Frocht, Max M., "Photoelasticity," John Wiley and Sons, New York, Volume II, 1948, pp. 333-496.

[15] Hetényi, M., "Handbook of Experim ental Stress Analysis," John Wiley and Sons, New York, 1950, pp. 924-976.

[16] Weller, R. and Bussey, J. K., "Photoelastic Analysis of Three-Dimensional Stress Systems using Scattered Light," National Advisory Committee for Aeronautics, Washington, D. C., Technical Notes No. 737, November 1939.

[17] Hetényi, M., "The Fundamentals of Three-Dimensional Photoelasticity," Journal of Applied Mechanics, Volume 5, December 1938, pp. A149-A155.

[18] Fisher, W.A.P., "Basic Physical Properties Relied upon in the Frozen Stress Technique," Proceedings of the Institute of Mechanical Engineers, London, Volume 158, 1948, pp. 230-235.

[19] Heywood, R.B., "Modern Applications of Photo-elasticity," Proceedings of the Institute of Mechanical Engineers, London, Volume 158, 1948, pp. 235-240.

[20] Drucker, Daniel C. and Mindlin, Raymond D., "Stress Analysis by Three-Dimensional Photoelastic Methods," Journal of Applied Physics, Volume 11, November 1940, pp. 724-732.

[21] Taylor, C. E., Stitz, E. O., and Belsheim, R. O., "A Casting Material for Three-Dimensional Photoelasticity," Proceedings of the Society for Experimental Stress Analysis, Volume VII, Part 2, 1950, pp. 155-172.

[22] Frocht, M. M., "The Growth and Present State of Three-Dimensional Photoelasticity," Applied Mechanics Reviews, Volume 5, Number 8, August 1952, pp. 337-340.

[23] Frocht, Max M. and Guernsey, R., Jr., "A Special Investigation to Develop a General Method for Three-Dimensional Stress Analysis," National Advisory Committee for Aeronautics, Washington, D. C., Technical Notes No. 2822, December 1952.

The Photoelastic Interferometer

[24] Neuber, H., "New Method of Deriving Stresses Graphically from Photoelastic Observations," Proceedings of the Royal Society, London, Volume 141, 1933, pp. 314-324.

[25] Brahtz, J.H.A., "Mathematical Theory of Elasticity--Part I," U. S. Bureau of Reclamation, Technical Memorandum No. 591, 1939.

[26] Favre, H., "Sur une nouvelle méthode optique de détermination des tensions intérieures," Revue d'Optique, Volume 8, 1929, pp. 193-213, 241-261, and 289-307.

[27] Vose, R. W., "An Application of the Interferometer Strain Gage in Photoelasticity," Journal of Applied Mechanics, Volume 2, 1935, pp. A99-A102.

[28] Coker, E. G., "Lateral Extensometers," Engineering, London, Volume 129, 1930, pp. 465-467.

[29] Taylor, L. W., "College Manual of Optics," Ginn and Co., New York, 1924.

[30] Maxwell, J. C., "On the Equilibrium of Elastic Solids," Transactions of the Royal Society of Edinburgh, Volume 20, 1853, pp. 87-120.

[31] Neumann, F. E., "Über die Gesetze der Doppelbrechung des Lichts in comprimierten oder ungleichförmig erwärmten unkrystallinischen Körpern," Abhandlungen der königlich preussischen Akademie der Wissenschaften Zu Berlin, 1841, Part II, pp. 1-254.

[32] Coker, E. G. and Filon, L. N. B., "A Treatise on Photo-elasticity," Cambridge University Press, London, 1931.

The Babinet Compensator

[33] Hetényi, M., "Handbook of Experimental Stress Analysis," John Wiley and Sons, New York, 1950, pp. 839-843.

[34] Jessop, H. T. and Harris, F. C., "Photoelasticity, Principles and Methods," Dover Publications, New York, 1950, pp. 62-64.

[35] Frocht, Max M., "Photoelasticity," John Wiley and Sons, New York, Volume 1, 1941, Chapter 5.

The Beggs Deformeter

[36] Beggs, G. E., "An Accurate Solution of Statically Indeterminate Structures by Paper Models and Special Gages," Proceedings of the American Concrete Institute, Volume XVIII, 1922, pp. 58-78.

[37] McCullough, C. B. and Thayer, E. S., "Elastic Arch Bridges," John Wiley and Sons, New York, 1931, pp. 282-300.

[38] Deformeter Bulletin No. 2, "The Beggs Deformeter," George E. Beggs, Jr. Co., Warrington, Pa., Undated.

[39] Bulletin 161-48, "Gaertner Measuring Microscopes for Laboratory and Shop," The Gaertner Scientific Corp., Chicago, Illinois, Undated.

The Electrical Analogy Tray

[40] Zangar, C. N., "Hydrodynamic Pressures on Dams due to Horizontal Earthquake Effects," U. S. Bureau of Reclamation, Engineering Monograph No. 11, May 1952.

[41] Zangar, Carl N., "Theory and Problems of Water Percolation," U. S. Bureau of Reclamation, Engineering Monograph No. 8, April 1953.

[42] Los Angeles District, Corps of Engineers, U. S. Army, "The Electric Analogy for Percolating Water," Technical Memorandum, May 1939, revised June 1953.

The Membrane Analogy

[43] Timoshenko, S., "Theory of Elasticity," McGraw-Hill, New York, 1934, p. 233.

[44] Prandtl, L., "Zur Torsion von prismatischen Stäben," Physikalische Zeitschrift, Volume 4, 1903, pp. 758-759.

[45] Hetényi, M., "Handbook of Experimental Stress Analysis," John Wiley and Sons, New York, 1950, pp. 704-716.

[46] Johnson, Bruce, "Torsional Rigidity of Structural Sections," Civil Engineering, Volume 5, No. 10, November 1935, pp. 698-701.

Photoelastic Materials and Model Preparation

[47] Frigon, R. A., "Report of the Eastern Photoelasticity Conference Committee on Materials Research," Proceedings of the 13th Eastern Photoelasticity Conference, 1941, pp. 62-66.

[48] Pittsburgh Plate Glass Co., "Properties of Columbia Resin, CR-39," Technical Service Department, Plastics Bulletin No. 2, 1943, pp. 9-11.

[49] Jessop, H. T. and Harris, F. C., "Photoelasticity, Principles and Methods," Dover Publications, New York, 1950, pp. 181-182.

[50] Vidosic, J. P., "Plastics for Photoelastic Analysis," Proceedings of the Society for Experimental Stress Analysis, Volume IX, No. 2, 1952, pp. 113-124.

[51] Catalin Corporation of America, "Catalin Cast Resins for Photoelastic Analysis of Stress," undated pamphlet.

[52] Unpublished results of tests made in Materials Laboratory, U. S. Bureau of Reclamation, 1946 to 1952.

[53] B. F. Goodrich Chemical Co., "Kriston Thermosetting Resin--Properties and Processing Information," Technical Bulletin PM-5, undated.

[54] Taylor, C. E., Stitz, E. O., and Belsheim, R. O., "A Casting Material for Three-Dimensional Photoelasticity," Proceedings of the Society for Experimental Stress Analysis, Volume VII, Part 2, 1950, pp. 155-172.

[55] Rohm and Haas Co., "Technical Data--Plexiglas--Mechanical Properties," unnumbered bulletin, 1943.

[56] The Marblette Corporation, "Marblette--The Versatile Plastic," unnumbered bulletin, undated.

ACKNOWLEDGEMENTS

H. J. Kahm and I. E. Allen reviewed the entire monograph and made valuable suggestions. H. E. Willmann prepared the figures.

GPO 834-118